

Hypoxia in Tendinopathies: From Epigenomics to Chondroid Metaplasia

BY

Katie Trella

B.S. Rose-Hulman Institute of Technology, Terre Haute, IN, 2011

THESIS

Submitted as partial fulfillment of the requirements
for the degree of Doctor of Philosophy in Bioengineering
in the Graduate College of the
University of Illinois at Chicago, 2016

Chicago, Illinois

Defense Committee:

Dr. Anna Plaas, Advisor

Dr. Vincent M. Wang, Advisor

Dr. David Eddington, Chair

Dr. Yang Dai

Dr. Robert Wysocki, Rush University Medical Center

Acknowledgements

First and foremost, I would like to thank all of my advisors (Dr. Anna Plaas, Dr. Vincent Wang, and Dr. John Sandy) for their continued support and dedication to my graduate school career. Thank you for always believing in me even when I was ready to give up. The things I have learned from you all in these 5 years will be invaluable not only in my career but in my life. I would also like to thank Dr. Jun Li for his immense support in all the animal work for these projects, and for his beautiful histology seen throughout. Many thanks are also owed to Dr. Rebecca Bell, Dr. Daniel Gorski, and Dr. Deva Chan who taught me many of the lab protocols and mostly importantly how to endure through graduate school. Finally, there are not enough thanks to be given to Elizabeth Shewman for her support (emotional and physical) throughout these past years and for welcoming me into her “research” family!

I will forever be grateful to my family and friends who have stood with me through all the ups and downs these past 5 years, especially Derik, my parents, Marian, Chris, Maria, Emma, Megan, Randy, Trevor, and Patty. I would like to dedicate this thesis to Kim Sikes who always believed in me and taught me that no matter which direction I choose, that life was meant to be lived with a smile, a good book, and a cup of coffee. I would not have gotten through graduate school without all three!

Abstract

Tendon overuse, due to work- and sports-related activities, is the initiating factor for tendinopathy in the majority of patients, accounting for 30-50% of all sports medicine related injuries. The severity of subsequent impaired mechanical function, pain, and inflammation is influenced by age, activity level, genetic predisposition, co-morbidities, and adverse drug effects. Due to the complexity of this musculoskeletal disease, successful pharmacological and physical therapies are still lacking. While the current model of pathogenesis includes published data on the nature of the initiating extrinsic factors (e.g. acute micro-injury and chronic overuse) and provides a molecular link between collagen fibril disorganization and loss of biomechanical function, it fails to provide any details on the nature of the cellular responses that produce a chronic non-functional tissue. The over-arching goal of this project was to advance the understanding of those cellular mechanisms involved in the initiation and progression of tendinopathy using epigenomic, transcriptomic, and proteomic methods.

Firstly, a murine model of Achilles tendinopathy was utilized to determine novel pathways associated with tendinopathy through epigenetic mechanisms (Aim 1). Methylome analyses in WT mice allowed for the discovery of differential methylation in the promoter regions of 5 genes (*Leprel2*, *Foxf1*, *Mmp25*, *Igfbp6*, and *Peg12*) during the pathogenesis of tendinopathy. Notably their known functional roles are all relevant collagen dis-organization and development of chondroid metaplasia, typically associated with tendinopathy.

Histological evaluation of end stage diseased human tendons has suggested a potential involvement of hypoxia-mediated damage patterns to tendon cells and matrix, however, no molecular evidence has been reported to date. The murine Achilles tendinopathy model was used to examine the expression of a range of genes known to be affected by cellular responses to

hypoxia (Aim 2). Overall expression levels of hypoxia signaling genes, specifically those involved in angiogenesis/coagulation and metabolism/transport were significantly altered with injury. Moreover, expression changes coincided with appearance of chondroid deposits in the pericellular and interfibrillar spaces of the tendon.

Lastly, given the changes in expression of genes involved in metabolism and those regulated by metabolism, a murine Achilles tendon explant system was developed to study the role of oxygen tension where intrinsic tendon cells could be studied within their native ECM (Aim 3). Injured explanted tendons demonstrated an inability to respond to changes in oxygen tension and exhibited altered metabolism (increased glucose uptake and NADH/NADPH production). All aims were also conducted with the *Adamts5*^{-/-} mouse which exhibited a severe tendinopathic phenotype. In summary, using both *in-vivo* and *ex-vivo* murine systems, we have shown altered metabolic measures following tendon injury, which correlated with chondroid matrix deposition, a classic marker of tendinopathy. We postulate that altered tendon cellular metabolism following tendon injury may contribute to a chronic pathology and altered tendon healing.

Table of Contents

Acknowledgments.....	ii
Abstract.....	iii
Table of Contents.....	v
List of Figures.....	vi
List of Tables.....	vii
Chapter 1 – Introduction	
Significance.....	1
Background.....	1
Specific Aims.....	10
Chapter 2 – Specific Aim 1	
Introduction.....	11
Methods.....	12
Results.....	16
Discussion.....	29
Chapter 3 – Specific Aim 2	
Introduction.....	33
Methods.....	35
Results.....	37
Discussion.....	54
Chapter 4 – Specific Aim 3	
Introduction.....	58
Methods.....	59
Results.....	63
Discussion.....	75
Chapter 5 – Summary and Future Directions	
Discussion.....	78
Study Limitations.....	80
Future Directions.....	81
Appendix.....	82
Full Protocols.....	111
References.....	122
Vita	139

List of Figures

Figure 1: Diagram of the collagen fibril.....	2
Figure 2: Hierarchical structure of tendon.....	3
Figure 3: Organization of proteoglycans in the tendon ECM.....	4
Figure 4: Hematoxylin and Eosin stained sections of WT and TS5KO Achilles tendons.....	18
Figure 5: <i>Hif1a</i> expression of WT and TS5KO Achilles tendons.....	38
Figure 6: HIF1A stained sections of WT and TS5KO Achilles tendons.....	39
Figure 7: Components of the glycomatrix in WT and TS5KO Achilles tendons at 3d.....	48
Figure 8: Components of the glycomatrix in WT and TS5KO Achilles tendons with CA.....	49
Figure 9: Components of the glycomatrix in WT and TS5KO Achilles tendons with TM.....	50
Figure 10: Lectin staining of adjacent stroma for confirmation of staining specificity for neovascularization.....	52
Figure 11: Lectin staining in WT and TS5KO Achilles tendons with TM.....	53
Figure 12: Explant mechanical testing setup.....	63
Figure 13: Production of NADH/NADPH reducing equivalent in UI WT and TS5KO tendon explants.....	67
Figure 14: Change in media glucose concentration in UI WT and TS5KO tendon explants.....	68
Figure 15: Material properties in UI WT and TS5KO tendon explants	68
Figure 16: Production of NADH/NADPH reducing equivalent in injured WT and TS5KO tendon explants.....	73
Figure 17: Change in media glucose concentration in injured WT and TS5KO tendon explants.....	74
Figure 18: Material properties in injured WT and TS5KO tendon explants.....	75

List of Tables

Table 1: Experimental groups, outcome measures, and mouse numbers for Aim 1.....	13
Table 2: Fold-changes in transcript abundance of chromatin-modifying enzymes at 3 days.....	20
Table 3: Fold-changes in transcript abundance of chromatin-modifying enzymes with TM.....	22
Table 4: Significantly altered expression of chromatin modifying enzymes in TS5KO mice with injury relative to WT.....	23
Table 5: Methylation of CpG sites of DNA in WT murine tendon in response to TGF- β 1.....	25
Table 6: DM CpG sites in gene promoters of WT murine tendon in response to TGF- β 1.....	26
Table 7: Fold changes in transcript abundance for genes with DM promoter regions in response to TGF- β 1 in WT mice.....	27
Table 8: Fold changes in transcript abundance in TS5KO mice for tendinopathy related genes identified via methylome analysis.....	29
Table 9: Experimental groups, outcomes measures and mouse numbers for Aim 2.....	35
Table 10: Fold-changes in transcript abundance of hypoxia signaling genes at 3 days.....	41
Table 11: Fold-changes in transcript abundance of hypoxia signaling genes with CA.....	43
Table 12: Fold-changes in transcript abundance of hypoxia signaling genes with TM.....	44
Table 13: Significantly altered expression of hypoxia signaling genes in TS5KO mice with injury relative to WT.....	45
Table 14: Experimental groups, outcomes measures and mouse numbers for Aim 3.....	60
Table 15: Transcript abundance of <i>Hif1a</i> with UI explant.....	64
Table 16: Fold-changes in transcript abundance of hypoxia signaling genes with explant.....	65
Table 17: Altered expression of hypoxia signaling genes in TS5KO mice with explant relative to WT.....	66

Table 18: Concentration of glucose in media before and after UI explant culture.....	67
Table 19: Transcript abundance of <i>Hif1a</i> in injured tendons with explant.....	69
Table 20: Fold-changes in transcript abundance of hypoxia signaling genes in injured tendons with explant.....	70
Table 21: Altered expression of hypoxia signaling genes in injured TS5KO tendons with explant relative to WT.....	71
Table 22: Altered expression of hypoxia signaling genes in injured explants relative to un-injured explants.....	72
Table 23: Concentration of glucose in media before and after injured explant culture.....	74

Chapter 1 – Introduction

Significance

Tendon overuse, due to work and sports-related activities, is the initiating factor for tendinopathy in the majority of patients [1], accounting for 30-50% of all sports medicine related injuries [2]. The severity of subsequent impaired mechanical function, pain, and inflammation is influenced by age, activity level, genetic predisposition, co-morbidities [3], and adverse drug effects [4]. Due to this complex etiology, successful pharmacological and physical therapies are lacking. While the current model of pathogenesis includes published data on the nature of the initiating extrinsic factors (e.g. acute micro-injury and chronic overuse) and provides a molecular link between collagen fibril disorganization and loss of biomechanical function, it fails to provide any details on the types of the cellular responses that lead to a non-functional extracellular matrix.

Background

Collagen in the Tendon ECM – Molecular Structure and Function

The extracellular matrix (ECM) of tendons and ligaments are comprised of highly organized, longitudinally aligned collagen fibers (primarily types I, III, and V) which make up approximately 80% of the dry weight of the tissue. As the predominant molecular components of the tendon ECM, triple helical type I (COL1) and type III (COL3) monomers are assembled into aligned fibrils once secreted from the cell [5]. Type II collagen (COL2) fibrils are also present, but are confined to fibrocartilaginous regions at the bone/tendon interphase. “Minor collagens”, such as type V (COL5) IX (COL9), XII (COL12), and XIV (COL14) and function in regulating fibrillogenesis or mediate interactions between integrins and fibronectin [6] (Figure 1).

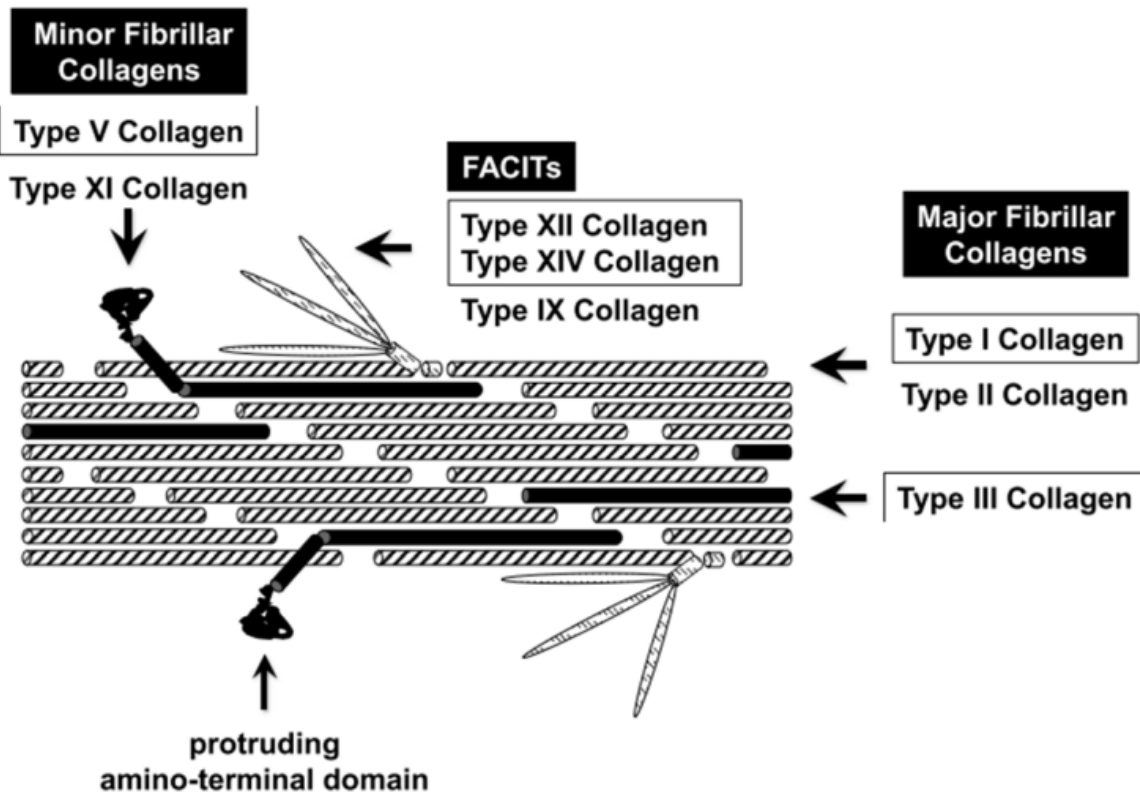


Figure 1: Diagram of the collagen fibril in tendon [5]

The detailed macromolecular organization of collagen in the tendon ECM is shown in (Figure 2). Collagen fibres and fasicles are surrounded by the endotendon (interfascicular matrix) which is essential for sliding during transmission of mechanical loads throughout the tissue [7, 8]. A large number of studies have demonstrated the complexity of the tendon loading micro-environment. The organization of collagen along the long axis of the tissue allows for the transmission of tensile forces from muscle to bone, essential for joint mobility.

At the molecular level, compression of the tissue along the perpendicular axis (changes in cross sectional area during stretching), rotation, and sliding of collagen fibres have been reported [9]. These inhomogeneous mechanical responses require additional macromolecular components e.g. elastin, lubricin, and collagen associated proteoglycans (such as decorin and fibromodulin)

within the collagen matrix contribute in varying degrees to the elasticity and viscoelasticity of the tissue. Specifically, high levels of lubricin have been implicated in the loose connective tissue sheath known as the peritenon, which is thought to confer sliding [10], but overall it has not been implicated in the structural integrity of the tissue. Therefore, changes to the molecular organization of the tendon ECM, due to traumatic or overuse injuries, comorbidities, drug side effects, genetic defects, or aging will affect overall biomechanical mechanical function of the tissue as well as the transduction of signals from the ECM to resident tendon cells.

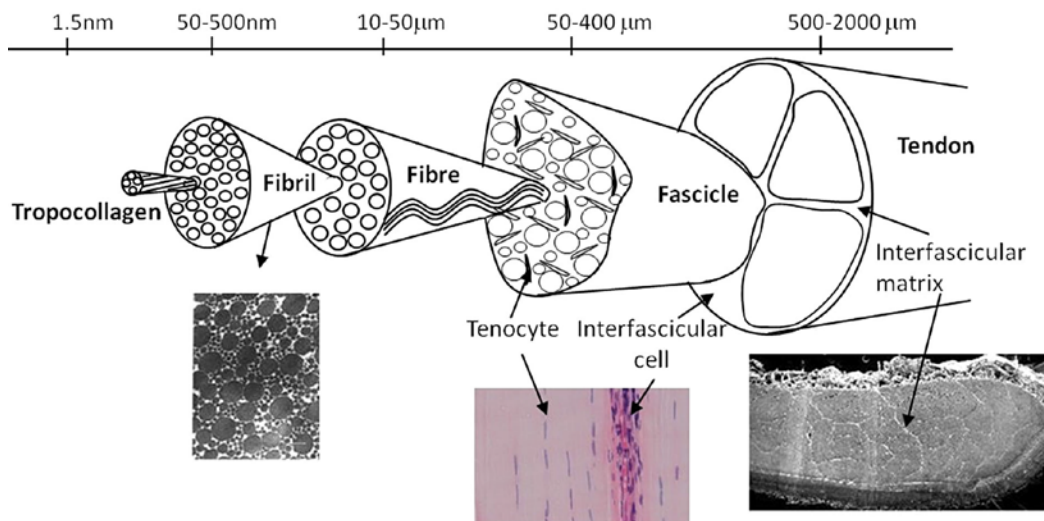


Figure 2: Hierological structure of tendon [11]

Non-Collagenous Components in the Tendon ECM – Molecular Structure and Function

The ECM of the tendon body and peritenon (loose connective sheath that surround the tendon) contain other macromolecules such as proteoglycans (PG) (biglycan, fibromodulin, decorin, versican, and aggrecan), as well as hyaluronan (HA) [12]. Together these account for approximately 2% of the dry weight of tendon. These components primarily sit between collagen

fibrils and interact directly with tenocytes (Figure 3). The leucine rich proteoglycans (SLRPs), decorin, biglycan, and fibromodulin, [11] bind to specific sites on the collagen fibrils for regulation of fibrillogenesis [13-15]. Due to the size of the larger PGs, such as aggrecan and versican, they reside in the pericellular region [11] and are closely associated with collagen fibres within the ECM. They contain numerous negatively charged glycosaminoglycan (GAG) chains for attraction of water, which when accumulated can provide resistance to compression [6, 16]. The distribution of PGs varies greatly along the length of the tendon, with a higher proportion, specifically of aggrecan, present near the tendon-bone insertion (fibrocartilaginous zones) where adaptations to compressive loading are necessary [17].

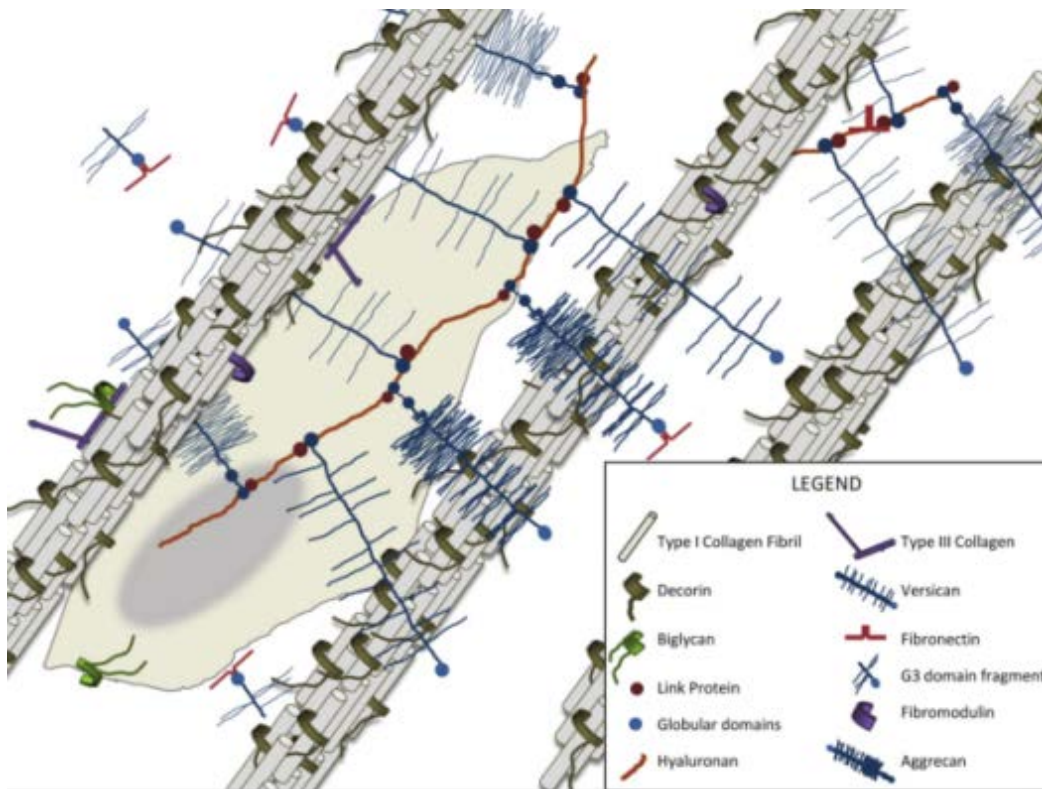


Figure 3: Organization of proteoglycans in the tendon extracellular matrix [6]

There is a paucity of studies aimed at identifying differences in proteoglycan content between tendon types and between different species. Recent studies have highlighted the

differences between positional and energy storing tendons using an equine model. The common digital flexor tendon (CDET), which is functionally comparable to the human anterior tibialis tendon [18], is a positional tendon exhibiting small strains of 2-3% [11]. The superficial digital flexor tendon (SDFT), which is comparable to the human Achilles [19], which also performs a positional role, can reach strains up to 10% allowing for the storage of energy [11]. However, the ability to reach higher strains (less stiff) makes these tendons more prone to injury [11]. While the CDET overall has fewer SLRPs than the energy storing SDFT, the SLRP's of the CDET are more highly localized in the interfascicular matrix allowing for enhanced fibril sliding and contributing to the higher viscoelasticity of these tendons [20-22]. Conversely, the SDFT has higher levels of GAG, non-mature collagen cross-linking, and larger proportions of lubricin and elastin in the interfascicular matrix allowing for elastic, or recoverable, sliding [11, 23]. Few differences were seen in the presence of decorin and biglycan between the tendon types, with the chondroitin sulfate side chains within these PGs most likely contributing to fibril sliding [23, 24]

Extra-tendinous cell sources involved in tendon repair

With regards to cellular responses to tendon injury, recent studies have suggested that cells residing in the peritenon and even the endotendon may be important in regulating tendon repair [25]. In relation to tenocytes found adjacent to tendon fibres, cells derived from the tendon proper (peritenon, endotendon) demonstrated a multi-potent potential through increased expression of tenogenic and matrix assembly genes [26], and a higher capacity to differentiate towards osteogenic, adipogenic, and myogenic lineages [27].

Tissue Pathologies in Tendinopathy

A diagnostic feature of human and animal model tendinopathy is the appearance of cell clusters in a “chondroid matrix” as defined by Alcian Blue or SafraninO positive staining [28-32]. At the biochemical level, chondrogenic markers (aggrecan and collagen type II) have been reported to be increased in human Achilles tendinopathy [30], and in cells from human tendinopathic lesions [31]. Further, in a histopathological study of human patellar tendinopathy 28 patients showed chondroid deposits in the tendon matrix, with similar ECM alterations in only 3 of 39 age- and sex-matched tissues from cadaveric donors with no history of tendinopathy [32]. Additionally, histological GAG accumulation, largely due to aggrecan chondroitin sulfate was shown to be strongly correlated to advanced clinical symptoms (pain, tenderness, overall weakness) [33], suggesting the direct link of this chondroid pathology to mechanical dysfunction.

In summary, the pathway to chronicity in tendinopathy favored by many in the field is that intra-tendinous stressors (metabolic or biomechanical) persist following an initiating injury, such as acute overload, and maintain the cellular activities responsible for chondroid deposition, collagen disorganization, and a loss of tissue material properties [34, 35]. For example, overload of bovine flexor tendon *in-vitro* generates areas of rounded cells in the ECM, accompanied by collagen disorganization and increased cellular staining for IL6 and MMP13 [36]. As commonly seen in other connective tissues, such as cartilage [37] or skin [38], repair deficiencies in tendinopathy also appear to be associated with chronic turnover of pericellular components without a concomitant increase in the production of stable, long-lived matrix structures.

Murine Model of Achilles Tendinopathy

A more direct demonstration on the pathogenic role of such chondroid deposits has come from previous studies from our lab using a murine model, in which Achilles tendinopathy was induced by a single injection of transforming growth factor- β 1 (TGF- β 1) into the midportion of the tendon of skeletally mature, 12 week old male C57/Bl6 mice. This resulted in tendon swelling, deposition of chondroid (aggrecan-rich deposits), collagen disorganization, and a loss of tensile properties [39]. Mechanical stimulation of the impaired tendon via treadmill running was accompanied by elimination of chondroid and recovery of mechanical properties [39]. While this model appears very useful for studies on acute tendinopathy, it does not provide an opportunity to examine the pathways associated with chronic disease.

While there are anatomical and biomechanical differences in tendon structure and functions between animals and humans [40], animal models of tendinopathy offer the ability to study the ignition and progression of the disease following chemical and biomechanical stressor which mimic human disease etiology. In this context, the following guidelines for criteria an injury model should meet for relevance to the human pathology have been proposed: 1) collagen disorganization, 2) hypercellularity, 3) hypervascularity, 4) rounding of cells, 5) chondroid accumulation, 6) expression of chondrogenic markers, 6) tissue swelling 7) gait changes or activity-related pain, and 7) long term impaired biomechanical function [41].

The mouse model of tendinopathy used in the current studies meets the majority of these criteria. Mouse models offer the additional benefit of conditional and inducible knockouts which can allow for the study of heritable disorders, or genetic backgrounds which are susceptible to tendinopathy, or impaired tendon function [42]. In this way specific genes can be studied in the initiation and progression of tendinopathy.

Enhanced Tendinopathic Response of Achilles Tendons in ADAMTS-deficient mice

Our lab previously demonstrated that knockout of ADAMTS5 (TS5KO), a disintegrin and metalloproteinase with thrombospondin motifs, essential for collagen organization in wound healing, resulted in pericellular aggrecan accumulation, decreased material properties, and increased collagen fibril density [43] compared to tendons from wild-type (WT) mice. Significantly, tendinopathy (e.g. chondroid deposition and decreased mechanical strength) induced by TGF- β 1 injection in the ADAMTS5 knockout mice was exasperated and not eliminated by the treadmill exercise as seen with WT mice [44]. This mimics the apparent deficiency in ADAMTS5 seen in horses with degenerative suspensory ligament desmitis [45], which is characterized by high levels of proteoglycans.

Additionally, the presence of ADAMTS5 has been shown to be necessary for the deposition of fibrous tissue, as ADAMTS5 null mice were protected from dermal fibrosis in joints wounds [46] and scarring in dermal wounds [38]. Interestingly, TS5KO stromal cells exhibited reduced synthesis and secretion of aggrecan and versican proteoglycans which appeared to be correlated to reduced cellular uptake of glucose, not through the previously established metalloproteinase activity [47].

Therapeutic Treatments for Tendinopathy

Due to the complexity and chronicity of tendinopathy, to date there are no standardized treatments for the disease. Conservative non-surgical treatment options include shockwave, ultrasound, low-level laser, and hyperthermia therapies, injections of corticosteroids, platelet rich plasma (PRP), and poli-docanol (sclerosing agent for vessel proliferation), as well as oral or local administration of NSAIDs (ibuprofen, naproxen sodium, or celebrix). While many of these

modalities have been shown to reduce pain and inflammation associated with the disease [48, 49], allowing for mobility of the affected joint, their beneficial or adverse effects on long-term ECM structural regeneration and subsequent functional tissue healing are currently unknown.

Rehabilitative exercise, specifically eccentric loading (e.g. heel drop exercise), has been shown as the most effective long-term non-operative therapy for Achilles tendinopathy resulting in pain reduction and improved tendon function [50-52]. However, the mechanism by which this type of “physical” therapy contributes to tendon healing and restoration of function is currently unknown. Surgery is used as the last option for treatment if previous pharmacological and physical therapies have failed. Such invasive treatments usually involve debridement of the tendon and peritendinous tissue to remove fibrotic adhesions and calcified tissue [48]. Failure rates following surgical debridement remain at 20-30%, therefore other options including stem cell and growth factor treatments are being explored [48]. However, the development of successful and predictive therapeutic options largely depends on improved understanding of the cellular events involved in the initiation in progression of tendinopathy, which ultimately results in pathological tissue remodeling and a loss of mechanical function.

Specific Aims

The over-arching goal of this project is to advance the understanding of the cellular mechanisms involved in the initiation and progression of tendinopathy. Successful identification of pathway components using *in-vivo* and *in-vitro* murine models is expected to guide the future development of novel therapeutics to effectively treat tendinopathies.

Aim 1

To characterize mechanisms of epigenetic regulation in an *in-vivo* model of Achilles tendinopathy in skeletally mature C57Bl6 WT and TS5KO male mice

Aim 2

To determine the role of hypoxia and its downstream signaling pathway in the *in-vivo* Achilles tendinopathy model, using skeletally mature male C57Bl6 WT and TS5KO mice.

Aim 3

To develop an explant culture system for short term *ex-vivo* maintenance of murine Achilles tendons from skeletally mature male C57Bl6 WT and TS5KO to study the metabolic responses of un-injured and *in-vivo* injured tendon cells to varying O₂ concentrations

Chapter 2 – Specific Aim 1

This chapter and the ‘Tendinopathy’ and ‘Murine Model of Achilles Tendinopathy’ sections of Chapter 1 were submitted to the Journal of Orthopedic Research on April 26th, 2016, under the citation: Genome-wide alterations in DNA methylation identify *Leprel2*, *Foxf1*, *Mmp25*, *Igfbp6* and *Peg12* as disease-associated genes in murine Achilles tendinopathy. Co-Author affiliations and contributions can be seen in Appendix A. Copyright permission from the Journal of Orthopedic Research can be seen in Appendix B.

Introduction

The cellular basis for repair of connective tissues includes proliferation and differentiation of endogenous multipotent cells [53] and in this regard it has been suggested, among many other approaches, that connective tissue growth factor stimulated recruitment of endogenous tendon CD146+ cells may be an effective first step [54]. However, much as for any human complex disease, an understanding of the epigenomic regulation of the transcriptome will ultimately be needed to delineate the complex interplay between multipotent cells, matrix structure, and biomechanical factors. The epigenome involves chemical modifications to DNA (methylation) and histone proteins (methylation, acetylation, phosphorylation, and ubiquitination), as well as expression of micro-RNAs, which modulate the transcriptome. The application of epigenetics has previously been successfully used to identify novel therapeutics in complex diseases such as cancer, diabetes, chronic kidney disease, and fibrosis as the DNA methylome can be passed down through cell lineages, suggesting that epigenetic identities may contribute to the chronicity of a disease [55].

In relation to tendon biology, expression of G9a, a methyltransferase with specific affinity to the ninth lysine residue of histone three, was shown to regulate cellular differentiation

in mouse tenocytes by expression of tenogenic transcription factors [56], including Scleraxis and Mohawk, which have been heavily studied as necessary modulators for proper tendon development [57]. Additionally, the use of fluoroquinolones (linked to tendinopathy in human patients [58]) in human embryonic kidney cell cultures resulted in the inhibition of DNA methylases, collagen prolyl 4-hydroxylases, and hypoxia inducible factor 1a (also linked to tendinopathy [59]), suggesting a mechanistic epigenetic link to chronic tendinopathy [60].

While these recent studies suggest the important role of epigenetics in tendon biology, to our knowledge there are no published studies on analyses for altered DNA methylation and histone modification in human tendinopathies or animal models of the disease. The current aim was carried out, using a murine model of Achilles tendinopathy, to identify changes in expression of epigenetic modification enzymes, and to subsequently perform a genome-wide screening for changes in methylation of gene promoter regions associated with the development of the disease.

Methods

Murine model of Chronic Tendinopathy in WT and TS5KO C57/B16 Mice:

All animal use was approved by the IACUC of Rush University. We have previously published on the induction of tendinopathy in murine Achilles tendon by a single injection of TGF- β 1 into the body of the tendon, and we noted that the early loss of biomechanical properties and matrix disorganization was largely reversed by extended treadmill running [39]. To generate a model in which structural, biochemical, and cell biological changes become chronic, a more severe injury was generated by injections of TGF- β 1 on days 0 and 2. Experimental groups, outcome measures, and mouse numbers are summarized in Table 1. Mouse weights tracked each week during the experimental time-course can be seen in Appendix C.

Table 1: Experimental groups and outcomes for Aim 1

Group	Abbreviation	Outcome Measures				
		Histology ¹		QPCR ²		DNA Methylation ²
		WT	TS5KO	WT	TS5KO	WT
Un-Injured	UI	N=4	N=4	N=3 (12,20,22)	N=3 (20,18,20)	N=1 (6)
3 days	3d	N=4	N=2	N=3 (12 each)	N=3 (13,10,10)	N=1 (6)
14 days	14dCA	N=2	N=3	N=3 (20,20,21)	N=3 (20,18,21)*	N=1 (5)
28 days	28dCA	N=3	N=4	N=3 (18,16,18)	N=3 (18,15,15)	N=1 (5)
14 days + TM	14dTM	N=3	N=3	N=3 (16 each)	N=1 (16,11,11)	N=1 (6)
28 days + TM	28dTM	N=3	N=3	N=3 (16 each)	N=1 (20,15,16)	N=1 (6)
Un-Injured 14 days + TM	UI 14dTM	N=3	N=3	N=1 (15)	N=1 (20)	-
Un-Injured 28 days + TM	UI 28dTM	N=3	N=3	N=1 (17)	N=1 (20)	-

1 - Individual legs

2 - Tissue pools with number of tendons per pool in parenthesis

* 3rd pool removed from post-analysis due to outlier (Δ Ct values for all genes approximately 1.5 STDs below the average). Abundance values can be seen in Appendix D

Histology

Histological evaluation was performed as described previously [39]. Briefly, after formalin fixation and decalcification, specimens were embedded in paraffin and 5 μ m thin sections were stained with Hematoxylin and Eosin and images taken at 40x magnification.

Gene Expression Assays

Freshly harvested Achilles tendons were immediately isolated from all surrounding tissue with the peritenon left intact. RNA was isolated and purified, as previously described [39], from three separate pools of 12-20 combined Achilles tendons from un-injured (UI) mice and from each experimental group (Table 1). Briefly, tendon pools were fragmented by hammer impact at

-196°C in a Bessman Tissue Pulverizer, recovered, and extracted in 1 mL of Trizol by vortexing for 60 seconds. RNA was purified with an RNeasy MiniKit (Qiagen, Cat #: 74104) and yields were approximately 305ng/tendon for UI, 805ng/tendon for 3d, 1800ng/tendon and 800ng/tendon for 14 and 28 days post-injury, respectively. RNA quality was established from A260:280 of at least 1.90. cDNA was synthesized with 0.5ug of mRNA (RT² First Strand Kit, Qiagen, Cat #: 33404) and chromatin modification enzyme transcript abundances were determined with SYBR qt-PCR array plates (PAMM-085Z, Qiagen), as described by the manufacturer. The array was made up 84 genes separated into the following functional groups: DHD (DNA/Histone Demethylases; n=6), DM (DNA Methyltransferases; n=3), HA (Histone Acetyltransferases; n=17), HD (Histone Deacetylases; n=11), HM (Histone Methyltransferases; n=16), HP (Histone Phosphorylation; n=7), HU (Histone Ubiquitination; n=9), SET (SET Domain Proteins; Histone Methyltransferase Activity; n=15). The RNA preparations used to synthesize DNA for transcript assay of chromatin modification enzymes were also used for Taqman qt-PCR [39] of transcripts chosen from the DNA methylome analysis, with primers from Thermo-Lifetech. Primer information for individual assays can be found in Appendix E. Each individual qt-PCR assay was conducted in triplicate with a coefficient of variation of less than 7%. While each qt-PCR array was conducted singularly for each sample, three individual replicate array assays of a typical sample (WT 3d Pool #3) showed a coefficient of variation of less than 5% between each of the triplicates.

Changes in transcript abundance ($\Delta Ct = Ct$ for transcript of interest minus Ct for the housekeeping gene *B2m*) were used to calculate the fold change ($2^{-\Delta\Delta Ct}$) from UI levels for each experimental group. The genes *Aurkc* and *Prmt8* were removed from down analysis as transcripts were undetected by qt-PCR in all groups. A 1-way ANOVA with Tukey's post-hoc

test was conducted using GraphPad Prism 5 (La Jolla, CA) on the Δ Ct values to determine the significance ($p < 0.05$) in expression of genes in the injured relative to UI groups for each genotype. For genotypic comparisons a Student's t-test was used to compare TS5KO and WT values for each experimental group. For additional interpretation we have marked genes in **BOLD** that are also >3.5 -fold differentially regulated suggesting biological significance and genes marked with an * which were >3.5 -fold but not statistically significant. No statistical evaluation was performed on the un-injured plus treadmill running condition since only one pool of tendons was used per group. Instead, a >3.5 -fold change in expression relative to UI was considered "biologically significant"

Methyl-MiniSeqTM library construction (WT mice only)

Libraries were prepared from 200-500 ng of genomic DNA (from 5-6 tendons) digested with 60 units of Taq α I and 30 units of MspI (NEB) sequentially and then extracted with Zymo Research (ZR) DNA Clean & ConcentratorTM-5 kit (Cat#: D4003). Fragments were ligated to pre-annealed adapters containing 5'-methyl-cytosine instead of cytosine according to Illumina's specified guidelines (www.illumina.com). Adaptor-ligated fragments of 150–250 bp and 250–350 bp in size were recovered from a 2.5% NuSieve 1:1 agarose gel (ZymocleanTM Gel DNA Recovery Kit, ZR Cat#: D4001). The fragments were then bisulfite-treated using the EZ DNA Methylation-LightningTM Kit (ZR, Cat#: D5020). Preparative-scale PCR was performed and the resulting products were purified (DNA Clean & ConcentratorTM - ZR, Cat#D4005) for sequencing on an Illumina HiSeq.

Methyl-MiniSeqTM Sequence alignments and data analysis (WT mice only)

Sequence reads from bisulfite-treated EpiQuest libraries were identified using standard Illumina base-calling software and then analyzed using a Zymo Research proprietary analysis pipeline, which is written in Python and used Bismark (<http://www.bioinformatics.babraham.ac.uk/projects/bismark/>) to perform the alignment. Index files were constructed using the *bismark_genome_preparation* command and the entire reference genome. The *--non_directional* parameter was applied while running Bismark. All other parameters were set to default. Filled-in nucleotides were trimmed off during methylation calling. The methylation level of each sampled cytosine was estimated as the number of reads reporting a C, divided by the total number of reads reporting a C or T. Fisher's exact test or t-test was performed for each CpG site which has at least five reads coverage, and promoter, gene body, and CpG island annotations were added for each CpG included in the comparison. For post-processing, CpG sites with methylation differentials greater than 80% (0.8) for any experimental group relative to UI were used. Data was further analyzed to identify site specific methylation events across groups and within CpG islands using the UCSC Genome Bioinformatics database (<https://genome.ucsc.edu/>).

Data Access (WT mice only)

The data reported in this publication have been deposited in NCBI's Gene Expression Omnibus (Trella *et al.*, 2016) and are accessible through GEO Series accession number GSE80396 (<http://www.ncbi.nlm.nih.gov/geo/query/acc.cgi?acc=GSE80396>).

Results

Histological Evaluation in WT and TS5KO mice

Hematoxylin and Eosin staining was used to evaluate the collagen matrix and cellular responses during CA and TM, subsequent to the two TGF- β 1 injections into the Achilles tendon body (Figure 4 and 5; histopathological alterations denoted by arrows for collagen disorganization and asterisk for hypercellularity). UI TS5KO mice exhibited collagen disorganization relative to UI mice which is indicative of the decreased mechanical properties seen in the Achilles tendon of these mice [43]. In the both genotypes, a 3d acute response (1 day after second injection) consisted of cell proliferation in the body of the tendon, the peritenon, and the stroma of the adjoining adipose tissue, as well as localized collagen disorganization of the tendon at the presumed injection sites (Figure 4b). In mice maintained with CA, hypercellularity, collagen disorganization, and chondroid deposits were still evident at 14dCA, (Figure 4c) but had largely dissipated by 28dCA (Figure 4d), with small areas of increased cellularity seen in only one of the three mice examined (Figure 4e). When TM was applied after the injury, this pathology was also evident at 14dTM (Figure 4f) , but had worsened by 28dTM, with large areas of collagen disruption extending throughout the tendon body, and chondroid and occasional calcified deposits (WT only) in between fiber bundles in the area surrounding the TGF- β 1 injection sites (Figure 4g, h). Minimal changes in pathology were seen in UI WT mice which underwent TM for 14 and 28 days (Figure 4i, j). TM in UI TS5KO mice allowed for the maintenance of collagen organization as compared to UI mice (Figure 4i,j).

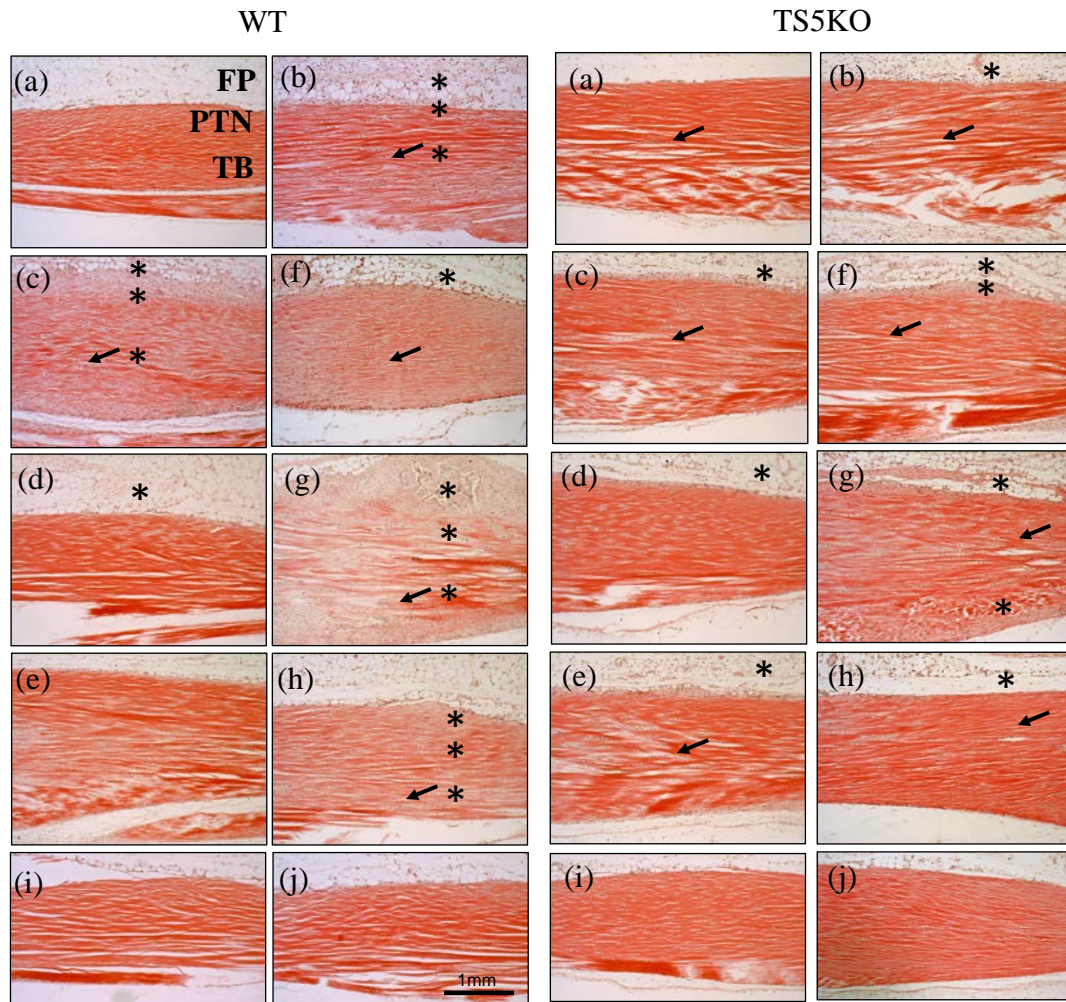


Figure 4: Hematoxylin and Eosin stained sections of WT and TS5KO Achilles tendons: (a) UI; (b) acute (3d) TGF- β 1 injury; (c) 14dCA; (d,e) 28dCA (f) 14dTM, (g,h) 28dTM. (i) UI 14dTM, (j) UI 28dTM. Fat Pad (FP), Peritenon (PTN), tendon body (TB). *hypercellularity, arrows denote collagen disorganization

Expression of chromatin-modifying enzymes in WT and TS5KO mice

The intra-tendinous injections of TGF- β 1 resulted in alterations in transcript abundance of genes involved in epigenetic modifications (Table 2). In the WT 3d acute group, 34 genes covering both histone and DNA modification enzymes showed significant ($p < 0.05$) increases in expression and three histone-modifying genes (*Kat2b*, *Hdac11*, and *Smyd1*) showed a significant decrease. Most notably, 8 genes were >4-fold up-regulated (*Dnmt1*, *Esco2*, *Prmt1*, *Suv39h1*,

Aurka, *Aurkb*, *Pak1*, and *Whsc1*) and *Hdac11* was >4-fold down-regulated suggesting additional biological significance. In the TS5KO 3d acute group only 15 genes were significantly increased, and 2 were significantly decreased relative to UI levels (Table 2). 7 out of the 15 genes (*Dnmt1*, *Esco2*, *Suv39h1*, *Aurka*, *Aurkb*, *Pak1*, and *Whsc1*) were >4-fold up-regulated. All genes were similarly altered in the WT 3d group; however *Aurkb* and *Esco2* were further up-regulated in TS5KO mice.

Table 2: Fold-changes in transcript abundance of chromatin-modifying enzymes at 3 days

Gene Group	Genes	WT	TS5KO
DHD	<i>Kdm1a</i>	2.00 (0.22)	3.01 (1.50)
DM	<i>Dnmt1</i>	5.24 (0.26)	4.49 (0.83)
	<i>Dnmt3b</i>	2.46 (0.56)	NS
HA	<i>Esco2</i>	26.51 (3.07)	70.78 (30.69)
	<i>Hat1</i>	3.31 (0.19)	2.26 (0.22)
	<i>Kat2a</i>	3.10 (0.42)	3.47 (1.36)
	<i>Ciita</i>	2.49 (0.25)	NS
	<i>Csrp2bp</i>	2.12 (0.23)	NS
	<i>Kat7</i>	1.74 (0.11)	NS
	<i>Kat2b</i>	0.57 (0.02)	0.44 (0.02)
HD	<i>Hdac1</i>	2.25 (0.14)	NS
	<i>Hdac2</i>	2.03 (0.18)	NS
	<i>Hdac3</i>	1.95 (0.12)	NS
	<i>Hdac6</i>	1.92 (0.16)	NS
	<i>Hdac11</i>	0.27 (0.02)	NS
HM	<i>Prmt1</i>	3.81 (0.45)	3.46 (1.18)
	<i>Suv39h1</i>	3.57 (0.40)	5.19 (2.61)
	<i>Prmt3</i>	2.90 (0.06)	2.96 (0.83)
	<i>Prmt5</i>	2.69 (0.17)	2.14 (0.22)
	<i>Carm1</i>	2.61 (0.34)	NS
	<i>Prmt6</i>	2.09 (0.30)	NS
	<i>Prmt7</i>	2.08 (0.25)	NS
	<i>Setdb2</i>	2.08 (0.24)	NS
HP	<i>Smyd1</i>	0.36 (0.09)	NS
	<i>Aurkb</i>	61.26 (2.30)	97.72 (41.79)
	<i>Aurka</i>	33.57 (1.17)	21.68 (8.50)
	<i>Pak1</i>	10.13 (0.84)	6.82 (1.55)
HU	<i>Nek6</i>	3.34 (0.29)	2.68 (0.57)
	<i>Dzip3</i>	2.63 (0.22)	NS
	<i>Usp16</i>	2.11 (0.28)	NS
	<i>Rnf20</i>	2.01 (0.10)	NS
	<i>Ube2a</i>	1.98 (0.17)	NS
	<i>Usp22</i>	1.82 (0.31)	NS
SET	<i>Ube2b</i>	NS	0.57 (0.03)
	<i>Whsc1</i>	5.03 (0.89)	5.77 (3.23)
	<i>Setd8</i>	2.52 (0.31)	1.99 (0.09)
	<i>Setd4</i>	1.80 (0.31)	NS
	<i>Setd1a</i>	1.60 (0.13)	NS
	<i>Setdb1</i>	NS	2.26 (0.63)

All expression changes shown are significant ($p < 0.05$) relative to genotype matched UI levels. Average (STD). NS = not significant. Bolded values are >3.5-fold. Groups: DHD (DNA/Histone Demethylases), DM (DNA Methyltransferases), HA (Histone Acetyltransferases), HD (Histone Deacetylases), HM (Histone Methyltransferases), HP (Histone Phosphorylation), HU (Histone Ubiquitination), SET (SET Domain Proteins; Histone Methyltransferase Activity).

When WT mice were maintained with CA, the altered transcript levels with the exception for *Aurkb* (3.70-fold) and *Kdm5c* (2.44-fold) were reversed to UI levels by 14dCA and remained stable by 28dCA. Similarly, when TS5KO mice were maintained with CA, all altered transcript levels reversed to UI levels at 14dCA except for *Kdm1a* (2.11-fold) and *Pak1* (1.90-fold). At 28dCA, *Kat2b* (0.70-fold), *Prmt7* (0.59-fold), and *Setd8* (0.48-fold) being significantly down-regulated in TS5KO mice. However, only *Aurkb* at 14dCA in WT mice was >4-fold differentially regulated suggesting biological significance.

In contrast, when WT injured mice were exposed to TM (Table 3), mRNA abundance for 6 of the TGF- β 1 injury activated genes (*Dnmt3b*, *Ciita*, *Aurka*, *Aurkb*, *Pak1*, and *Whsc1*) remained slightly elevated at 14dTM, and *Pak1* remained at 28dTM. Furthermore, transcript levels of two genes (*Dnmt3a*, *Setd5*) which were not altered by TGF- β 1 injection, showed significant increases at 14dTM. In addition, three genes (*Hat1*, *Setd6*, and *Setd8*) and two genes (*Atf2* and *Ehmt1*) were slightly decreased after 14dTM and 28dTM in WT mice, respectively. In TS5KO mice with TM, *Kdm1a*, *Hat1*, *Pak1*, and *Kat2b* remained regulated at 14dTM while all other activated genes at 3d normalized to UI levels (Table 3). *Ehmt2* and *Prmt7*, which were not affected at 3d, were significantly regulated with 14dTM, but only *Ehmt2* and *Pak1* were significantly altered at 28dTM. As with CA, only *Aurkb* in WT mice was >4-fold differentially regulated with TM

Very few epigenetic modification genes demonstrated a direct response to mechanical stimulation as seen by comparing age and genotype matched TM groups to CA groups. In WT mice, *Ube2b* (1.50-fold) and *Atf2* (0.53-fold) was significantly ($p < 0.05$) dependent on activity level at 14 days, and *Ehmt1* (0.56-fold) was dependent at 28 days, however none were >4-fold

differentially regulated in TS5KO mice, *Setd8* was differentially regulated at both 14dTM (1.80-fold) and 28dTM (1.88-fold) time-points relative to CA, although not >4-fold.

Table 3: Fold-changes in transcript abundance of chromatin-modifying enzymes with TM

Gene Group	Genes	WT		TS5KO	
		14dTM	28dTM	14dTM	28dTM
DHD	<i>Kdm5c</i>	2.68 (0.16)	NS	NS	NS
	<i>Kdm1a</i>	NS	NS	2.50 (0.19)	NS
DM	<i>Dnmt3a</i>	2.22 (0.34)	NS	NS	NS
	<i>Dnmt3b</i>	2.05 (0.09)	NS	NS	NS
HA	<i>Atf2</i>	NS	0.52 (0.09)	NS	NS
	<i>Ciita</i>	2.24 (0.35)	NS	NS	NS
	<i>Hat1</i>	0.47 (0.04)	NS	0.65 (0.04)	NS
	<i>Kat2b</i>	NS	NS	0.68 (0.07)	NS
HD	-	NS	NS	NS	NS
HM	<i>Ehmt1</i>	NS	0.57 (0.10)	NS	NS
	<i>Ehmt2</i>	NS	NS	2.64 (0.25)	2.70 (0.28)
	<i>Prmt7</i>	NS	NS	0.58 (0.16)	NS
HP	<i>Aurkb</i>	3.84 (0.55)	NS	NS	NS
	<i>Aurka</i>	2.91 (0.18)	NS	NS	NS
	<i>Pak1</i>	2.51 (0.09)	2.15 (0.35)	2.54 (0.80)	2.28 (0.32)
SET	<i>Setd5</i>	2.50 (0.35)	NS	NS	NS
	<i>Whsc1</i>	2.06 (0.18)	NS	NS	NS
	<i>Setd6</i>	0.66 (0.06)	NS	NS	NS
	<i>Setd8</i>	0.46 (0.04)	NS	NS	NS

All expression changes shown are significant ($p < 0.05$) relative to genotype matched UI levels. Average (STD). NS suggests that no significant changes in expression of genes in that group were detected. Bolded values are >3.5-fold. Groups: DHD (DNA/Histone Demethylases), DM (DNA Methyltransferases), HA (Histone Acetyltransferases), HD (Histone Deacetylases), HM (Histone Methyltransferases), HP (Histone Phosphorylation), HU (Histone Ubiquitination), SET (SET Domain Proteins; Histone Methyltransferase Activity)

Additionally, very few genes showed significant differences when directly comparing experimental matched WT and TS5KO mice (Table 4), suggesting the similarity between the injury responses in both strains of mice. Interestingly the significant genes are dependent on experimental time-point with 9 genes differentially regulated at 3d, 5 genes with CA, and 12

genes with TM. In most cases, the TS5KO mice experience a blunted response as compared to WT mice (Table 2 and Table 3), suggesting that the presence of TS5 may be contributing to the robust response seen in the WT mice, especially at the 3d time-point, and may also be involved in mechanical induced regulation with TM.

Table 4: Significantly altered expression of chromatin modifying enzymes in TS5KO mice with injury relative to WT

Gene Group	Genes	3d	14dCA	28dCA	14dTM	28dTM
DHD	<i>Kdm4a</i>	NS	NS	NS	0.76 (0.09)	NS
	<i>Kdm5c</i>	NS	NS	NS	0.67 (0.06)	NS
DM	<i>Dnmt1</i>	0.61 (0.11)	NS	NS	NS	NS
HA	<i>Atf2</i>	NS	1.07 (0.05)	NS	NS	NS
	<i>Kat2b</i>	0.79 (0.03)	NS	NS	NS	NS
	<i>Hat1</i>	0.61 (0.06)	NS	NS	1.24 (0.08)	NS
	<i>Ciita</i>	NS	NS	NS	0.60 (0.05)	NS
	<i>Esco2</i>	NS	NS	NS	NS	0.55 (0.42)
HD	<i>Hdac2</i>	0.59 (0.14)	NS	NS	NS	NS
	<i>Hdac9</i>	NS	1.45 (0.05)	NS	1.84 (0.06)	NS
	<i>Hdac6</i>	NS	NS	0.64 (0.12)	NS	NS
HM	<i>Prmt7</i>	0.62 (0.07)	NS	NS	NS	NS
	<i>Prmt5</i>	0.58 (0.06)	NS	NS	NS	1.12 (0.14)
	<i>Ehmt1</i>	NS	NS	NS	0.73 (0.05)	NS
HU	<i>Ube2a</i>	0.70 (0.10)	NS	NS	NS	NS
	<i>Usp21</i>	NS	NS	0.67 (0.12)	0.68 (0.15)	NS
	<i>Usp22</i>	NS	NS	NS	0.77 (0.08)	NS
SET	<i>Setd6</i>	0.74 (0.04)	NS	NS	NS	NS
	<i>Setd8</i>	0.68 (0.03)	NS	0.51 (0.04)	NS	NS
	<i>Setd5</i>	NS	NS	NS	0.73 (0.10)	NS
	<i>Setdb1</i>	NS	NS	NS	0.74 (0.01)	NS

Fold changes (Average (STD)) listed are significantly altered ($p < 0.05$) relative to experimentally matched WT mice, NS = not significant. Bolded values are >3.5 -fold. Groups: DHD (DNA/Histone Demethylases), DM (DNA Methyltransferases), HA (Histone Acetyltransferases), HD (Histone Deacetylases), HM (Histone Methyltransferases), HP (Histone Phosphorylation), HU (Histone Ubiquitination), SET (SET Domain Proteins; Histone Methyltransferase Activity)

Importantly, no biologically significant change (>4-fold) in expression of chromatin modification enzymes was observed in WT UI mice after 14dTM and 28dTM suggesting that there is minimal epigenetic regulation without the initiating TGF- β 1 injury in WT mice. In TS5KO, only *Kdm6b* was up-regulated (5.15-fold) at UI 28dTM without the initiating TGF- β 1 injury. Heat map representations for all groups can be seen in Appendix F and G for WT and TS5KO groups, respectively. Baseline expression levels of chromatin modification enzymes in UI mice can be seen in Appendix H.

Genome-wide alterations in the DNA Methylome in WT mice

Changes in mRNA transcript abundance for DNA methylases and DNA/Histone demethylases (Table 2, 3) indicated that changes in the DNA methylome were likely to occur at different stages of the tendinopathy model in WT mice. Therefore, a genome-wide DNA methylome analysis was conducted on tendons from each of the WT experimental groups (Table 1). Following the acute TGF- β 1 injury, 1058 individual CpG sites, with an additional 27 in CpG islands (CpG I), showed methylation differentials of > 80% (0.8) compared to UI levels. After 14 and 28 days, for both CA and TM, this was reduced to approximately 650 CpG sites with differential methylation (DM) (Table 5). Most importantly for the present study, 3-5% of the DM sites for each experimental group were within promoter gene regions and a variable proportion of these were in CpG islands (Table 5). Overall, hypo-methylation was the predominant response to TGF- β 1 induced injury, accounting for 74% (3d), 58% (14d), 57% (28d), 87% (14dTM), and 75% (28dTM) of all modified promoter CpG sites in these experimental groups.

Table 5: Methylation of CpG sites of DNA in murine tendon in response to TGF- β 1 in WT mice

Group	Genome-Wide		Non-Coding		Intron		Exon		Promoter	
	CpG I	Other	CpG I	Other	CpG I	Other	CpG I	Other	CpG I	Other
3d	27	1058	6	539	9	412	13	99	4	31
14dCA	9	622	0	347	4	232	5	29	0	26
28dCA	17	620	0	338	4	230	14	47	9	23
14dTM	19	693	1	357	2	280	15	45	4	26
28dTM	17	609	0	333	2	230	11	37	5	27

All sites exhibited greater than >80% DM compared to the same sites in UI

Genes with differential promoter methylation and effects on transcript abundance in WT mice

It has been proposed that the methylation status of CpGs within promoters is most likely to affect transcription if it is located within a CpG I, or if it is one of multiple DM non-island sites [61]. Table 6 lists the genes for each experimental group with CpG sites which fulfill these criteria, and their chromosomal location is provided in (Appendix I). All genes (except *Foxr1*) were present in only one experimental group showing that both the gene identified and its modified methylation status are dependent on the injury time-course and activity level in this murine tendinopathy model. In addition all sites (except for *Sfi1*) were found to be hypomethylated. In the 3d group, these sites were evenly distributed between CpG I and non-island locations, whereas of the 13 genes identified in the 14dTM, 28d, and 28dTM groups, 12 were associated with methylation changes in CpG island locations. Although there were DM genes at 3d no DM genes were identified in the 14dCA group.

Table 6: DM CpG sites in gene promoters of murine tendon in response to TGF- β 1 in WT mice

Group	CpG I		Non CpG I	
	Gene	Methylation status	Gene	Methylation Status
3d	<i>Baiap2l1</i> (1)	80% HYPO	<i>Cend1</i> (3)	90% HYPO
	<i>Foxr1</i> (1)	86% HYPO	<i>Gm19557</i> (2)	80% HYPO
	<i>Grm4</i> (1)	80% HYPO	<i>Mirlet7c-2</i> (2)	80% HYPO
	<i>Rbmxl2</i> (1)	80% HYPO		
14dCA	NONE	NONE	NONE	NONE
28dCA	<i>Gnas</i> (2)	91% HYPO	<i>Hoxc4</i> (3)	80% HYPO
	<i>Leprel2</i> (4)	100% HYPO		
	<i>Foxf1</i> (1)	80% HYPO		
	<i>Foxr1</i> (1)	83% HYPO		
	<i>Zrsr1</i> (1)	84% HYPO		
14dTM	<i>Igfbp6</i> (1)	80% HYPO	NONE	NONE
	<i>Mmp25</i> (1)	80% HYPO		
	<i>Sfi1</i> (1)	80% HYPER		
28dTM	<i>Cnot7</i> (2)	80% HYPO	NONE	NONE
	<i>Peg12</i> (1)	80% HYPO		
	<i>Shisa7</i> (1)	96% HYPO		
	<i>Usp9x</i> (1)	80% HYPO		

Number after gene in parenthesis denotes the number of effected sites within that gene promoter. Methylation status is relative to UI levels (average % methylation given for multiple sites)

To examine the potential effect of these methylation changes on transcription, the fold-changes in transcript levels were determined for each gene for the five experimental groups relative to UI levels (Table 7). *Foxr1*, *Grm4*, and *Shisa7* transcripts were below the level of detection at all time points, and *Gm19557* (gene without any known function) was not assayed. Due to large variations in expression levels between the pools for each experimental time-point (Appendix J), statistical significance was not achieved ($p > 0.05$). However, large fold changes were observed, and therefore an altered abundance of transcripts (>4 -fold) seen for *Cnot7*, *Usp9x*, *Peg12*, and *Cend1* should be considered as relevant to the pathology. This line of thinking follows guidelines recently released by the American Statistical Association [62] for evaluating the significance of the data in this paper. Due to the need for tissue pooling for mRNA

assays and the available number of mice for this study (Table 1) the n values for biological replicates was not sufficient for a robust statistical test.

Table 7: Fold changes in transcript abundance for genes with DM promoter regions in response to TGF- β 1 in WT mice

Gene	3d		14dCA		28dCA		14dTM		28dTM		
	RNA	DM	RNA	DM	RNA	DM	RNA	DM	RNA	DM	
CpG I (Multiple Sites)											
<i>Cnot7</i>	4.50 (2.28)	-	1.54 (0.88)	-	1.03 (0.15)	-	1.74 (1.00)	-	0.61 (0.56)		HYPO
<i>Gnas</i>	1.18 (0.63)	-	1.23 (0.51)	-	0.58 (0.12)	HYPO	1.36 (1.10)	-	0.93 (0.49)		-
<i>Leprel2</i>	1.90 (0.10)	-	2.41 (1.18)	-	0.98 (0.36)	HYPO	3.87 (2.47)	-	1.29 (0.65)		
CpG I											
<i>Usp9x</i>	4.39 (2.32)	-	2.45 (1.36)	-	0.61 (0.52)	-	3.76 (3.63)	-	1.22 (0.53)		HYPO
<i>Baiap211</i>	2.94 (0.60)	HYPO	1.59 (0.45)	-	1.01 (0.49)	-	1.99 (1.55)	-	1.48 (0.81)		-
<i>Peg12</i>	2.86 (1.23)	-	2.02 (1.55)	-	0.98 (0.35)	-	20.92 (23.1)	-	6.14 (10.2)		HYPO
<i>Mmp25</i>	2.43 (0.31)	-	3.59 (1.55)	-	0.62 (0.24)	-	3.79 (2.80)	HYPO	1.10 (0.35)		-
<i>Sfi1</i>	1.97 (0.37)	-	1.53 (1.13)	-	1.05 (0.39)	-	2.65 (1.46)	HYPER	1.66 (0.71)		-
<i>Foxf1</i>	1.65 (0.58)	-	1.81 (2.27)	-	0.87 (0.16)	HYPO	3.05 (2.12)	-	1.55 (0.65)		-
<i>Zrsr1</i>	0.60 (0.20)	-	1.13 (0.16)	-	0.99 (0.24)	HYPO	1.08 (0.47)	-	0.85 (0.45)		-
<i>Igfbp6</i>	0.43 (0.13)	-	1.55 (0.40)	-	0.71 (0.07)	-	1.35 (1.25)	HYPO	0.98 (0.31)		-
<i>Rbmxl2</i>	0.37 (0.13)	HYPO	0.95 (0.17)	-	1.06 (0.39)	-	1.00 (1.00)	-	0.89 (0.38)		
Non CpG I (Multiple Sites)											
<i>Cend1</i>	3.56 (0.90)	HYPO	1.85 (0.81)	-	0.65 (0.20)	-	2.69 (2.24)	-	1.29 (0.93)		-
<i>Hoxc4</i>	1.47 (0.60)	-	1.30 (0.58)	-	0.88 (0.28)	HYPO	1.72 (1.21)	-	1.22 (0.53)		-
<i>Mirlet7c</i>	0.49 (0.19)	HYPO	1.59 (1.37)	-	0.99 (0.43)	-	0.76 (0.43)	-	0.93 (0.55)		-

Average (Standard deviation) relative to UI levels. No values are significantly ($p < 0.05$) relative to UI. Bolded values are >3.5 -fold (rounded).

Despite such computational limitations, several potentially important biological response patterns between promoter methylation status and transcript abundance were evident (Table 7). For instance, hypo-methylation of the *Mmp25* promoter at 14dTM was accompanied by the predicted high transcript abundance (3.79-fold), relative to UI, and was higher than increased transcript levels at 3d and 28dTM at which time the gene promoter had normal methylation. Conversely, hyper-methylation of the *Sfi1* promoter at 14dTM was accompanied by slightly increased transcript abundance (2.65-fold). For *Igfbp6*, with promoter hypo-methylation at 14dTM there was no effect on transcripts. Hypo-methylation at 3d of *Cend1*, *Baiap211*, *Mirlet7c-2*, and *Rbmlx2* promoters was associated with borderline increased abundance of transcripts for *Cend1* (3.56-fold) and *Baiap211* (2.94-fold) and decreased abundance of *Mirlet7c-2* (0.49-fold) and *Rbmlx2* (0.37-fold) transcripts. Moreover, *Cend1* transcripts remained elevated in 14dTM groups (2.69-fold), despite normalization of the promoter methylation, and could be explained by long half-lives of this mRNA species. For *Leprel2*, *Hoxc4*, and *Foxf1* with promoter hypo-methylation in the 28dCA group, the transcript abundance was unaltered relative to the UI group, however, for these genes the late hypo-methylation may have resulted in increased transcription at >28d post-injury time points, which were not included in the current study. It should also be noted that the increased transcript abundance for *Leprel2* in the 3d and 14dCA groups (2.41-fold and 3.87-fold respectively), where promoter methylation was not changed relative to UI, suggests that expression of this gene is controlled by factors other than promoter methylation, such as histone modification or miRNAs. Lastly, for the three genes (*Usp9x*, *Cnot7*, and *Peg12*) showing hypo-methylation at 28dTM, the changes in transcript abundance was correlated with an increased expression in *Peg12* (6.14-fold), but not *Cnot7* or *Usp9x*.

Expression levels of genes identified by methylome analysis in TS5KO mice

Five of the genes identified by methylome analysis in WT mice had functions which suggest a strong relevance to tendinopathy (see discussion). When assayed in TS5KO mice (Table 8) significant differences were detected relative to UI TS5KO mice. Most notably, *Igfbp6* was >4-fold down-regulated at 3d and *Mmp25* was up-regulated throughout the injury time-course with cage activity. These mimic the trends seen in WT mice, but a much more robust response is observed. When directly comparing the expression in TS5KO mice to experimentally matched WT mice (Tables 7 and 8) it is evident that *Peg12* and *Igfbp6* are less expressed at 3d and 14dCA/28dTM, respectively. UI expression levels for all five genes can be seen in Appendix K.

Table 8: Fold changes in transcript abundance in TS5KO mice for tendinopathy related genes identified via methylome analysis

Genes	3d	14dCA	28dCA	14dTM	28dTM
<i>Foxf1</i>	2.48 (0.48)	1.70 (0.47)	0.53 (0.28)	1.45 (0.25)	0.91 (0.33)
<i>Igfbp6</i>	0.24 (0.02)*	0.54 (0.01)^	0.31 (0.16)*	0.43 (0.08)	0.54 (0.10)^
<i>Leprel2</i>	2.44 (0.45)	2.69 (0.09)	0.93 (0.47)	1.43 (0.39)	1.41 (1.08)
<i>Mmp25</i>	31.08 (16.62)*	11.07 (0.97)*	4.14 (0.55)	4.39 (2.74)	3.25 (2.56)
<i>Peg12</i>	1.55 (0.79)^	0.78 (0.03)	0.25 (0.20)	1.30 (0.90)	0.96 (0.49)

Values presented as fold changes (Average (STD)). *p<0.05 relative to UI levels. ^p<0.05 relative to experimentally matched WT mice. No genes identified as significant (p>0.05) in age-matched TM to CA groups. Bolded values are >3.5-fold.

Discussion

The primary objective of this aim was to use a murine Achilles tendinopathy model with acute, intermediate, and chronic phases to investigate whether tissue changes in the model (such as collagen disorganization, chondroid metaplasia, and loss of tensile properties), which are broadly characteristic of human tendinopathies, are accompanied by changes in the methylation

status of promoter regions of tendon DNA. Secondly, we aimed to determine whether promoter methylation status was predictive of changes in transcript abundance and whether the identity of the transcripts might provide novel insights into tendinopathic changes.

In summary, 19 genes displayed differential promoter methylation in a treatment-group specific manner in WT mice and, notably 18 of these genes involved hypo-methylation. Four (*Cnot7*, *Usp9x*, *Peg12*, and *Cend1*) of the identified genes also exhibited marked differences (>4-fold) in mRNA transcript abundance between the WT groups. To investigate whether DM of one or more of the 19 genes might impact tendon function we undertook a limited literature search using the murine gene function on PubMed and identified studies relating the gene to multipotent mesenchymal cells, fibroblasts, tendon, and/or extracellular matrix. In this way we identified five genes (*Leprel2*, *Foxf1*, *Mmp25*, *Igfbp6* and *Peg12*) which demonstrate strong relevance. Notably, three of the five exhibit functions closely related to collagen fiber organization. While not significant, >4-fold changes in expression are seen in WT mice during the injury time-course and most notably, significant and >4-fold changes are seen in expression of those genes in TS5KO mice. These findings give merit to the methylome analysis which was not conducted in TS5KO mice, but the discovery of novel genes using WT mice is clearly relevant to the TS5KO injury pathology

Firstly, *Leprel2* has the potential to profoundly affect collagen matrix organization in the tendon as it has a critically important and tissue-specific role in the unique assembly and packing of tendon type I collagen fibrils [63, 64]. Thus, modulation of *Leprel2* expression in the tendon could readily explain the fiber disorganization which is a hallmark of tendon pathologies, including tendinopathy. Secondly, *Foxf1* induces integrin $\beta 3$ expression, with high specificity in mouse embryonic fibroblasts [65]. This finding appears to be important since this integrin was

identified through the BORG database of genomic and biomedical knowledge as one of four strong candidate risk genes for human tendinopathy (which included *COL11A2*, *ELN*, *ITGB3*, and *LOX*) [66]. Thirdly, proteomic analysis of pericellular proteins in developing tendons has shown that *Mmp25* (like *Leprel2* and *Foxf1*) is likely involved in collagen fibril and matrix assembly [67], which is relevant to the robust (>30-fold) expression in the 3d TS5KO group. Fourthly, a significance for *Igfbp6* modulation in this model is suggested by its reported capacity to regulate cell proliferation in connective tissue disorders [68], and also by its sensitivity to hypoxia [69], which has often been implicated in tendinopathic change [59]. Lastly, the dramatic increase in *Peg12* expression in the WT 14dTM group might be related to its capacity to bind Gsk3 [70] and potentially reduce production of inflammatory cytokines in macrophage-type cells in response to Toll-like receptors [71]. Additionally, significant baseline differences between WT and TS5KO UI mice (Appendix K) suggest the importance of *Peg12* in normal tendon maintenance. Furthermore, in this regard it is interesting that analysis of the array data for chromatin-modifying enzymes shows that six of the genes most affected overall in WT and/or TS5KO mice with injury (*Dnmt3b*, *Ciita*, *Aurka*, *Pak1*, *Hat1*, *Atf2*) have been implicated in the control of macrophage polarization in innate inflammation. While the role of inflammation in tendon injury is still heavily debated [72], recent evidence suggests that early macrophage involvement in ligament wound healing is necessary for maintenance of repair responses including angiogenesis, cell differentiation, and collagen production [73].

It should be noted that there was no clear relationship between methylation status and transcript abundance in WT tendon for many of the genes identified by this study. In this regard, recent reviews [74, 75] have underlined the complexity of the causes and effects of cytosine methylation on downstream transcription, so that the earlier supposition [76] that hypo-

methylation necessarily results in high transcription (and vice-versa) is, while possible in a context-dependent fashion, an over-simplification of the multiple possible effects of DM levels. In addition, changes in transcript levels may partly or entirely result from other methods of regulation (e.g. enhancer methylation, transcription factor binding, and miRNA levels) which could contribute to the complexities of transcript abundance reported here. In addition, cell populations from surrounding tissue (fat pad, synovial tissue, peritenon) may be present in the samples at varying levels and potential contribute to the variability exhibited. In summary, despite these caveats, we postulate that a study of the molecular genomics of *Leprel2*, *Foxf1*, *Mmp25*, *Igfbp6* and *Peg12* in animal and human tendon could further delineate the pathogenesis of this multifactorial disease.

Chapter 3 – Specific Aim 2

Introduction

Tendon is a sparsely vascularized tissue, with a few blood vessels present at the musculotendinous and osseotendinous junctions, the peritenon, and adjacent adipose tissues [77]. Thus, nutrient diffusion and gas exchange into the main body of the Achilles tendon occurs via the peritenon and adjacent synovial bursa [77]. Studies with tendon derived stem cells have suggested that 2-4% atmospheric oxygen is typical for healthy tendon *in-vivo* [78, 79], which is substantially lower than skeletal muscles (7.5x) [80], but similar to that of cartilaginous tissues.

Regulation of oxygen levels for normal wound healing is vital, as oxygen is required for cellular metabolism and energy production, which in turn regulates cell proliferation, collagen synthesis, angiogenesis, and growth factor signal transduction. Furthermore, since packing of collagen fibers through formation of intra- and inter-chain cross linking is essential for the biomechanical function of tendon tissues, enzymes which modify pro-collagens (proyl-hydroxylase, lysyl-hydroxylase, and lysyl-oxidase) require oxygen [81-84]. In this regard, our novel finding (Aim 1, Chapter 2) that *Leprel2*, a proyl hydroxylase, is up-regulated in response to tendon injury is noteworthy, as proyl hydroxylation is the rate limiting step of collagen synthesis [83, 84].

Histopathological examination of human tissues from end-stage tendinopathies reported hypoxic and mucoid degeneration as the two central pathological changes associated with spontaneous rupture of human Achilles, lone head of the biceps, and quadriceps tendons [29]. The hypoxic degeneration of tenocytes was characterized as changes in shape of the mitochondria and nuclei, cytoplasmic and mitochondrial calcification, and necrosis. Additionally, these cells were localized within an abnormal collagen matrix with varied fibril

orientations and diameters. Therefore, it has also been hypothesized that hypoxia following tendon injuries can lead to the development of chronic tendinopathy and subsequent rupture in tendons [29, 32, 77].

Whereas the molecular basis of mucoid degeneration in human and animal models of tendinopathy has been studied by our group and others [29-31, 33, 34, 39, 44], less is known about cellular pathways leading to hypoxic degeneration. It is well established that in response to injury, resident tissue cells have a protective response to changes in oxygen levels via activation of *hypoxia inducible factor1a (Hif1a)* controlled pathways, which include angiogenesis, metabolism, and cell fate [85]. Indeed, high expression of *Hif1a* in torn human rotator cuff tendon tissues was correlated with apoptosis [86] and hypo-vascularity was identified at sites where tendon ruptures are known to occur [87]. Furthermore, *in-vitro* experiments with cells isolated from torn human hamstring tendon tissue showed that exposure of such cells to hypoxia (1% O₂) resulted in increased expression of *Hif1a* and *collagen Type III* [59].

While involvement of hypoxia-induced changes has been identified in human tendon tissue and tendon-derived cell cultures, the timing of such cellular responses during the pathogenesis of tendinopathy *in-vivo* remains to be determined. In addition, the potential mechanistic link between hypoxic responses, accumulation of mucoid and chondroid deposits and collagen fibrillar disorganization, has not been studied. The goal of the current aim, therefore, was to characterize hypoxia signaling pathways in a murine model of Achilles tendinopathy utilizing both WT and TS5KO mice, as it relates to the development of chondroid metaplasia and progression of tendinopathy. The inclusion of the TS5KO mouse strain, where persistent chondroid deposition occurs [44] allowed for the determination if the aggrecan

deposition was primarily attributable to the lack of degradation by the ADAMTS5 protease or if it was linked to the metabolic defect recently described in this mouse [47].

Methods

Murine model of Chronic Tendinopathy in WT and TS5KO C57/Bl6 Mice:

All animal use was approved by the IACUC of Rush University and experimental groups, outcome measures, and mouse numbers are summarized in Table 9. Overall animal health and food intake was tracked by daily observation of activity levels, water consumption and determination of body weight (Appendix C).

Table 9: Experimental groups and outcomes for Aim 2

Group	Abbreviation	Outcome Measures			
		Histology ¹		qt-PCR ²	
		WT	TS5KO	WT	TS5KO
Un-Injured	UI	N=4	N=4	N=3 (12,20,22)	N=3 (20,18,20)
3 days	3d	N=4	N=2	N=3 (12 each)	N=3 (13,10,10)
14 days	14dCA	N=2	N=3	N=3 (20,20,21)	N=3 (20,18,21)*
28 days	28dCA	N=3	N=4	N=3 (18,16,18)	N=3 (18,15,15)
14 days + TM	14dTM	N=3	N=3	N=3 (16 each)	N=1 (16,11,11)
28 days + TM	28dTM	N=3	N=3	N=3 (16 each)	N=1 (20,15,16)
Un-Injured 14 days + TM	UI 14dTM	N=3	N=3	N=1 (15)	N=1 (20)
Un-Injured 28 days + TM	UI 28dTM	N=3	N=3	N=1 (17)	N=1 (20)

1 - Individual legs

2 - Tissue pools with number of tendons per pool in parenthesis

* 3rd pool removed from post-analysis due to outlier (Δ Ct values for all genes approximately 1.5 STDs below the average). Abundance values can be seen in Appendix L

Histology and Immunohistochemistry

The methods were conducted as described previously [39]. Briefly, the leg was dissection of all skin and placed into formalin for at least 1 day and followed by decalcification in EDTA for 2 weeks. The specimens were processed, embedded in paraffin, and 5 μ m thin sections were

cut through the entire joint. Routinely 3-6 sections from the midpoint of the joint were stained with SafraninO, imaged and scored for severity of tendinopathy (e.g. chondroid deposits).

For immunohistochemistry, sections were deparaffinized, and incubated overnight at 4°C with antibodies to aggrecan core protein (*anti-DLS*, rabbit anti-peptide [37]) and HIF1a (*ab114977*, rabbit polyclonal from Abcam). For HIF1A and anti-DLS, the secondary antibody was biotinylated anti-rabbit IgG. Hyaluronan (HA) was localized using a biotinylated HA Binding Protein (*bhrTSG6*, under MTA from Halozyme), and terminal alpha- galactose residues which has been widely used to identify endothelium of newly forming blood vessels [88] was identified via biotinylated *Griffonia (Bandeiraea) Simplicifolia* Lectin I (*B-1105LECTIN-1*, from Vector Labs). All sections were counterstained with methyl green

Gene Expression Assays via qt-PCR

Following euthanasia, freshly harvested Achilles tendons were immediately isolated from all surrounding tissue with the peritenon left intact. RNA was isolated from three separate pools of 12-20 combined Achilles tendons from each experimental group (Table 9). Briefly, tendon pools were fragmented by hammer impact at -196°C in a Bessman Tissue Pulverizer, recovered, and extracted in 1 mL of Trizol by vortexing for 60 seconds. RNA was purified with an RNeasy MiniKit (Qiagen, Cat #: 74104) and yields were approximately 305ng/tendon for UI, 805ng/tendon for 3d, 1800ng/tendon and 800ng/tendon for 14 and 28 days post-injury, respectively. RNA quality was established from A260:280 of at least 1.90. cDNA was synthesized with 0.5ug of mRNA (RT² First Strand Kit, Qiagen) and hypoxia signaling transcript abundances were determined with SYBR qt-PCR array plates (PAMM-032ZA, Qiagen), as described by the manufacturer. The array was made up 84 genes separated into the following functional groups: Hif1a signal transduction (n=25), Angiogenesis and Coagulation (n=16), Cell

Fate Determination (n =19), and Metabolism and Transport (n=24). While each qt-PCR array was conducted singularly for each sample, three individual replicate array assays of a typical sample (WT 3d Pool #3) showed a coefficient of variation of less than 5% between each of the triplicates.

Changes in transcript abundance ($\Delta Ct = Ct$ for transcript of interest minus Ct for the housekeeping gene *B2m*) were used to calculate the fold change ($2^{-\Delta\Delta Ct}$) from UI levels for each experimental group. The genes *Epo* and *Hnf4a* were removed from down analysis as transcripts were undetected by qt-PCR in all groups. A 1-way ANOVA with Tukey's post-hoc test was conducted using GraphPad Prism 5 (La Jolla, CA) on the ΔCt values to determine the significance ($p < 0.05$) in expression of genes in the injured relative to UI groups for each genotype. For genotypic comparisons a student's t-test was used to compare TS5KO and WT values for each experimental group. For additional interpretation we have marked genes in **BOLD** that are also >3.5 -fold differentially regulated suggesting biological significance and genes marked with an * which were >3.5 -fold but not statistically significant. No statistical evaluation was performed on the un-injured plus treadmill running condition since only one pool of tendons was used per group. Instead, a >3.5 -fold change in expression relative to UI was considered "biologically significant".

Results

Hif1a expression and localization in WT and TS5KO mice

Following TGF- β 1 induced injury, *Hif1a* expression increased significantly at 3d and returned to uninjured levels by 14dCA (Figure 5). This response was similar in both WT and

TS5KO mice; however, in WT mice exposed to TM running, *Hif1a* gene expression remained high at 14dTM and returned to uninjured levels at 28dTM.

In WT mice, the maximally activated gene expression of *Hif1a* at 3d was not accompanied by increases in protein levels (Figure 6b) Cell associated HIF1a immunoreactivity was clearly visible by 14d with both CA and TM activity levels (Figure 6c,e) and then returned to pre-injury levels by 28d CA or TM (Figure 6d,f). In TS5 KO mice, there was also no clear correlation between increased *Hif1a* gene expression and HIF1A immunoreactivity at 3d (Figure 6h) but increased cellular staining observed at the 14d time points in both CA and TM activity (Figure 6i,k). However, whereas HIF1A immunoreactivity in WT mice returned to essentially UI levels by 28d CA and TM, cellular staining remained high in the TS5KO mice, under both conditions (Figure 6j,l).

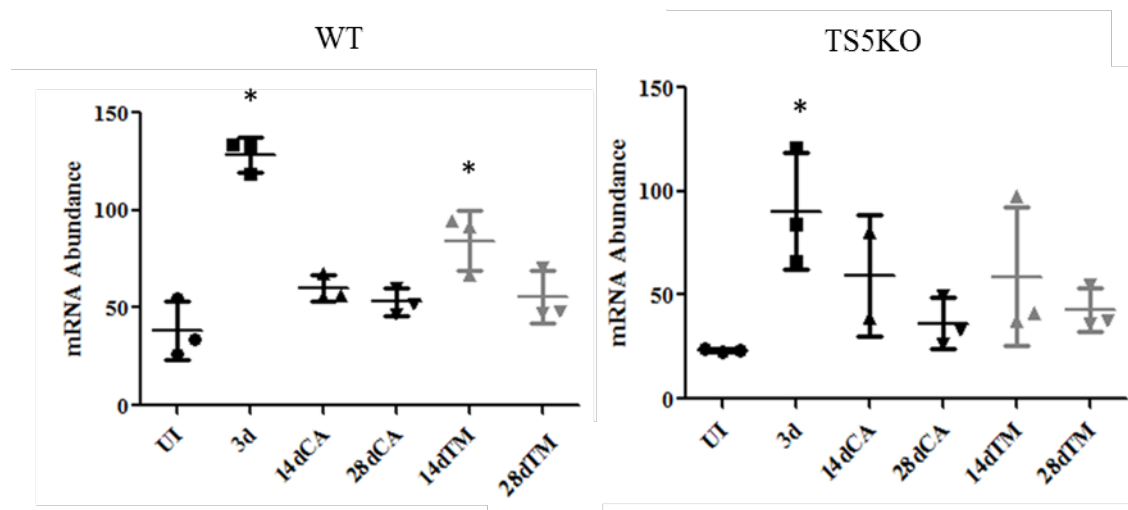


Figure 5: Hif1a expression of A) WT and B) TS5KO Achilles tendons (* $p < 0.05$ relative to genotype specific naïve; NS differences detected between genotypes).

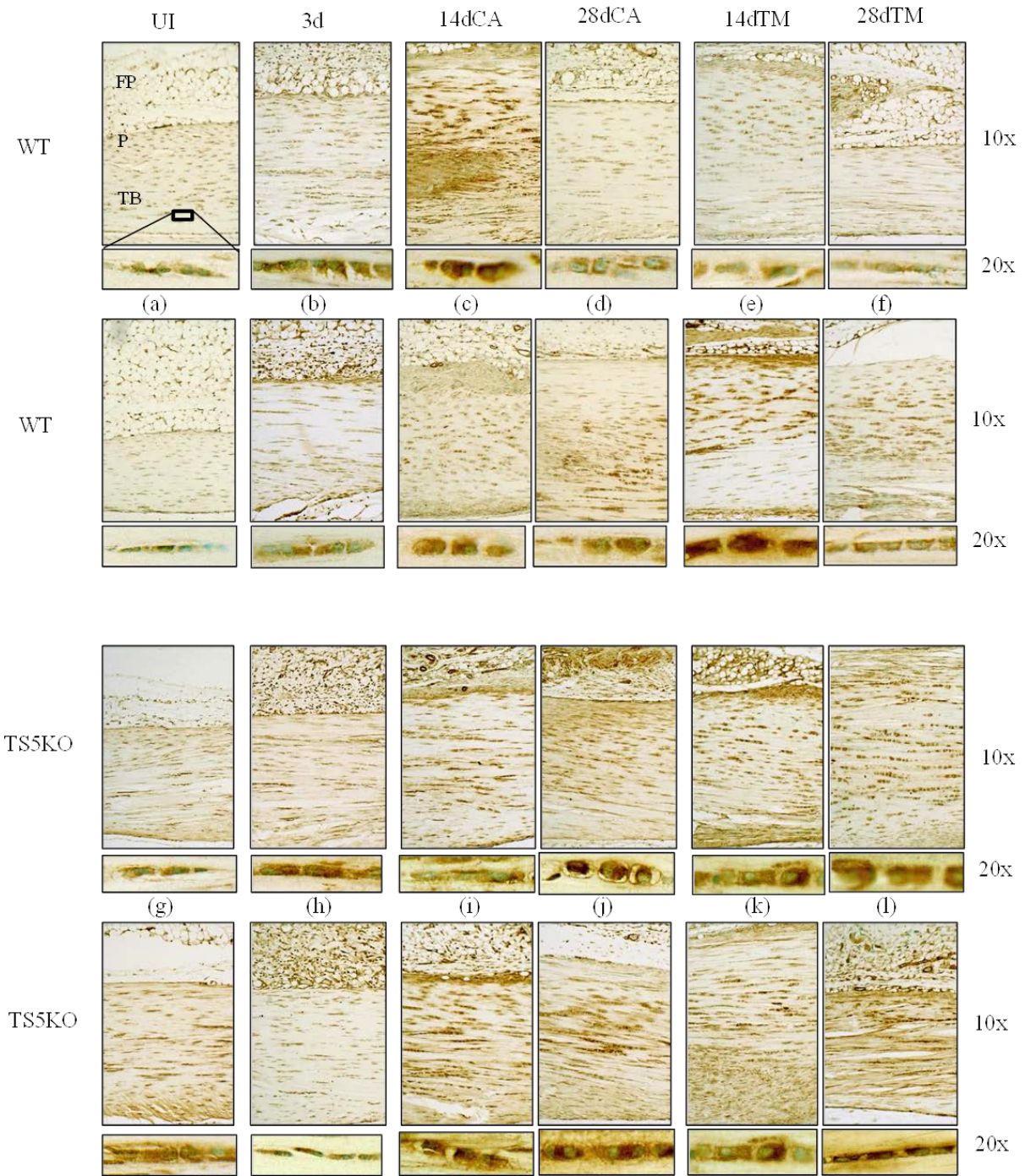


Figure 6: HIF1A stained sections of WT and TS5KO Achilles tendons

Expression of hypoxia signaling genes in WT and TS5KO mice

To examine the downstream activation of hypoxia related responses further, the expression levels of 84 genes identified as being regulated in response to this cellular stressor were determined in UI and post-injury tendons. Patterns of modification for these group during the initiation and progression of the tendinopathy in both strains of mice is provided as heat maps in Appendix M and N with expression levels in UI tendons from WT and TS5KO mice seen in Appendix O.

In WT mice following the injury at 3d, significant ($p < 0.05$) alterations in the expression of 43 genes were observed, with 40 genes up-regulated and only 3 down-regulated relative to UI levels (Table 10). When genes were further selected for a >3.5 -fold biologically significant change, 7 *Hif1a* signaling, 8 angiogenesis/coagulation, 6 cell fate, and 8 metabolism/transport genes were found to exhibit this robust response. By comparison, in TS5KO mice, the initial injury caused only minimal modulation in expression of genes in the *Hif1a* signaling pathway and also fewer genes in the metabolism/transport pathways were affected. However, modulation of expression of genes in angiogenesis/coagulation and cell fate groups were similarly affected in injured tendons of WT and KO mice.

Table 10: Fold-changes in transcript abundance of hypoxia signaling genes at 3d

Group	Gene	WT	TS5KO	Group	Gene	WT	TS5KO
Hif1a Signaling	<i>P4hb</i>	5.29 (0.34)	3.39 (0.63)	Metabolism Transport	<i>Pkm</i>	12.7 (0.33)	7.37 (2.21)*
	<i>Bhlhe40</i>	4.54 (1.14)	NS		<i>Pgam1</i>	11.8 (0.38)	5.55 (1.05)*
	<i>P4ha1</i>	3.66 (0.17)	NS		<i>Eno1</i>	11.0 (1.00)	6.44 (1.33)
	<i>Apex1</i>	3.65 (0.39)	3.01 (0.80)		<i>Slc2a1</i>	7.62 (0.40)	3.74 (0.46)
	<i>Trp53</i>	3.61 (0.24)	NS		<i>Slc16a3</i>	7.62 (0.75)	NS
	<i>Cops5</i>	2.15 (0.12)	NS		<i>Pgk1</i>	4.76 (0.15)	NS
	<i>Usf2</i>	2.10 (0.14)	NS		<i>Car9</i>	4.45 (0.71)	NS
	<i>Nfkb1</i>	2.09 (0.07)	NS		<i>Pfkl</i>	3.80 (0.04)	2.23 (0.32)
	<i>Eif4ebp1</i>	1.77 (0.16)	1.78 (0.32)		<i>Ero1l</i>	2.79 (0.03)	2.37 (0.26)
	<i>Hif3a</i>	0.14 (0.03)	NS		<i>Pdk1</i>	2.45 (0.22)	NS
	<i>Ctsa</i>	NS	2.64 (0.88)		<i>Ldha</i>	2.29 (0.12)	NS
	Angiogenesis Coagulation	<i>Serpine1</i>	173 (20.70)		30.21 (7.61)	<i>Gpi1</i>	2.17 (0.17)
<i>F10</i>		23.90 (6.68)	54.35 (6.10)	<i>Pfkl</i>	1.84 (0.15)	1.02 (0.22)	
<i>Hmox1</i>		15.50 (4.57)	21.21 (2.39)	<i>Gbe1</i>	0.61 (0.07)	0.45 (0.13)	
<i>Lox</i>		11.50 (0.99)	4.90 (1.74)	<i>Tpil</i>	NS	0.86 (0.20)	
<i>Plau</i>		5.10 (1.19)	3.27 (0.61)	<i>Vdac1</i>	NS	0.49 (0.07)	
<i>Angptl4</i>		4.94 (0.32)	5.39 (1.76)	<i>Aldoa</i>	NS	0.47 (0.09)	
<i>Mmp9</i>		4.84 (1.30)*	18.43 (2.74)*				
<i>Adora2b</i>		4.28 (0.75)	9.39 (1.07)				
<i>Anxa2</i>		3.78 (0.31)	2.74 (0.73)				
<i>Jmjd6</i>		3.07 (0.02)	1.98 (0.26)				
<i>Vegfa</i>		2.56 (0.26)	NS				
<i>F3</i>		1.72 (0.18)	0.41 (0.08)				
<i>Bnip3</i>		NS	0.37 (0.07)				
Cell Fate		<i>Ier3</i>	6.97 (1.94)	3.93 (0.49)			
	<i>Mif</i>	6.80 (1.13)	3.93 (0.33)				
	<i>Blm</i>	4.69 (0.43)	4.35 (2.07)				
	<i>Odc1</i>	4.23 (0.13)	NS				
	<i>Ruvbl2</i>	4.07 (0.23)	2.41 (0.56)				
	<i>Nampt</i>	0.58 (0.04)	0.55 (0.11)				
	<i>Txnip</i>	0.25 (0.01)	0.26 (0.11)				
	<i>Pim1</i>	NS	1.50 (0.46)				
	<i>Ndrgl</i>	NS	0.46 (0.19)				

Fold changes (Average (STD)) listed are significantly altered ($p < 0.05$) relative to genotype matched UI mice, NS = not significant. Bolded values are >3.5-fold (rounded). *values are NS, but reached >3.5-fold.

When WT and TS5KO mice were underwent CA or TM activity for 14 days and 28 day post injury, (Tables 11 and 12, respectively) the majority of hypoxia pathway genes returned to either UI levels, or to values less than the biologically significant cutoff (<3.5 fold). However, in both genotypes, the expression of the angiogenesis/coagulation pathway genes *Mmp9* and *F10* remained highly up-regulated at both time points. *Serpine1* expression remained high in WT tendons only (14d and 28d, CA and TM) and *Adora2b* was activated at 14dTM and 28dTM in TS5KO tendons. When examining the data based on statistically significant modified expression levels ($p < 0.05$ relative to UI tissue), it was noted that a group of genes in cell metabolism pathways, *Gbe1*, *Vdac1*, and *Aldoa*, were down-regulated at 14dCA in both genotypes and *Tpi1*, *Hk2*, *Gys1*, *Pfkfb3*, and *Tfrc* were additional regulated in the WT only.

Statistically significant ($p < 0.05$) differences were also observed between genotypes at each time-point (Table 13). TS5KO mice exhibited an overall reduction in the expression of hypoxia signaling genes. Throughout the injury time-course 61/82 genes involved in hypoxia signaling are significantly ($p < 0.05$) down-regulated in TS5KO relative to WT mice. The genes span all signaling groups including angiogenesis/coagulation, cell fate determination, and metabolism/transport, but most are differentially regulated at 3d with 10 genes >3.5-fold down-regulated. During the longer time-points with CA and TM, there are only minor differences detected between the two genotypes.

Notably, only a few genes were significantly different between TM and CA genotype matched groups. For TS5KO mice, at 14dCA *Aldoa* (0.47-fold) and at 28dCA *Aldoa* (2.04-fold), *Blm* (2.37-fold), *Ddit4* (3.34-fold), *Ldha* (2.05-fold), *Per1* (2.04-fold), and *Usf2* (3.86-fold) were altered. In WT tendons *Map3k1* was the only differentially regulated gene, (1.68-fold) gene between 14 CA and TM groups.

Table 11: Fold-changes in transcript abundance of hypoxia signaling genes with CA

Group	Gene	WT		TS5KO	
		14dCA	28dCA	14dCA	28dCA
Hif1a Signaling	<i>Map3k1</i>	0.62 (0.09)	NS	NS	NS
	<i>Hif3a</i>	0.29 (0.04)	NS	NS	NS
	<i>Nfkb1</i>	NS	1.52 (1.10)	NS	NS
Angiogenesis Coagulation	<i>Mmp9</i>	9.01 (8.79)*	6.98 (4.82)*	6.19 (8.05)*	15.90 (11.37)*
	<i>F10</i>	5.51 (3.30)	4.92 (3.17)	5.05 (2.75)	5.47 (1.47)
	<i>Serpine1</i>	4.00 (1.19)	2.61 (0.81)	NS	NS
	<i>Hmox1</i>	3.31 (0.83)	NS	NS	NS
	<i>F3</i>	0.48 (0.11)	NS	0.36 (0.25)	NS
	<i>Bnip3</i>	0.40 (0.08)	NS	NS	NS
	<i>Vegfa</i>	0.37 (0.08)	NS	NS	NS
Cell Fate	<i>Nampt</i>	0.57 (0.11)	NS	NS	NS
	<i>Txnip</i>	0.54 (0.08)	NS	NS	NS
	<i>Igfbp3</i>	NS	NS	2.57 (0.94)	NS
	<i>Nos3</i>	NS	NS	NS	1.30 (0.89)
Metabolism Transport	<i>Pgam1</i>	1.81 (0.23)	NS	NS	NS
	<i>Tpi1</i>	0.55 (0.14)	NS	NS	NS
	<i>Gbe1</i>	0.50 (0.09)	NS	0.32 (0.19)	NS
	<i>Gys1</i>	0.43 (0.18)	NS	NS	NS
	<i>Vdac1</i>	0.42 (0.12)	NS	0.33 (0.20)	0.55 (0.10)
	<i>Aldoa</i>	0.42 (0.21)	NS	0.40 (0.02)	NS
	<i>Hk2</i>	0.40 (0.11)	NS	NS	NS
	<i>Pfkfb3</i>	0.37 (0.09)	NS	NS	NS
	<i>Tfrc</i>	0.34 (0.09)	NS	NS	NS

Fold changes (Average (STD)) listed are significantly altered (p<0.05) relative to genotype matched UI mice, NS = not significant. Bolded values are >3.5-fold (rounded). *values are NS, but reached >3.5-fold.

Table 12: Fold-changes in transcript abundance of hypoxia signaling genes with TM

Gene Group	Genes	WT		TS5KO	
		14dTM	28dTM	14dTM	28dTM
Hif1a Signaling	<i>Hif1a</i>	2.30 (0.42)	NS	NS	NS
	<i>P4hb</i>	1.80 (0.10)	NS	NS	NS
	<i>Nfkb1</i>	1.63 (0.17)	1.55 (0.39)	NS	NS
	<i>Ctsa</i>	NS	NS	2.54 (0.29)	2.67 (0.62)
	<i>Per1</i>	NS	NS	2.34 (0.37)	2.53 (0.60)
	<i>Map3k1</i>	NS	NS	NS	2.35 (0.56)
	<i>Arnt</i>	NS	NS	NS	2.30 (0.58)
	Angiogenesis Coagulation	<i>Mmp9</i>	14.11 (13.19)*	31.58 (44.60)*	4.97 (4.59)*
<i>F10</i>		8.06 (1.63)	5.33 (3.83)	12.84 (3.68)	4.85 (1.11)
<i>Hmox1</i>		4.60 (0.32)	NS	NS	NS
<i>Serpine1</i>		4.42 (0.73)	3.38 (1.93)	NS	NS
<i>Vegfa</i>		0.56 (0.00)	NS	NS	NS
<i>Bnip3</i>		0.43 (0.05)	NS	NS	NS
<i>F3</i>		0.39 (0.09)	NS	NS	NS
<i>Adora2b</i>		NS	NS	4.63 (1.38)	3.95 (0.96)
<i>Pgf</i>		NS	NS	2.07 (0.13)	NS
Cell Fate	<i>Igfbp3</i>	2.19 (0.22)	NS	2.46 (0.29)	1.77 (0.32)
	<i>Nampt</i>	0.54 (0.06)	NS	NS	NS
	<i>Mif</i>	NS	1.64 (0.35)	NS	NS
	<i>Ccng2</i>	NS	NS	NS	2.15 (0.41)
	<i>Ddit4</i>	NS	NS	1.60 (0.25)	2.20 (0.45)
	<i>Ndrgr1</i>	NS	NS	NS	1.69 (0.42)
	Metabolism Transport	<i>Pkm</i>	2.45 (0.44)	NS	NS
<i>Eno1</i>		2.20 (0.33)	2.11 (0.64)	2.32 (0.39)	2.41 (0.43)
<i>Pgam1</i>		2.15 (0.30)	1.85 (0.54)	NS	NS
<i>Tpi1</i>		0.60 (0.07)	NS	NS	NS
<i>Vdac1</i>		0.50 (0.04)	NS	0.55 (0.08)	NS
<i>Gbel</i>		0.50 (0.07)	NS	NS	NS
<i>Tfrc</i>		0.48 (0.05)	NS	NS	NS
<i>Gys1</i>		0.40 (0.02)	NS	NS	NS
<i>Slc2a1</i>		NS	NS	1.90 (0.10)	2.19 (0.44)
<i>Pfkip</i>		NS	NS	1.08 (0.18)	1.25 (0.30)

Fold changes (Average (STD)) listed are significantly altered ($p < 0.05$) relative to genotype matched UI mice, NS = not significant. Bolded values are >3.5-fold (rounded). *values are NS, but reached >3.5-fold.

Table 13: Significantly altered expression of hypoxia signaling genes in TS5KO mice with injury relative to WT

Group	Gene	3d	14d	28d	14dTM	28dTM
Hif1a Signaling	<i>Nfkb1</i>	0.67 (0.13)	NS	NS	0.74 (0.05)	NS
	<i>Cops5</i>	0.67 (0.13)	NS	NS	NS	NS
	<i>Ankrd37</i>	0.64 (0.08)	NS	0.61 (0.10)	NS	NS
	<i>Trp53</i>	0.58 (0.13)	NS	NS	NS	NS
	<i>Per1</i>	0.57 (0.11)	NS	0.40 (0.13)	NS	NS
	<i>P4hb</i>	0.57 (0.11)	NS	0.64 (0.16)	NS	NS
	<i>Usf2</i>	0.56 (0.16)	NS	NS	NS	NS
	<i>Hif1an</i>	0.53 (0.14)	NS	NS	NS	NS
	<i>Egln1</i>	0.51 (0.18)	NS	NS	1.11 (0.08)	NS
	<i>Dnajc5</i>	0.47 (0.15)	NS	NS	NS	NS
	<i>Rbpj</i>	0.45 (0.22)	NS	0.56 (0.17)	NS	NS
	<i>P4hal</i>	0.29 (0.07)	NS	NS	0.68 (0.08)	NS
	<i>Bhlhe40</i>	0.25 (0.06)	NS	0.40 (0.17)	NS	NS
	<i>Ncoal</i>	NS	0.67 (0.08)	NS	NS	NS
	<i>Ctsa</i>	NS	0.61 (0.14)	NS	NS	NS
	<i>Eif4ebp1</i>	NS	NS	0.81 (0.03)	NS	NS
	<i>Lgals3</i>	NS	NS	0.69 (0.09)	NS	NS
	<i>Fos</i>	NS	NS	0.21 (0.08)	NS	0.52 (0.13)
	Angiogenesis Coagulation	<i>Mmp9</i>	2.16 (0.32)	NS	NS	NS
<i>Plau</i>		0.58 (0.11)	NS	NS	0.69 (0.07)	NS
<i>Jmjd6</i>		0.58 (0.08)	NS	NS	NS	NS
<i>Adora2b</i>		0.54 (0.06)	0.41 (0.18)	NS	NS	NS
<i>Anxa2</i>		0.45 (0.12)	NS	NS	NS	NS
<i>Bnip3</i>		0.41 (0.08)	NS	NS	NS	NS
<i>Lox</i>		0.34 (0.12)	NS	NS	NS	NS
<i>Vegfa</i>		0.24 (0.06)	NS	NS	1.39 (0.22)	NS
<i>F3</i>		0.18 (0.04)	NS	NS	NS	NS
<i>Serpine1</i>		0.16 (0.04)	NS	NS	NS	NS
<i>Bnip3l</i>		NS	NS	0.72 (0.11)	NS	NS
<i>Pgf</i>		NS	NS	NS	0.75 (0.18)	NS
<i>Edn1</i>		NS	NS	NS	NS	1.80 (0.30)
Cell Fate	<i>Btg1</i>	0.68 (0.15)	NS	NS	NS	NS
	<i>Mif</i>	0.66 (0.06)	NS	NS	NS	NS
	<i>Igfbp3</i>	0.63 (0.10)	NS	NS	NS	NS
	<i>Nampt</i>	0.61 (0.12)	NS	0.68 (0.11)	NS	NS
	<i>Pim1</i>	0.56 (0.17)	NS	NS	NS	NS
	<i>Mxi1</i>	0.48 (0.06)	NS	NS	NS	NS
	<i>Atr</i>	0.47 (0.14)	NS	NS	NS	NS
	<i>Odc1</i>	0.47 (0.09)	NS	NS	NS	NS
	<i>Ruvbl2</i>	0.46 (0.11)	NS	NS	NS	NS
	<i>Ndr1</i>	0.44 (0.18)	NS	0.54 (0.22)	NS	NS
	<i>Met</i>	0.42 (0.24)	NS	NS	NS	NS

	<i>Ier3</i>	0.37 (0.05)	NS	0.51 (0.03)	NS	NS
	<i>Egr1</i>	0.22 (0.06)	NS	0.38 (0.08)	NS	NS
	<i>Blm</i>	NS	NS	0.48 (0.04)	1.39 (0.10)	NS
Metabolism Transport	<i>Vdac1</i>	0.73 (0.11)	NS	NS	1.32 (0.18)	NS
	<i>Pfkfb4</i>	0.65 (0.08)	NS	NS	NS	NS
	<i>Hk2</i>	0.63 (0.16)	NS	NS	NS	NS
	<i>Ero1l</i>	0.60 (0.07)	NS	0.66 (0.17)	NS	NS
	<i>Slc2a3</i>	0.57 (0.16)	NS	NS	NS	NS
	<i>Tpi1</i>	0.56 (0.13)	NS	NS	NS	NS
	<i>Ldha</i>	0.54 (0.14)	NS	NS	NS	NS
	<i>Tfrc</i>	0.50 (0.08)	NS	NS	NS	NS
	<i>Pgk1</i>	0.42 (0.12)	NS	NS	NS	NS
	<i>Pkm</i>	0.40 (0.12)	NS	NS	0.70 (0.06)	NS
	<i>Pfkp</i>	0.39 (0.09)	NS	NS	NS	NS
	<i>Eno1</i>	0.39 (0.08)	NS	NS	0.70 (0.12)	NS
	<i>Pfkl</i>	0.39 (0.06)	NS	NS	NS	NS
	<i>Pgam1</i>	0.34 (0.06)	NS	NS	NS	NS
	<i>Car9</i>	0.28 (0.05)	NS	NS	NS	NS
	<i>Slc2a1</i>	0.27 (0.03)	NS	NS	NS	NS
	<i>Pdk1</i>	0.26 (0.08)	NS	NS	NS	NS
	<i>Slc16a3</i>	0.24 (0.02)	NS	NS	NS	NS
	<i>Aldoa</i>	NS	NS	NS	1.92 (0.57)	NS
	<i>Pfkfb3</i>	NS	NS	NS	1.38 (0.19)	NS

Fold changes (Average (STD)) listed are significantly altered ($p < 0.05$) in TS5KO mice relative to experimentally matched WT mice, NS = not significant. Bolded values are > 3.5 -fold.

Importantly, only expression of *Adora2b* was down-regulated (0.24-fold) in WT UI mice after 14dTM. No genes were modified at UI 28dTM. Conversely, in TS5KO mice, while no genes were modified at the UI 14dTM time-point, 4 genes were up-regulated at the UI 28dTM time-point (*Adora2b*, 3.94-fold, *Fos*, 6.33-fold, *Hmox1*, 4.90-fold, and *Serpine1*, 6.08-fold).

Evaluation of S-GAG, ACAN, and HA Deposition in WT and TS5KO mice

Histopathological scoring of the WT and TS5 specimens showed collagen disorganization in the tendon and cellular hyperplasia in the peritenon and stroma of adjacent adipose tissue at 3d (Figure 7g,j) relative to UI mice (Figure 7a,d). In both genotypes, this

response was accompanied by a robust accumulation of HA throughout the tendon body, peritenon, and the adjacent adipose stroma (Figure 7i,l). In both genotypes, after 14dCA and 28dCA (Figure 8c,f,i,l), HA was largely eliminated from those regions. Pericellular and interfibrillar ACAN accumulation in the tendon was greatest at 14dCA (Figure 8b,e) and 14dTM (Figure 9b,e) time-points evidenced by both positive SafO and anti-DLS immunostaining. The peritenon and adipose stroma showed strong immunoreactivity for ACAN at 14dCA and 14dTM, with staining intensity returned to pre-injury levels at the longer 28d time-points (Figure 8 and 9h,k), in either activity level.

Whereas overall the histologically detectable changes in HA and ACAN contents were similar for both genotypes throughout the time frame of the model, the most robust responses for all stains were observed for the WT tissue in the CA activity groups (Figure 8a-c,g-i) and for the TS5KO tissues in the TM activity groups (Figure 9d-f,j-l), supporting our previous observations of a difference in mechanosensitive responses between the two genotypes [39]. Notably, histological evaluation of tendons from UI mice exposed to 14dTM and 28dTM regimes, showed no marked changes in collagen orientation or histochemical staining of ACAN and HA (Appendix P). This supports our previous conclusions that an injurious event with subsequent cell responses is needed for the development of tendinopathy [39].

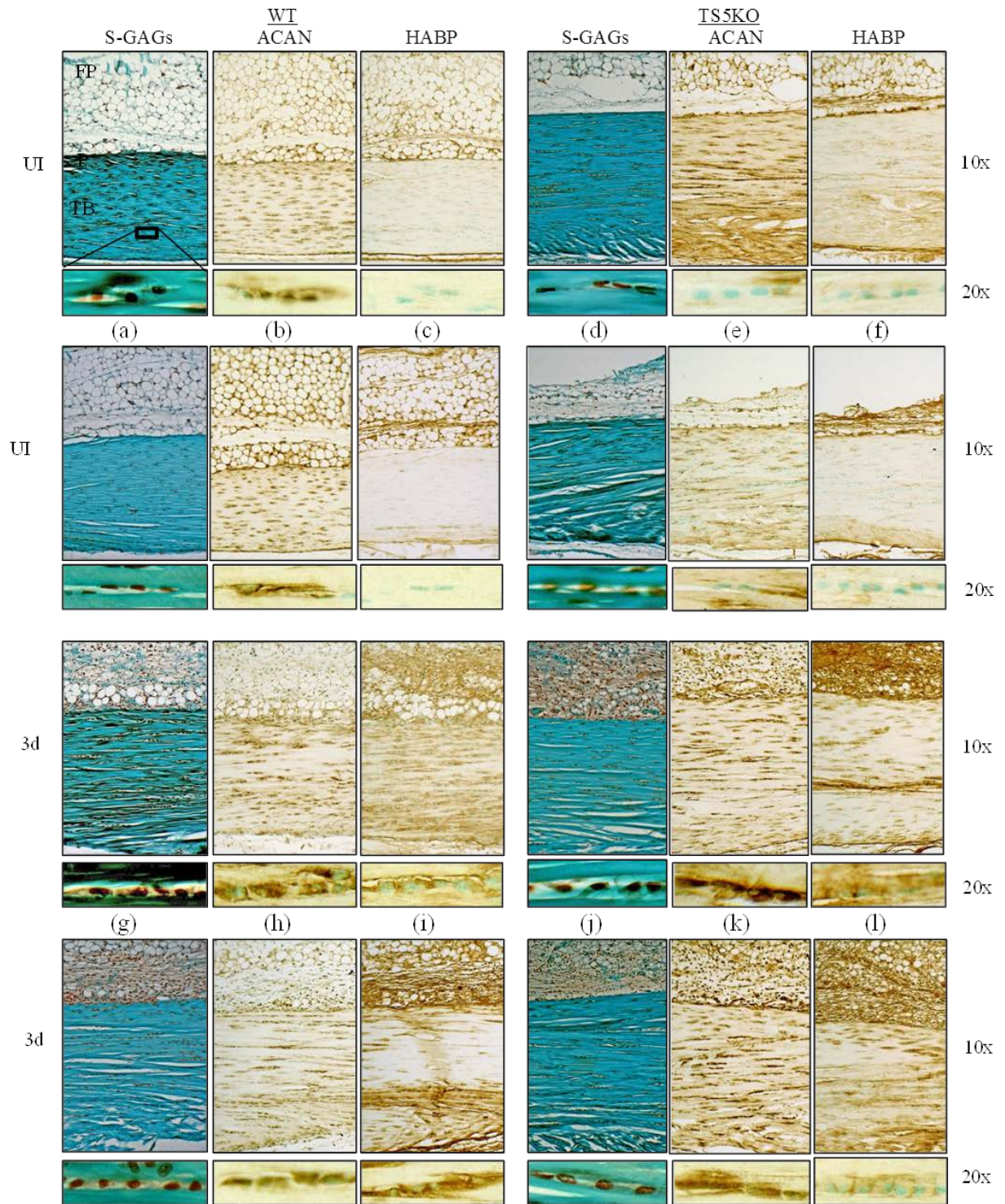


Figure 7: Components of the glycomatrix in WT and TS5KO Achilles tendons at 3d. Abbreviations: TB = tendon body, P=Peritenon, FP = Fat Pad.

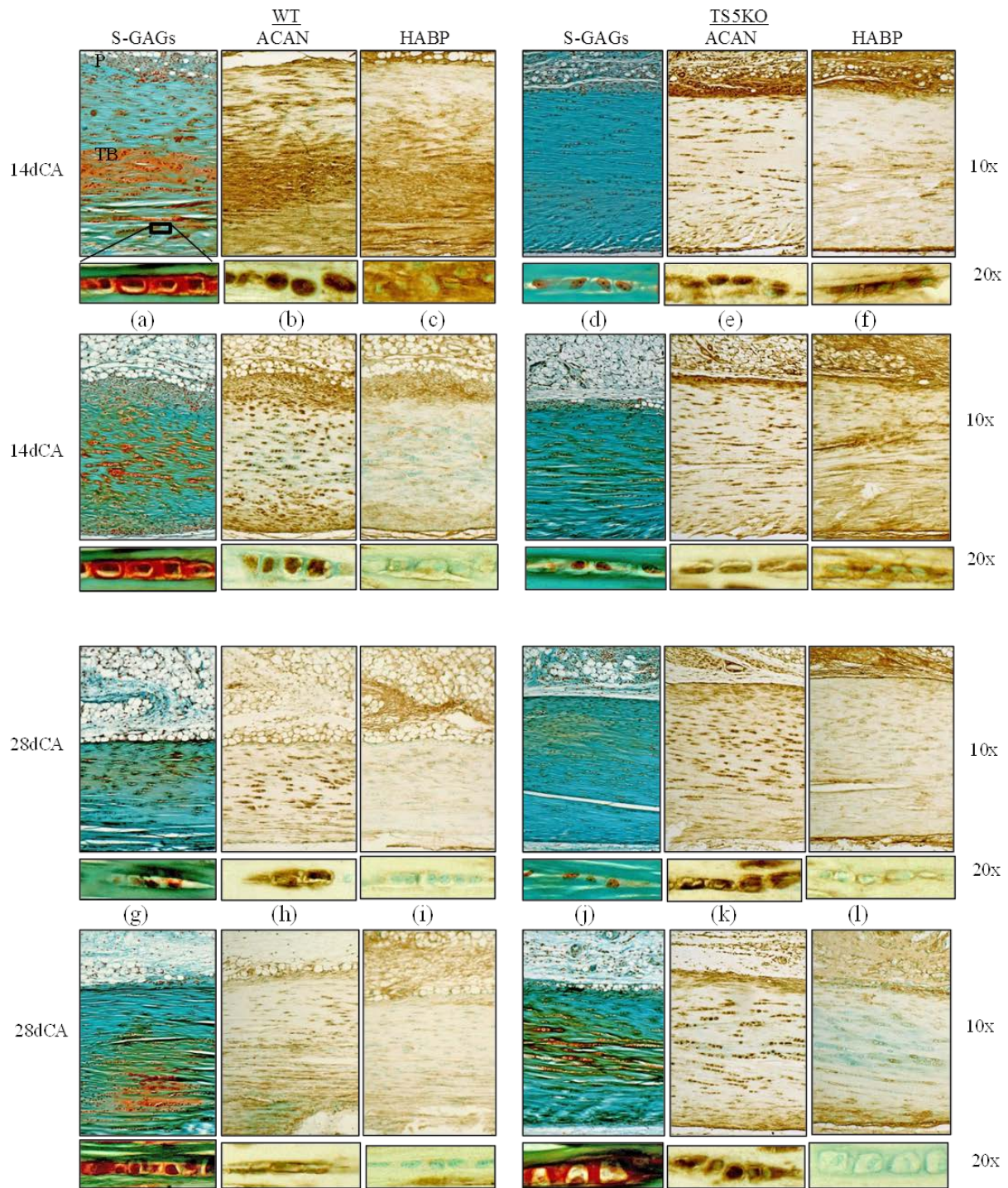


Figure 8: Components of the glycomatrix in WT and TS5KO Achilles tendons with CA. Abbreviations: TB = tendon body, P=Peritenon, FP = Fat Pad.

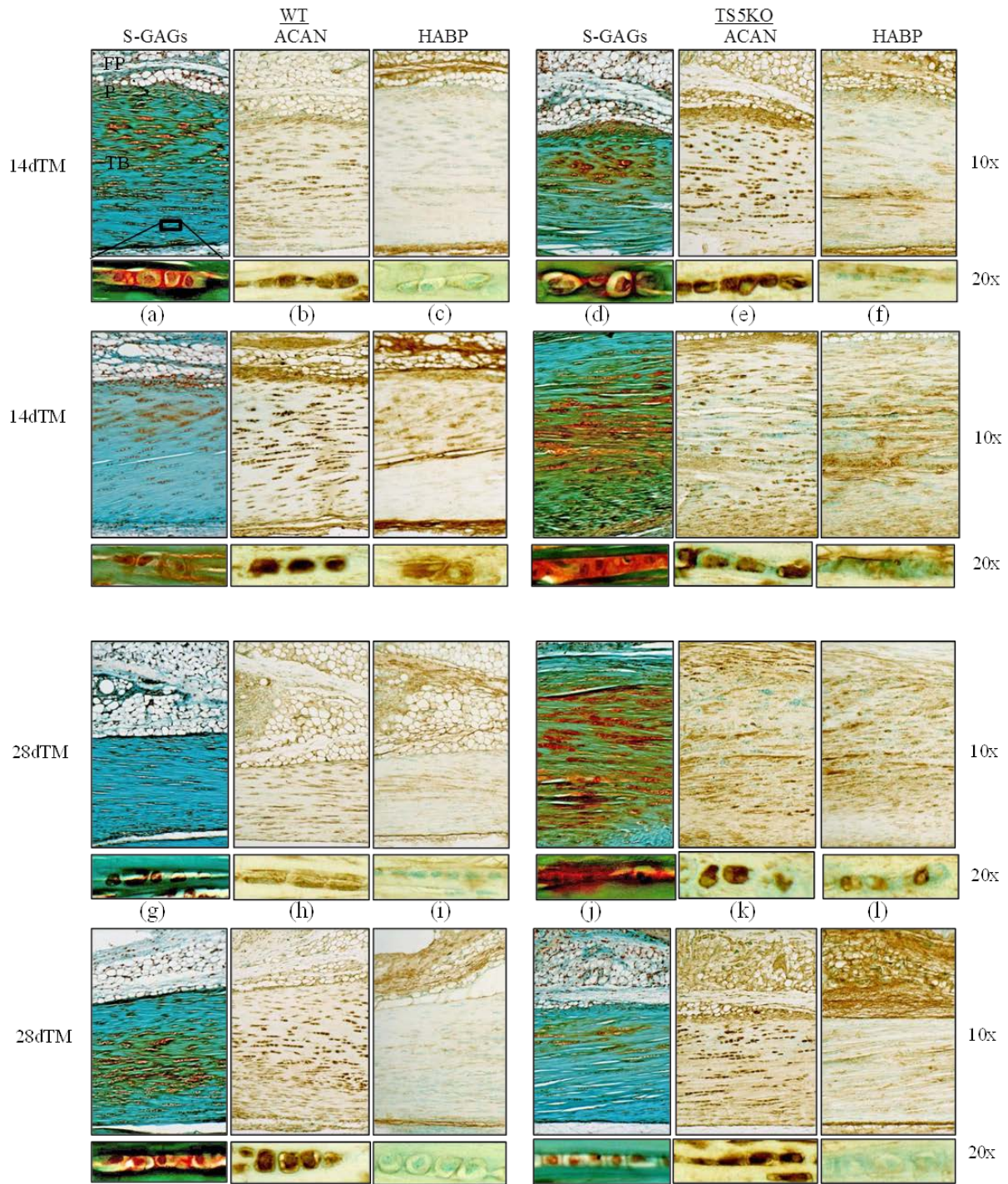


Figure 9: Components of the glycomatrix in WT and TS5KO Achilles tendons with TM. Abbreviations: TB = tendon body, P=Peritenon, FP = Fat Pad.

Histological Evaluation of Neovascularization using Griffonia (Bandeiraea) Simplicifolia Lectin Staining in WT and TS5KO mice

Application of the lectin reagent for histochemical analyses of tissue sections for specimens in the tendinopathy model, showed positive staining of cells in the adipose stroma, tendon cells ECM of both the tendon body and the peritenon (Figures 9 and 10).

Staining of cells in the adipose stroma (Figure 9) was used to evaluate neovascularization in the model. Notably, cells in mature blood vessels (indicated by black arrows in Figure 9) stained weakly in UI joints and during the development of tendinopathy. However, strong staining of cell aggregates and cells lining of small capillaries (indicated by black triangles in Figure 9) was evident in the post-injury period in both genotypes.

Staining in the tendon body demonstrated un-organized deposition of lectin into the extracellular matrix. During the early 3d time-point, increased lectin staining of WT mice was evident in the tendon body (Figure 11b), more so than with TS5KO mice (Figure 11h). With CA, deposition was evident in the ECM at 14dCA (Figure 11c) and 28dCA (Figure 11d) time-points in WT mice. With TS5KO mice, deposition peaks at the longer 28dCA (Figure 11j) time-point and remained confined to the pericellular matrix. Conversely, with TM (Figure 11k,l), a more robust deposition was evident in TS5KO mice as compared to WT mice. When UI mice were run on the TM little deposition was evident at both UI 14dTM and UI 28dTM time-points (Appendix P).

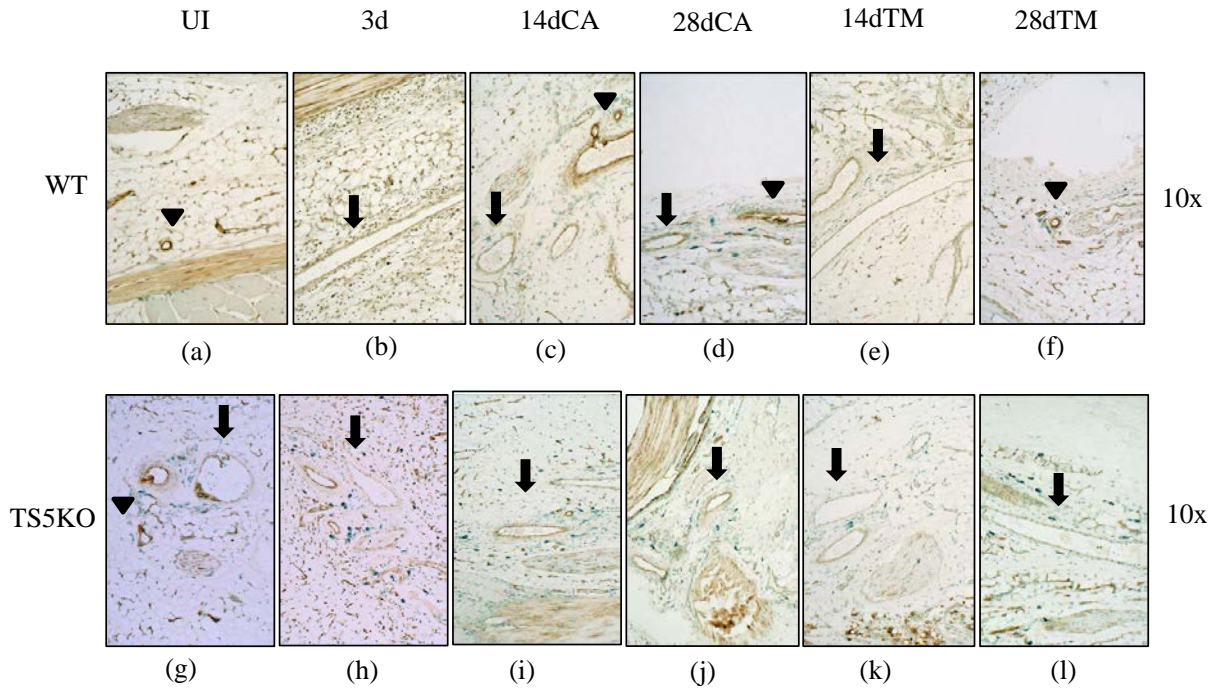


Figure 10: Lectin staining of adjacent stroma for confirmation of staining specificity for neovascularization

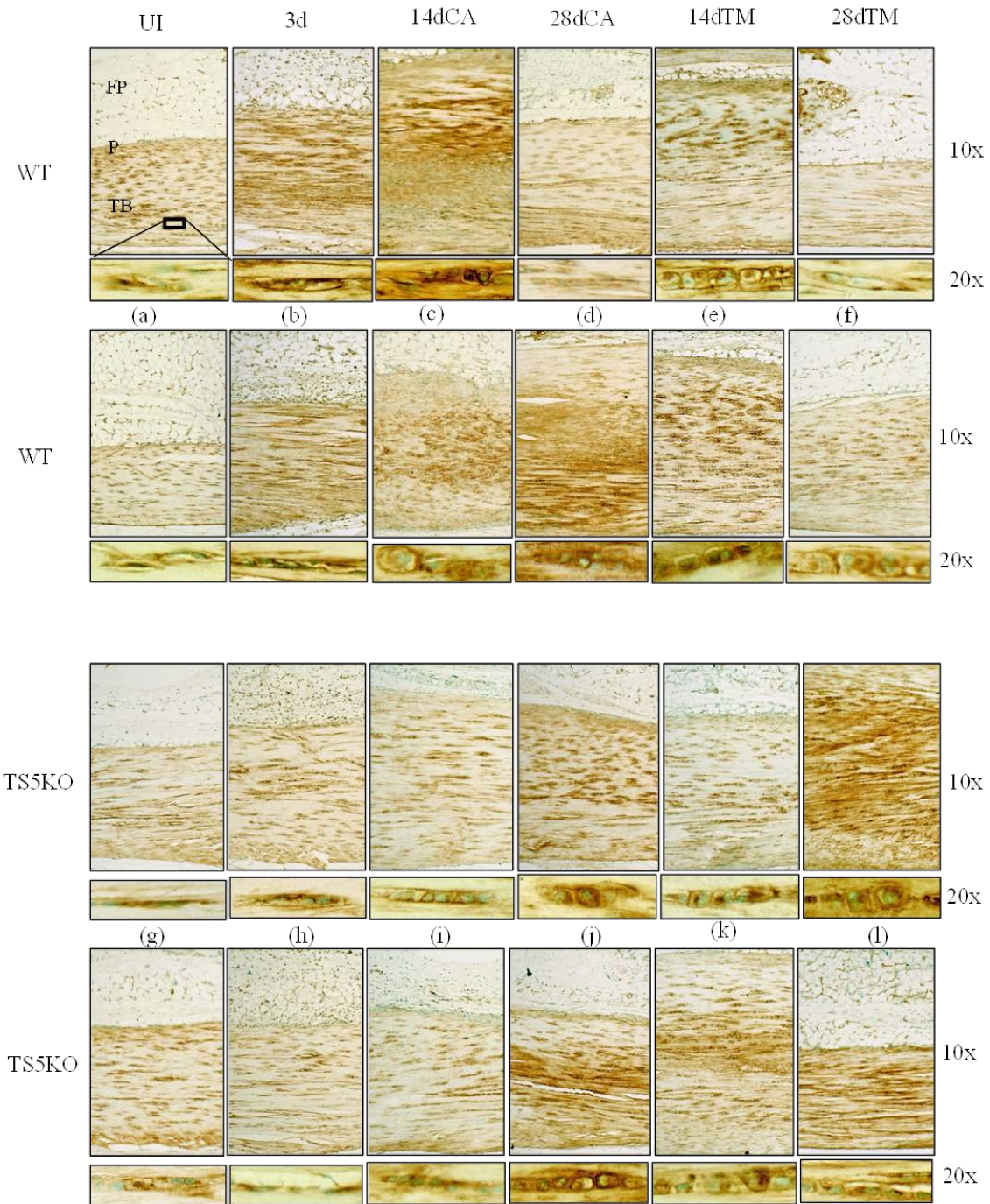


Figure 11: Lectin staining of WT and TS5KO Achilles tendons with TM. Abbreviations: TB = tendon body, P=Peritenon, FP = Fat Pad.

Discussion

The goal of this study was to identify the activation of hypoxia signaling pathways in a murine model of Achilles tendinopathy, as it relates to the development of chondroid metaplasia and progression of tendinopathy. Immediately following the injury (3d) a transient increase in expression of *Hif1a*, a transcription factor that modulates expression of a wide range of genes as a protective response to hypoxia (changes in O₂ concentration) occurred in both WT and TS5KO tendons (Figure 5). Furthermore, this was accompanied by changes in expression of genes involved in angiogenesis/coagulation, cell fate, and metabolism/transport, supporting the notion that injury to the tendon activates the hypoxia response pathway in this murine tendinopathy model. Interestingly, although *Hif1a* was increased in TS5KO tendons, this was accompanied by a less robust induction of the downstream genes during the injury time-course when compared to WT tendons (Table 13). The lack of an impaired hypoxic response at the mRNA transcript level could be explained by the altered glucose uptake in TS5KO tendon associated cells [47], as glucose uptake and glycolysis were shown to reduce cell fate changes associated with hypoxia [89].

Notably, TS5KO UI tendons showed higher immunoreactivity of intracellular HIF1A and also an increased deposition of the protein within the tendon ECM, peritenon, and adjacent stroma compared to WT specimens (Figure 6a,g). This apparent accumulation of HIF1A protein in TS5KO tendons may be reflected in the finding that fibroblastic cells from TS5KO have an impaired capacity for uptake and intracellular degradation of proteins such as LRP1, another mediator in the hypoxia pathway [47, 90]. Therefore, following de novo synthesis of HIF1a protein in the early stages of a hypoxic response, WT cells may down-regulate this response by proteolytic clearance of the HIF1A protein through post-translational modification pathways

[90]. Indeed, following injury, WT tendons exhibited decreased deposition of HIF1A as compared to TS5KO mice (Figure 6b-f,h-l) When mice were exposed to TM activity after the injury, increases in *Hif1a* signal transduction and downstream responsive genes in TS5KO mice were evident (Table 12). TS5KO mice also exhibited an increased number of genes significantly differentially regulated between TM and CA age-matched groups and increased baseline activation of genes in UI mice that underwent TM as compared to WT. These findings suggest a mechanical component for hypoxia signaling in the absence of *Adamts5*. Indeed, a more robust deposition of ACAN, HA and S-GAG in was evident in TS5KO with TM (Figure 9).

Most notable was the finding that following the early activation of a wide range of hypoxia response genes, only those associated with angiogenesis/coagulation remained highly upregulated in the tendon for up to 28d post-injury (Table 11-12). Specifically, transcript levels for *Serpine1*, *F10*, *Hmox1*, and *Mmp9* were increased, in both WT and TS5KO mice, maintained with either CA and TM activity. *Mmp9* has been studied in relation to tendon biology in a number of systems. For example, increased expression was correlated to painful and ruptured human Achilles tendons [91, 92], patellar tendinopathy [93], and rotator cuff disease [94], as well correlated to aging in rat tenocytes [95]. Low level laser therapy (LLLT) was found to promote MMP9 in the early inflammation phase of injury rat Achilles tendon healing model [96], with increased expression levels also seen in human dermal wound healing [97] and flexor tendon healing [98, 99]. However, direct inhibition of MMP9 did not affect adhesion formation in murine flexor tendon healing [100]. In relation to the changes in expression of metabolic genes in the current study, is the finding the high glucose up-regulates expression of *Mmp9* in tendon cells [101].

In this regard, it is notable, that the histochemical staining with biotinylated *Griffonia (Bandeiraea) Simplicifolia* (used to mark capillary endothelium) was also positive in tendon cells, supporting the gene expression studies that suggest the capacity for tenocytes to retain a degree of pluripotency that includes capacity to produce molecular components required for vasculogenesis and chondrogenesis. Injury induced activation of neovascularization events in the adipose tissue stroma adjacent to the tendon body was also detected by the lectin histochemical staining. Interestingly, while both WT and TS5KO mice showed post injury induced increases in cells that stained positive for the lectin, those were more organized into capillary structures in the WT compared to the TS5KO mice (Figure 10). The strong staining of the tendon ECM by the lectin after injury (Figure 11) could be the result of enhanced secretion of glycoproteins containing terminally galactose capped oligosaccharides. Alternatively, it might be result of increased diffusion of serum derived proteins with those oligosaccharide structures into the tendon ECM as a result of increased vascular permeability induced by an inflammatory response following the initial injury.

In summary, the activation of the hypoxic pathway in resident tendon cells in this murine model of tendinopathy may provide a mechanistic explanation for a biomechanically-independent (as supposed to near insertion sites and in regions of compression) of chondroid deposits commonly associated with human and animal tendinopathy [30, 31, 39, 102]. Thus, low oxygen tension and downstream activation of Hif1a has been associated with enhanced chondrogenesis (collagen type II and aggrecan production) in pluripotent connective tissue progenitor cells [103-106]. Furthermore, post-injury changes in expression of metabolic energy pathway genes were reflected in altered in glycosylation responses such as increased HA and aggrecan CS synthesis and NR-terminal alpha-galactose capping (Figure 7-9). These changes in

cell metabolism also have a profound effect on reparative collagen synthesis and extracellular assembly [107] , which are critically important to restore the biomechanical function of the tendon as a whole.

Chapter 4 – Specific Aim 3

Introduction

The complexity of tendinopathy arises from individualized factors such as genetic predisposition, co-morbidities such as diabetes [108, 109], obesity [110], hyper-cholesteremia [111], hyper-uricaemia [112], and congenital metabolism disorders [113], and drug related side effects [58] that have been linked to spontaneous tendon degeneration and rupture. In this context, the role of tendon cell metabolism on injury progression is highly relevant to the development of chronic tendinopathy and accompanying mechanical dysfunction [114]. For example, in diabetes, persistently elevated levels of extracellular glucose can result in the formation of advanced glycation end products (AGEs) which covalently bond to collagen fibers resulting in alterations to their structure and function [115], thus providing a likely mechanism for impaired flexor tendon and rotator cuff healing in diabetic rats [116, 117].

Tendon explant culture methodologies allow for mechanistic studies of cellular responses, independent of modulating contributions *in-vivo* from surrounding tissues such as bone and muscle while maintaining cells in their native ECM. Tendon explants from a range of sources including rat (tail tendon fascicles [118-125], anterior cruciate ligament [126], and *tibialis anterior* [127]), canine (*Flexor digitorum profundus* [128]), rabbit (anterior and medial collateral ligaments, flexor tendon, patellar tendon fascicles [129-133]), bovine (foot extensors and deep digital flexor tendons [134-136]), equine (superficial digital flexor tendon [137-139]), chick (*flexor digitorum profundus*) [140], and human (hamstring [141]) have been used to examine the effects of mechanical stimulation and growth factor treatments on tendon cell responses. The application of an explant model with the use of knockout mice in relation to genetic predispositions in tendon injury has not been heavily explored [142]. Additionally, while

most explant studies have focused on ECM turnover, few have focused on metabolism alterations associated with these deviations in normal tendon structure.

With relevance to injury initiation and progression in the *in-vivo* murine tendinopathy model was the finding that injury of the tendon results in activation of a hypoxia response by tendon cells that includes changes in expression of pro-angiogenic genes and genes encoding enzymes and transporters for energy metabolism, with one of more of such pathways being linked to chondroid deposits in the pericellular and interfibrillar matrix (Aim 2, Chapter 3).

The goal of the experiments carried out under this aim was firstly, to develop a murine Achilles explant culture system that showed a cellular response when exposed to different O₂ concentrations; secondly, to compare such responses in WT and TS5KO tendons, since previous work from our laboratory showed that fibroblastic cells lacking TS5 are unable to downregulate glucose uptake; and thirdly to examine the effect of *in-vivo* injury on the ability of the resident cells to respond to high and low O₂ concentration. Furthermore, in addition to metabolic responses we also determined whether explanting under the different conditions above modulate tissue structure and associated biomechanical properties.

Methods

Murine Achilles Tendon Explant Culture

All animal use was approved by the IACUC of Rush University. Achilles tendons were isolated from freshly excised 12 week old male WT and TS5KO C57/Bl6 mice, and placed directly into CO₂-independent media (Gibco[®]) supplemented with 1% penstrep. Tendons were then placed free floating in culture dishes for 4 days in AMEM/1% FCS/5mM glcNH₂ (1 mL media/tendon, 6 tendons per dish). Media changes were conducted on day 1 and 3 of the culture

period. Explant conditions were previously optimized for maintenance of mechanical properties and expression of extracellular components in murine Achilles tendons [143] (Appendix Q). Additional tendons for explant were taken from 3d injured mice (see Aim 1 or 2 for in-vivo injury protocol) and cultured under the same conditions. Experimental groups, outcome measures, and tendon numbers are summarized in Table 14.

Table 14: Experimental groups and outcomes for Aim 3

Group	Abbreviation	Outcome Measures					
		Alamar Blue		Biomechanics		qt-PCR	
		WT	TS5KO	WT	TS5KO	WT	TS5KO
<i>Freshly Excised</i>	FE	6	6	6	6	20	20
<i>Explanted</i>							
20% O ₂	HI O ₂	6	6	6	6	13	13
2.5% O ₂	LO O ₂	6	6	5	6	16	18
<i>Injured, Freshly Excised</i>	3d FE	6	5	6	6	12	13
<i>Injured, Explanted</i>							
20% O ₂	3d HI O ₂	5	5	5	6	15	14
2.5% O ₂	3d LO O ₂	6	6	6	6	22	19

Gene Expression Assays

RNA was isolated from one pool of 12-22 combined Achilles tendons from each explant experimental group (approximately 400-800ng/tendon). Briefly, tendon pools were fragmented by hammer impact at -196°C in a Bessman Tissue Pulverizer, recovered, and extracted in 1 mL of Trizol by vortexing for 60 seconds. RNA was purified with an RNeasy MiniKit (Qiagen, Cat #: 74104) and RNA quality was established from A260:280 of at least 1.90. cDNA was synthesized with 0.5ug of mRNA (RT² First Strand Kit, Qiagen) and hypoxia signaling transcript abundances were determined with SYBR qt-PCR array plates (PAMM-032ZA, Qiagen), as described by the manufacturer. The array was made up 84 genes separated into the following functional groups: Hif1a signal transduction (n=24), Angiogenesis and Coagulation (n=16), Cell

Fate Determination (n =19), and Metabolism and Transport (n=24). While each qt-PCR array was conducted singularly for each sample, three individual replicate array assays of a typical sample (WT 3d Pool #3 from Aims 1 and 2) showed a coefficient of variation of less than 5% between each of the triplicates.. Changes in transcript abundance ($\Delta\text{Ct}=\text{Ct}$ for transcript of interest minus Ct for the housekeeping gene *B2m*) were used to calculate the fold change ($2^{-\Delta\Delta\text{Ct}}$) from UI levels for each experimental group. The genes *Epo*, *Hif3a*, and *Hnf4a* were removed from down analysis as transcripts were undetected by qt-PCR in all groups. A >3.5-fold change in expression relative to UI was considered “biologically significant”.

Assay of Viability via Alamar Blue in Tendon Explants

On day 3 of the explant protocol, 5-6 tendons per group were placed into individual wells of 12 well plates with 1 mL of culture media and 10% (v/v) Alamar Blue reagent (Invitrogen) and incubated at 37°C in 20% O₂ [141]. After 24 hours, the media was removed and the fluorescence measured (excitation: 530nm, emission: 590nm) against a ‘medium blank’ which had no tissue during the 24 hour incubation period. This assay represents an index of cell viability/metabolic activity by measuring intracellular reducing activity (NADH/NADPH) via conversion of resazurin to resorufin. Statistically significant changes relative to FE tissue was determined by 1-way ANOVA followed by Tukey’s post-hoc tests (*p<0.05) using GraphPad Prism 5 (La Jolla, CA). For genotypic comparisons a student’s t-test was used to compare TS5KO and WT values for each experimental group.

Assay of Glucose Uptake by Tendon Explants

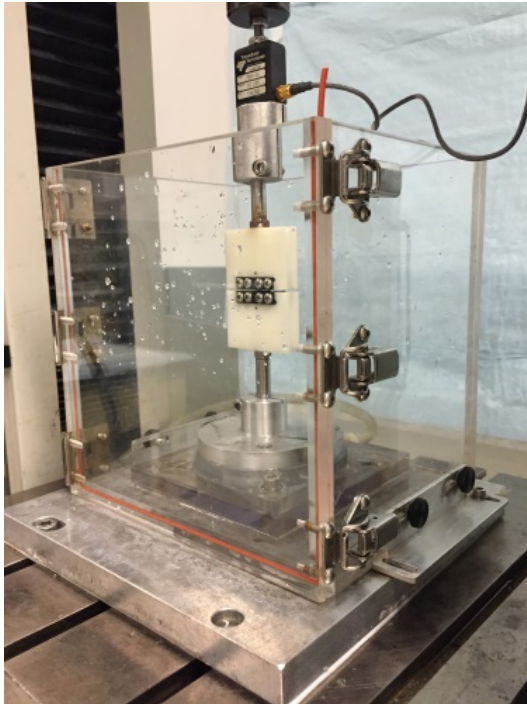
Triplicate media samples, removed on days 1, 3, and 4 of the culture period, were assayed for glucose content using the Amplex™ Kit (LifeTech, Inc.) [144]. The glucose

concentration was calculated relative to blank controls (day 0) and expressed as μmol of glucose in medium (per tendon). Statistically significant changes relative to UI tissue at each time-point was determined by 1-way ANOVA followed by Tukey's post-hoc tests ($*p<0.05$) using GraphPad Prism 5 (La Jolla, CA). For genotypic comparisons a student's t-test was used to compare TS5KO and WT values for each experimental group.

Mechanical Testing

The cross-sectional area of each tendon was measured using a precision caliper (width) and laser displacement sensor (thickness), assuming a rectangular geometry [43]. Tendons were clamped in custom grips (Figure 12) using an initial grip-to-grip length of 3.75mm and placed in an isotonic saline bath within a Mechanical Testing System (Eden Prairie, MN) equipped with 10 lb load cell. Following a ten minute equilibration in the saline bath and a preload of 0.05N for 2 minutes, tendons were loaded to failure at 0.05mm/sec. Following testing, maximum force, stiffness, maximum stress, and elastic modulus was determined. Groups were compared to FE tendons using a 1-way ANOVA and Tukey's post hoc tests ($p<0.05$). For genotypic comparisons a student's t-test was used to compare TS5KO and WT values for each experimental group.

Figure 12: Explant mechanical testing setup



Results

Expression of Hif1a and hypoxia signaling genes in UI WT and TS5KO tendons following explant

No biologically significant (>3.5-fold) changes in abundance of *Hif1a* were detected in FE WT and TS5KO tendons upon explant in HI O₂ or LO O₂ conditions (Table 15), indicating a cellular response to O₂ levels *in-vitro*. Assays for transcript abundance of 82 hypoxia signaling genes in WT and TS5 tendons cultured under both LO O₂ and LO O₂ demonstrated either unchanged or reduced expression relative to FE tendons (Table 16).

However some oxygen level dependent and genotypic specific activations were observed: The following genes were activated during culture in LO O₂ in both genotypes: *Ankrd3* (Hif1a Signaling), *Pgf* (Angiogenesis), *Mif* (Cell fate), *Car9*, *Eno1*, *Ero1l*, *Pgam1*, *Pkm*, and *Slc2a1* (Metabolism and transport). Additionally, the following were genes were up-regulated in TS5KO

tendons only: *Lgals3* (HIF1 Signaling), *Serpine1* (Angiogenesis), *Adm*, *Pfkl*, *Pfkp*, *Slc16a3*, and *Pgk1* (Metabolism and Transport). By comparison, culture in HI O₂ stimulated *Mmp9* (Angiogenesis), *Car9*, *Eno1*, *Pkm*, and *Slc2a1* (Metabolism and Transport) but only in TS5KO tendons. In addition, *Hmox1*, a gene commonly associated with cellular stress responses, was increased in both genotypes and under both oxygen conditions, indicating a generalized response to explant culture, similar to that reported for *Mmp3*. Heatmap representations for all genes are shown in Appendix R and direct comparisons of genotypic differences in expression of the hypoxia signaling genes are shown in (Table 17).

Table 15: Transcript abundance of *Hif1a* in UI mice with explant

WT			TS5KO		
FE	LO O ₂	HI O ₂	FE	LO O ₂	HI O ₂
36.67	21.53 (0.59)	15.44 (0.42)	23.35	43.64 (1.87)	34.81 (1.49)

Values presented are transcript abundance ($2^{-(\Delta Ct)} * 1000$) with fold change relative to FE in parenthesis. No >3.5-fold changes relative to UI or between experimentally matched WT and TS5KO tendons detected.

Table 16: Fold-changes in transcript abundance of hypoxia signaling genes in explanted relative to FE tendons

Group	Genes	WT		TS5KO		Group	Gene	WT		TS5KO	
		LO O ₂	HI O ₂	LO O ₂	HI O ₂			LO O ₂	HI O ₂	LO O ₂	HI O ₂
Hif1a Signaling	<i>Ankrd37</i>	3.68	0.28	4.71	NS	Metabolism Transport	<i>Car9</i>	19.61	NS	53.06	9.73
	<i>Arnt</i>	0.28	0.11	NS	NS		<i>Erol1</i>	6.00	NS	12.44	NS
	<i>Ncoa1</i>	0.25	0.09	NS	0.29		<i>Slc2a1</i>	5.83	NS	18.89	5.49
	<i>Hif1an</i>	0.24	0.06	NS	0.23		<i>Eno1</i>	5.77	NS	15.06	4.85
	<i>Fos</i>	0.12	0.03	NS	0.11		<i>Pgam1</i>	4.75	NS	11.01	NS
	<i>Per1</i>	0.12	0.01	NS	NS		<i>Pkm</i>	4.37	NS	12.50	4.26
	<i>Nfkb1</i>	NS	0.24	NS	NS		<i>Slc2a3</i>	0.28	0.08	NS	NS
	<i>Dnajc5</i>	NS	0.20	NS	NS		<i>Vdac1</i>	0.25	0.18	NS	0.13
	<i>Bhlhe40</i>	NS	0.12	NS	NS		<i>Pfkl</i>	NS	0.22	9.32	NS
	<i>Egln2</i>	NS	0.12	NS	NS		<i>Pfkp</i>	NS	0.21	3.54	NS
	<i>Egln1</i>	NS	0.10	NS	NS		<i>Ldha</i>	NS	0.19	NS	NS
	<i>Usf2</i>	NS	0.10	NS	0.23		<i>Gbel</i>	NS	0.18	NS	0.23
	<i>Map3k1</i>	NS	0.07	NS	NS		<i>Gpi1</i>	NS	0.16	NS	NS
	<i>Lgals3</i>	NS	NS	4.01	NS		<i>Tpi1</i>	NS	0.16	NS	NS
Angiogenesis Coagulation	<i>Hmox1</i>	17.23	4.92	34.72	11.42	<i>Tfrc</i>	NS	0.14	NS	NS	
	<i>Pgf</i>	6.86	NS	15.17	NS	<i>Aldoa</i>	NS	0.11	NS	0.19	
	<i>Edn1</i>	0.14	0.12	NS	0.23	<i>Gys1</i>	0.20	0.06	NS	0.09	
	<i>F3</i>	0.10	0.05	0.27	0.05	<i>Hk2</i>	NS	0.04	NS	0.14	
	<i>Lox</i>	NS	0.29	NS	NS	<i>Pfkfb4</i>	0.14	0.04	NS	0.22	
	<i>Vegfa</i>	NS	0.14	NS	NS	<i>Slc16a3</i>	NS	0.04	4.52	NS	
	<i>Bnip3</i>	NS	0.08	NS	NS	<i>Pfkfb3</i>	NS	0.03	NS	0.13	
	<i>Mmp9</i>	NS	NS	NS	4.25	<i>Pgk1</i>	NS	NS	4.10	NS	
	<i>Serpine1</i>	NS	NS	3.83	NS						
Cell Fate	<i>Mif</i>	6.82	NS	6.64	NS						
	<i>Pim1</i>	0.20	0.06	NS	0.24						
	<i>Egr1</i>	0.19	0.09	NS	0.19						
	<i>Txnip</i>	0.15	0.04	NS	0.13						
	<i>Btg1</i>	NS	0.27	NS	NS						
	<i>Atr</i>	NS	0.20	NS	NS						
	<i>Nampt</i>	NS	0.17	NS	NS						
	<i>Ndr1</i>	NS	0.16	NS	NS						
	<i>Adm</i>	NS	0.12	5.04	NS						
	<i>Ccng2</i>	NS	0.11	NS	NS						
	<i>Mxi1</i>	NS	0.10	NS	NS						
	<i>Ddit4</i>	NS	0.05	NS	NS						
<i>Nos3</i>	NS	0.04	NS	0.14							

Fold changes listed are altered (>3.5-fold) relative to genotype matched UI tendons, NS = not significant.

Table 17: Altered expression of hypoxia signaling genes in TS5KO mice with explant relative to WT

Group	Gene	FE	LO O ₂	HI O ₂
Hif1a Signaling	<i>Per1</i>	NS	3.95	NS
	<i>Egln1</i>	NS	NS	3.86
Angiogenesis Coagulation	<i>Adora2b</i>	0.28	NS	NS
	<i>F10</i>	NS	4.88	NS
	<i>Lox</i>	NS	NS	3.74
Metabolism Transport	<i>Car9</i>	NS	NS	19.66
	<i>Slc16a3</i>	NS	NS	12.98
	<i>Pfkl</i>	NS	NS	5.34
	<i>Pfkfb4</i>	NS	NS	4.35
	<i>Eno1</i>	NS	NS	4.16
	<i>Pkm</i>	NS	NS	3.86

Fold changes listed are altered (>3.5-fold) relative to experimentally matched WT tendons, NS = not significant.

Assay for Production of NADH/NADPH Reducing Equivalents in UI Tendon Explants

Production of NADH/NADPH reducing equivalent was measured using the Alamar Blue assay freshly excised tendons and tissue maintained under LO O₂ and HI O₂ (Figure 13). The data obtained showed statistically significant changes (increase over FE) only in WT tendon explants under HI O₂. A similar trend was seen in TS5KO tendons, but the difference to FE tissue did not reach statistical significance. Explant culture of tissue from both genotypes, under LO O₂ conditions had essentially identical levels of NADH/NADPH production as that seen in FE tissue, suggesting that LO O₂ conditions during explant culture maintain activity of this pathway at levels present in freshly harvested tissues.

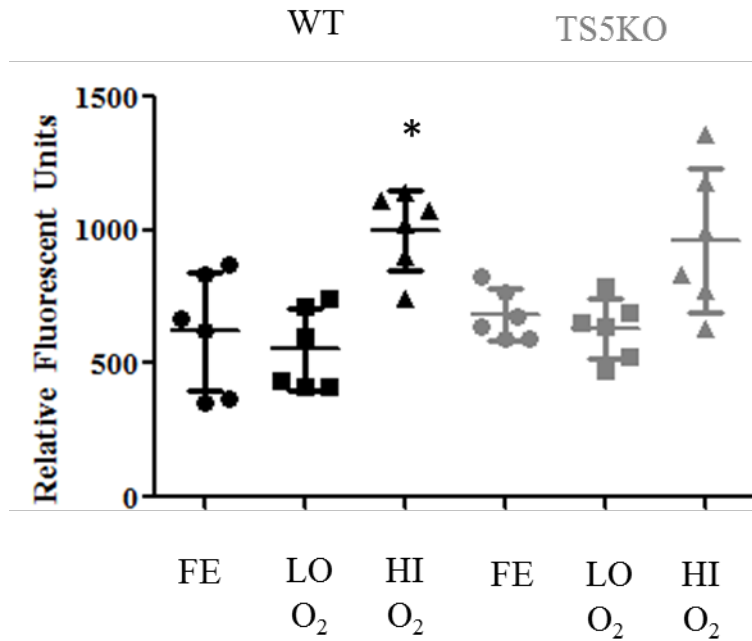


Figure 13: Production of NADH/NADPH reducing equivalent (Average +/- STD) in WT and TS5KO tendon explants (* $p < 0.05$ to genotype matched UI, NS detected between genotype for each condition)

Assay of Medium Glucose Concentration in UI WT and TS5KO tendon explants

Glucose levels in media collected at 1, 3 and 4 days of explant cultures maintained in either LO O₂ or HI O₂ demonstrate that glucose consumption or uptake was minimal for both WT and TS5KO tendons (Table 18 and Figure 14).

Table 18: Concentration of glucose in media before and after UI explant culture of WT and TS5KO tendons

Genotype	Group	Media Blank	Day 0-1	Day 1-3	Day 3-4
WT	LO O ₂	2.98 (0.43)	2.81 (1.07)	3.32 (1.56)	3.50 (1.38)
	HI O ₂	2.82 (0.46)	2.72 (0.53)	2.57 (1.31)	3.30 (0.78)
TS5KO	LO O ₂	2.28 (0.97)	1.86 (0.66)	2.41 (1.49)	2.60 (2.17)
	HI O ₂	2.33 (1.05)	2.95 (2.76)	2.69 (1.33)	2.07 (1.24)

Average (STD) glucose concentration of media from tendon explants (uM/mL)

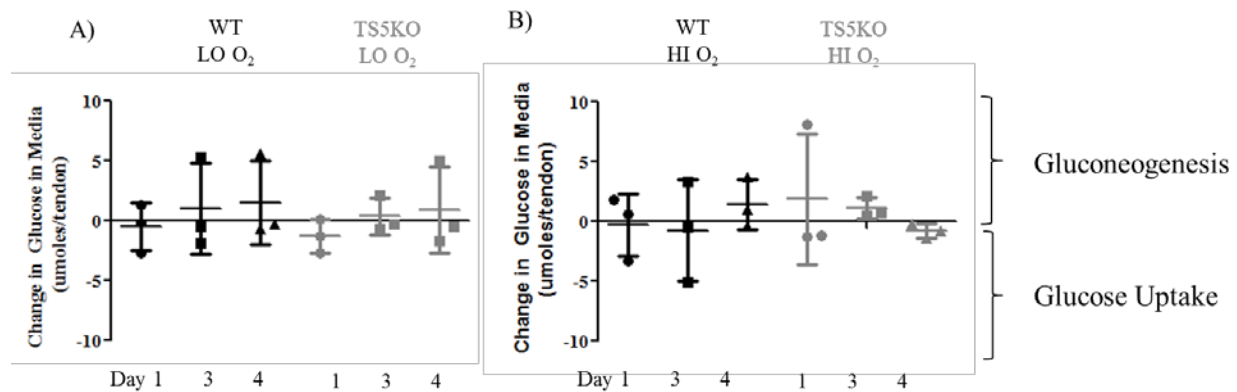


Figure 14: Changes in media glucose concentration in WT and TS5KO UI tendon explants (No statistically significant differences detected).

Material properties of UI WT and TS5KO tendons following explant

No significant changes in cross sectional area (CSA) or material properties (maximum stress and elastic modulus) were detected in WT explants relative to FE (Figure 15). Only a significant difference was detected in the elastic modulus of TS5KO tendons cultured in LO oxygen conditions relative to TS5KO FE tendons ($p < 0.05$). Experimentally matched genotypic differences were detected only between the elastic modulus of LO ($p = 0.0129$) and HI ($p = 0.0330$) TS5KO and WT tendons.

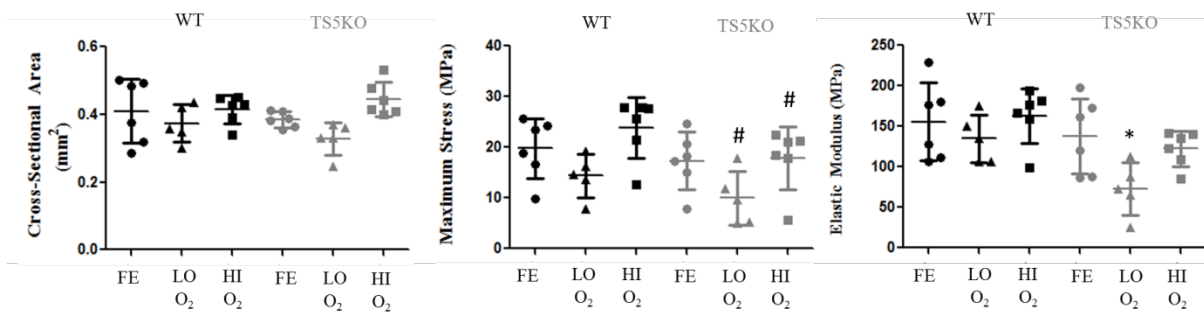


Figure 15: Material properties (Average +/- STD) in WT and TS5KO UI tendon explants (* $p < 0.05$ to genotype matched FE, # $p < 0.05$ between experimental matched genotypes)

Expression of Hif1a and hypoxia signaling genes in injured WT and TS5KO tendons following explant

When 3d injured tendons were explanted, the *in-vivo* injured induced increases in *Hif1a* transcript abundance (see Aim 2) was not maintained after the tissue was explanted for both WT and TS5KO tendons in either LO O₂ or HI O₂ (Table 19). As for uninjured tendons, the majority of hypoxia signaling genes in the injured tendons were decreased or not changed by the explant culture, when compared to the FE tissue (Table 20).

However some O₂ dependent and genotypic specific activations were observed. *Ankrd37* (Hif1 signaling) and *Adm* (cell fate) were activated by LO O₂ in both genotypes and *Ero11* (Metabolism) was activated in TS5KO tendons only. *Igfbp3* and *Ndr1* (Cell Fate) were upregulated by HI O₂ in TS5KO tendons only, and *Pgf* (Angiogenesis) showed increased expression under both culture conditions and for both genotypes. Heatmap illustrations of the entire set of genes for both culture conditions and genotypes can be seen in Appendix S

Data were further evaluated for differences between genotypes in gene expression responses to explant culture (Table 21). Trends showed that injured TS5KO tendons responded with more pronounced decreases in expression than WT injured tissues. Moreover, comparisons of genotype matched injured tendons and un-injured tendons cultured in the same oxygen conditions demonstrated differential changes in expression of hypoxia signaling genes primarily seen in the WT HI O₂ groups (Table 22).

Table 19: Transcript abundance of *Hif1a* in injured tendons with explant

WT			TS5KO		
3d FE	3d LO O ₂	3d HI O ₂	3d FE	3d LO O ₂	3d HI O ₂
128.10	33.05* (0.26)	61.66^ (0.48)	87.60	29.54 (0.34)	29.82 (0.34)

Values presented are transcript abundance ($2^{-(\Delta Ct)} \times 1000$) with fold change to 3d FE in parentheses. * >3.5-fold changes relative to FE 3d. ^ >3.5-fold relative to experimental and genotype matched non-injured tendons. No >3.5-fold changes between experimentally matched WT and TS5KO tendons.

Table 20: Fold-changes in transcript abundance of hypoxia signaling genes in 3d injured tendons with explant

Group	Gene	WT		TS5KO	
		3d LO O ₂	3d HI O ₂	3d LO O ₂	3d HI O ₂
Hif1a Signaling	<i>Ankrd37</i>	3.71	NS	5.70	NS
	<i>Cops5</i>	0.25	0.26	NS	0.26
	<i>Bhlhe40</i>	0.21	0.21	NS	NS
	<i>Fos</i>	0.13	0.13	0.25	0.19
	<i>Per1</i>	0.13	0.12	0.21	0.23
Angiogenesis Coagulation	<i>Pgf</i>	6.83	3.81	6.01	5.49
	<i>Mmp9</i>	0.28	NS	0.07	NS
	<i>Lox</i>	0.13	0.14	NS	0.27
	<i>F3</i>	0.04	0.06	0.28	0.24
	<i>Serpine1</i>	0.02	0.01	0.12	0.05
	<i>Anxa2</i>	NS	0.27	NS	NS
	<i>F10</i>	NS	0.06	NS	0.08
	<i>Bnip3</i>	NS	NS	5.22	NS
	<i>Edn1</i>	NS	NS	0.31	0.26
<i>Angptl4</i>	NS	NS	0.29	NS	
Cell Fate	<i>Adm</i>	5.47	NS	10.45	NS
	<i>Blm</i>	0.26	NS	NS	NS
	<i>Odc1</i>	0.16	0.12	NS	0.17
	<i>Egr1</i>	0.06	0.12	0.24	NS
	<i>Ier3</i>	NS	0.19	NS	NS
	<i>Ndr1</i>	NS	NS	6.39	3.74
	<i>Igfbp3</i>	NS	NS	NS	3.89
Metabolism Transport	<i>Car9</i>	11.39	4.23	41.50	16.12
	<i>Vdac1</i>	0.36	0.29	NS	NS
	<i>Eroll</i>	NS	NS	5.18	NS

Fold changes listed are altered (>3.5-fold) relative to genotype matched 3d FE tendons, NS = not significant.

Table 21: Altered expression of hypoxia signaling genes in TS5KO mice with explant relative to WT

Group	Gene	3d FE	3d LO O ₂	3d HI O ₂
Hif1a Signaling	<i>Egln1</i>	NS	NS	NS
	<i>Per1</i>	NS	NS	NS
	<i>Bhlhe40</i>	0.24	NS	NS
Angiogenesis Coagulation	<i>Vegfa</i>	0.23	NS	NS
	<i>F3</i>	0.18	NS	NS
	<i>Serpine1</i>	0.16	NS	NS
	<i>Hmox1</i>	NS	NS	0.24
Cell Fate	<i>Egr1</i>	0.21	NS	NS
Metabolism Transport	<i>Car9</i>	0.28	NS	NS
	<i>Slc2a1</i>	0.27	NS	NS
	<i>Pdk1</i>	0.25	NS	NS
	<i>Slc16a3</i>	0.24	NS	NS

Fold changes listed are altered (>3.5-fold) relative to experimentally matched WT tendons, NS = not significant.

Table 22: Altered expression of hypoxia signaling genes in injured explants relative to un-injured explants

Group	Gene	WT		TS5KO		Group	Gene	WT		TS5KO	
		LO O ₂	HI O ₂	LO O ₂	HI O ₂			LO O ₂	HI O ₂	LO O ₂	HI O ₂
Hif1a Signaling	<i>Per1</i>	13.85	NS	NS	0.25	Metabolism Transport	<i>Slc16a3</i>	57.48	NS	5.52	NS
	<i>Ankrd37</i>	10.36	NS	4.78	NS		<i>Car9</i>	37.04	NS	NS	NS
	<i>Fos</i>	10.05	NS	NS	NS		<i>Pfkl</i>	17.18	NS	NS	NS
	<i>Egln1</i>	9.50	NS	NS	NS		<i>Pdk1</i>	13.45	NS	5.10	NS
	<i>Map3k1</i>	9.23	NS	NS	NS		<i>Pfkfb3</i>	12.76	NS	4.36	NS
	<i>Bhlhe40</i>	7.72	NS	NS	NS		<i>Gpi1</i>	12.68	3.57	NS	NS
	<i>Hif1an</i>	7.36	NS	NS	NS		<i>Pfkfb4</i>	10.25	NS	NS	NS
	<i>Ctsa</i>	5.83	NS	NS	NS		<i>Pgam1</i>	9.92	NS	NS	NS
	<i>Egln2</i>	5.50	NS	NS	NS		<i>Hk2</i>	9.36	NS	NS	NS
	<i>P4ha1</i>	5.23	NS	NS	NS		<i>Pkm</i>	8.64	NS	NS	NS
	<i>Dnajc5</i>	5.01	NS	NS	NS		<i>Eno1</i>	7.60	NS	NS	NS
	<i>Arnt</i>	4.42	NS	NS	NS		<i>Slc2a3</i>	7.34	NS	NS	NS
	<i>Ncoa1</i>	4.42	NS	NS	NS		<i>Gys1</i>	6.26	NS	NS	NS
	<i>Hif1a</i>	3.99	NS	NS	NS		<i>Pgk1</i>	6.00	NS	NS	NS
	<i>Nfkb1</i>	3.89	NS	NS	NS		<i>Pfkp</i>	5.87	NS	NS	NS
	<i>Rbpj</i>	3.67	NS	NS	NS		<i>Ldha</i>	5.40	NS	NS	NS
	<i>P4hb</i>	2.49	NS	NS	NS		<i>Tpi1</i>	4.19	NS	NS	NS
<i>Usf2</i>	NS	NS	4.00	NS	<i>Eroll</i>	4.17	NS	NS	NS		
Angiogenesis Coagulation	<i>Pgf</i>	9.94	NS	6.67	NS	<i>Slc2a1</i>	3.77	NS	NS	NS	
	<i>Adora2b</i>	9.71	NS	4.00	NS	<i>Tfrc</i>	3.68	NS	NS	NS	
	<i>Vegfa</i>	7.14	NS	NS	NS						
	<i>Bnip3</i>	7.12	NS	NS	NS						
	<i>Lox</i>	5.53	NS	NS	NS						
	<i>Hmox1</i>	5.44	NS	NS	NS						
	<i>Plau</i>	4.76	NS	NS	NS						
	<i>Serpine1</i>	4.18	NS	NS	NS						
	<i>Edn1</i>	3.86	NS	NS	NS						
	<i>Angptl4</i>	3.57	NS	NS	NS						
	<i>F10</i>	NS	34.83	6.94	10.17						
<i>Mmp9</i>	NS	4.10	NS	NS							
Cell Fate	<i>Ddit4</i>	16.12	NS	3.58	NS						
	<i>Adm</i>	12.23	4.38	4.05	NS						
	<i>Pim1</i>	11.45	NS	NS	NS						
	<i>Nos3</i>	10.58	NS	4.64	NS						
	<i>Ccng2</i>	6.50	NS	NS	NS						
	<i>Ndr1</i>	5.87	NS	NS	NS						
	<i>Igfbp3</i>	5.86	NS	3.70	NS						
	<i>Mxi1</i>	4.82	NS	NS	NS						
	<i>Blm</i>	4.78	NS	NS	NS						
	<i>Txnip</i>	4.55	NS	NS	NS						
	<i>Btg1</i>	4.48	NS	NS	NS						
	<i>Atr</i>	3.77	NS	NS	NS						
	<i>Ier3</i>	2.14	NS	NS	NS						
	<i>Egr1</i>	NS	NS	NS	0.24						

Fold changes listed are altered (>4-fold) relative to oxygen level matched UI explanted tendons, NS = not significant.

Assay for Production of NADH/NADPH Reducing Equivalents in Injured Tendon Explants

Production of NADH/NADPH reducing equivalent measured via Alamar Blue assay was not significantly altered from 3d FE levels in explanted tendons from either genotype or oxygen condition (Figure 16). WT injured tendons explanted in HI O₂ and LO O₂ oxygen were also significantly altered relative to condition matched un-injured HI and un-injured LO tendons. For TS5KO tendons, similar comparisons only showed significance in the 3d LO O₂ group to un-injured tendons cultured in LO O₂ levels. No genotypic differences were detected between experimentally matched groups.

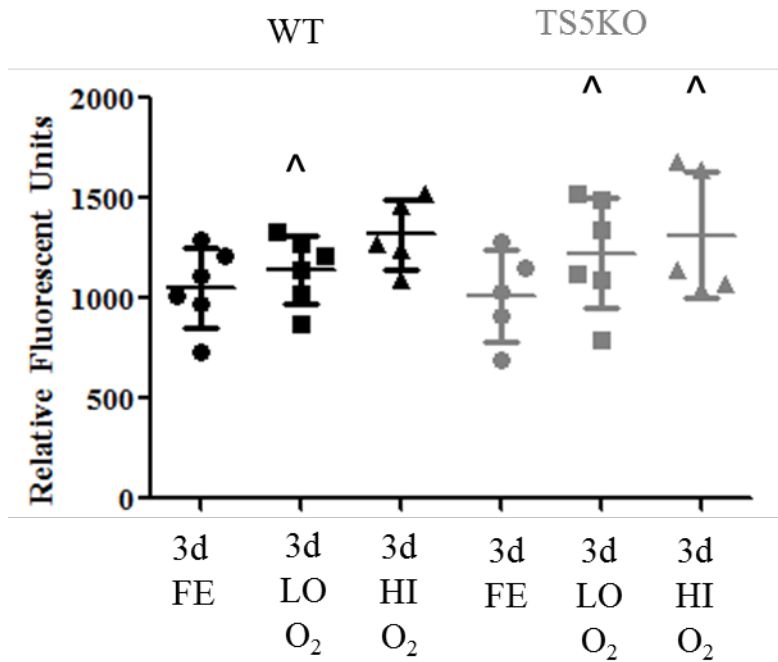


Figure 16: Production of NADH/NADPH reducing equivalent (Average +/- STD) in WT and TS5KO injured tendon explants (NS relative to genotype matched 3d FE, ^ p<0.05 to experimental and genotypic matched un-injured, NS detected between genotype for each condition)

Assay of Medium Glucose Concentration in Injured WT and TS5KO tendon explants

In contrast to uninjured tissues, glucose uptake by injured tendons over the 4 day explant was robust, under both O₂ conditions, with tissues from both genotypes (Table 23). Particularly notable was the significantly accelerated uptake of glucose between days 1-3 and 3-4 in both genotypes and both O₂ concentrations (Figure 17). Further experiments are required to determine the intracellular metabolic fate of the intracellular glucose in either ATP generating glycolysis/lactic acid production and or utilization for glycosylation reactions via conversion to UDP and CMP sugar precursors.

Table 23: Concentration of glucose in media before and after injured explant culture of WT and TS5KO tendons

Genotype	Group	Media Blank	Day 0-1	Day 1-3	Day 3-4
WT	3d LO O ₂	3.95 (2.27)	2.68 (1.17)	2.32 (0.94)	1.97 (1.24)
	3d HI O ₂	3.55 (1.78)	2.86 (0.25)	1.77 (0.51)	2.15 (0.92)
TS5KO	3d LO O ₂	6.81 (0.59)	5.39 (1.12)	4.00 (0.70)	2.29 (0.87)
	3d HI O ₂	3.18 (1.63)	3.45 (3.72)	1.28 (1.39)	1.85 (1.45)

Average (STD) glucose concentration of media from tendon explants (uM/mL)

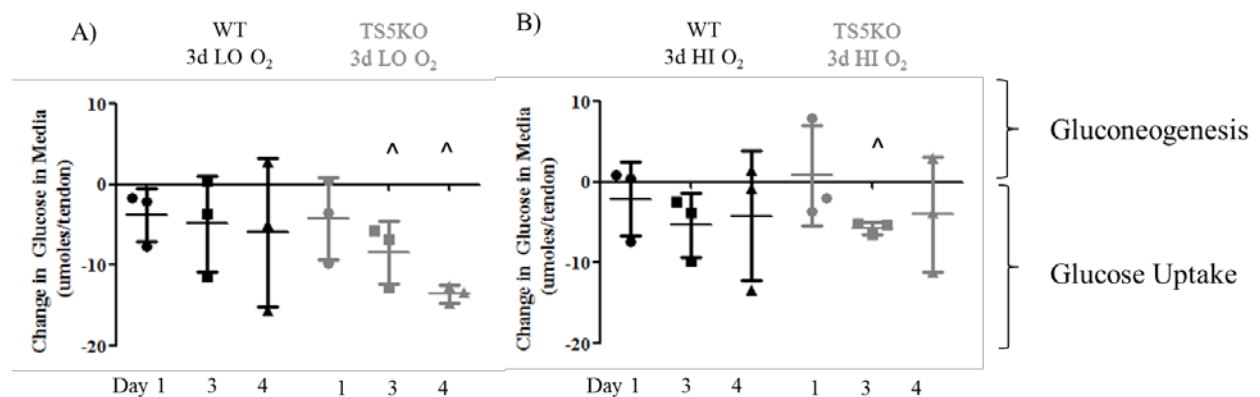


Figure 17: Change in media glucose concentration in WT and TS5KO injured tendon explants. (^ p<0.05 to experimentally matched UI, NS detected relative to original levels and between genotype for each condition). STD not shown

Material properties of UI WT and TS5KO tendons following explant

No significant changes in cross sectional area or material properties were detected in WT injured explants relative to WT 3d FE (Figure 18). TS5KO 3d injured tendons exhibited a significant decrease in CSA ($p=0.0006$) relative to 3d FE. However, material properties were not significantly altered. Genotypic differences were seen between 3d FE groups with TS5KO tendons exhibiting a significantly increased CSA ($p=0.0050$) and lower maximum stress relative to WT tendons ($p=0.0001$). Interestingly, when comparing injured tendons to experimentally and genotypically matched un-injured tendons, differences were detected in the maximum stress and elastic modulus for WT and TS5KO tendons cultured in HI oxygen conditions ($p<0.05$).

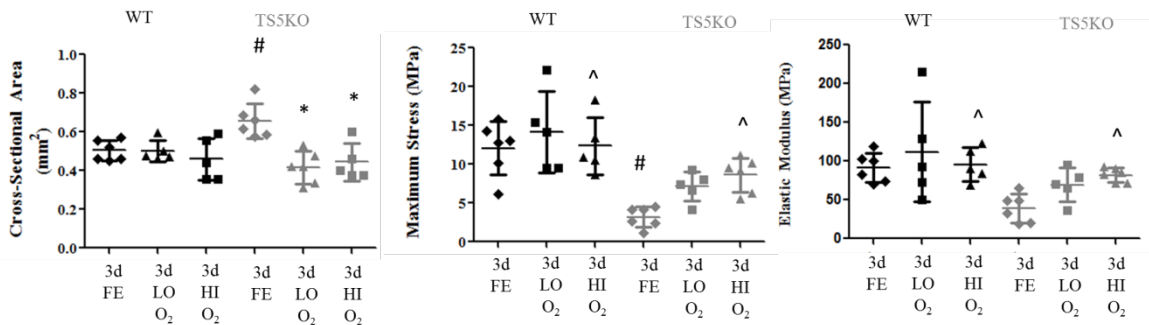


Figure 18: Material properties in WT and TS5KO injured tendon explants (* $p<0.05$ to genotype matched 3d FE, $^{\wedge}p<0.05$ to genotype, condition matched un-injured, $\#p<0.05$ to experimental matched WT).

Discussion

The goal of the current aim was to develop a murine Achilles tendon explant system to study the metabolic differences between un-injured and injured tendons in response to low oxygen tension as a means to comprehend the complex injury pathways which lead to the progression of a chronic disease state. Overall, injured tendon explants did not respond to changes in oxygen tension ex-vivo as very few metabolic gene expression changes were seen

compared to 3d FE tendons and between 3d HI O₂ and 3d LO O₂ groups for each genotype (Table 20). However, robust changes were evident seen between HI and LO un-injured explants (Table 16). These changes would suggest a change in cell metabolic state following an initiating injury. Interestingly, all injured explants (WT and TS5KO in HI O₂ and LO O₂ conditions) underwent glucose uptake (Figure 17), while un-injured explants trended towards gluconeogenesis or no changes in glucose utilization (Figure 14). Additionally, injured tendons underwent significantly increased production of NADH/NADPH equivalents.

Unfortunately, little has been published on the metabolic capacity of tendon cells *in-vivo* or *ex-vivo*. The current *ex-vivo* data suggests enhanced glucose utilization pathways (increased glucose uptake, glycolysis, and NADH/NADPH Kreb's cycle production) and metabolism following tendon injury. In accordance with this, a recently published article demonstrated similar trends of increased glucose uptake and vascularization following Achilles tendon repair [145]. Additionally, these outcomes which suggested enhanced metabolic capacity were correlated to poor clinical outcomes. In similar studies, healing Achilles tendons exhibited higher levels of the metabolites glutamate, pyruvate, and lactate [146], while exercise, which has been shown to be beneficial for tendon healing [51], promoted glucose uptake [147]. Interestingly, changes in glucose concentration were shown to regulate AGEs in porcine tendon explants [148] and chondrogenesis in mesenchymal stem cell (MSC) cultures through TGF- β 1 signaling pathways [149]. Since TGF- β 1 was the injury agent utilized in this study, AGE production and subsequent changes in collagen cross-linking may provide a mechanistic link to the decreased material properties seen in the injured explants and *in-vivo* tendinopathic specimens which utilized this model [39]. While AGE production was beyond the scope of the current aim chondroid deposition was associated with this TGF- β 1 induced injury (Aim 2). Indeed, UDP-

glucose dehydrogenase, which catalyzes the reaction of an essential monosaccharide in GAGs via a glucose dependent and TGF- β regulatory reaction, was shown to modulate HA and sGAG production as well as chondrogenesis [150].

Only minor differences in expression of hypoxia signaling genes and metabolic measurements were detected between 3d injured WT and TS5KO explanted tendons for each experimental group relative to 3d FE (Table 20). Comparisons of the WT LO O₂ and TS5KO HI O₂ groups demonstrated similar expression profiles specifically in up-regulated expression of genes involved in glucose transport (*Slc2a1*) and glycolysis (*Pgam1*, *Pgk1*, and *Pkm*). Additionally, while both genotypes exhibited glucose uptake with injury, TS5KO explants had higher differentials from baseline levels (Figure 17). These findings suggest a regulatory variance between WT and TS5KO in response to oxygen conditions, however additional studies are needed to explore these genotypic differences further. No evident correlation between changes in metabolic and material properties were evident, however TS5KO exhibited decreased material properties upon FE and upon injury as previously described [43]

In summary, the development and use of a murine Achilles tendon explant system allowed for the enhanced study of tendon cell reactions to oxygen conditions. Ex-vivo experiments of UI and injured tendons revealed variable metabolic capacities, with injured tendons exhibiting increased glucose utilization pathways which may be indicative of chondroid deposition and decreased material properties seen during *in-vivo* studies of this TGF- β 1 induced injury model. The altered metabolic capacity of injured tendon cells may contribute to reduced capacity for healing seen in tendinopathic patients.

Chapter 5 – Summary and Future Directions

Discussion

The over-arching goal of this project was to advance the understanding of the cellular mechanisms involved in the initiation and progression of tendinopathy using a multi-scale molecular approach (epigenomics, transcriptomics, and proteomics). Firstly, a murine model of Achilles tendinopathy was utilized to assess a role for epigenetic regulation in the pathogenesis of the disease, and to potentially discover novel pathways associated the chronic tissue degeneration (Aim 1). The data showed that expression of chromatin modification enzymes were altered when C57Bl6 wild type male mice were injured *in-vivo* through TGF- β 1 injection into the Achilles tendon. DNA Methylome analyses of un-injured and injured tendons led to the novel finding that 5 genes (*Leprel2*, *Foxf1*, *Mmp25*, *Igfbp6*, and *Peg12*) which showed differential methylation of their promoter regions and modulated mRNA transcript abundance throughout the pathogenesis of the tendinopathy also were likely players in tendon cell function and collagen synthesis. Most notably was the identification of *Igfbp6*, which has shown to be regulated by hypoxia, a previously identified indicator of tendinopathy. Interestingly, the identical injury model in TS5KO mice which results in persistent chondroid deposition and a severe tendinopathic response also showed differential expression in these genes.

Further examination of the potential role of a hypoxia response after tendon injury *in-vivo* revealed expression of injury induced increases in *Hif1a* mRNA transcripts and elevated cell-associated HIF1A in the tendon itself, as well as the peritenon, and the stroma of the adjoining adipose tissues. In addition, transcript levels of between 10-40 hypoxia signaling genes were significantly altered after injury at each time-point, primarily in WT mice with CA and TS5KO with TM. Interestingly, the modulated expression of genes in the hypoxia pathway

associated with metabolism/transport were concurrent with the increased deposition of S-GAGs, HA, and ACAN in the pericellular and interfibrillar matrix in the tendon body, and the development of chondroid deposits.

Another significant and novel observation of this study was the robust and persistent increase in hypoxia regulated genes with known functions in angiogenesis/coagulation (*Mmp9*, *Hmox1*, *F10*, and *Serpine1*). In support of this we demonstrated increased localization of endothelial markers in previously identified regions for tendinopathy associated neovascularization (such as the peritenon and the adjacent adipose stroma), but also, surprisingly by the tendon cells themselves. The later finding could potentially indicate a change in the phenotype of tendon cells that would impair their potential for effective functional regeneration of the damaged extracellular matrix structure and function.

Given the changes in expression of genes involved in metabolism and those regulated by metabolism, a murine Achilles tendon explant system was developed to study the role of oxygen tension where intrinsic tendon cells could be studied within their native ECM (Aim 3). Robust differences in expression of genes involved in the hypoxia pathway were seen in both genotypes when UI tendons cultured in HI and LO oxygen conditions were compared. Conversely, when 3d injured tendons were cultured, few differences were detected between HI and LO conditions, suggesting an inability of injured tendon cells to respond to variations in oxygen tension. Additionally, injured tendons trended towards gluconeogenesis and increased NADH/NADPH production while UI tendons showed few changes in glucose utilization and NADH/NADPH production. However, none of these metabolic changes were linked to altered material properties in explanted tendons. Overall, using both *in-vivo* and *ex-vivo* murine systems, we have shown altered metabolic measures following tendon injury, which correlate with chondroid matrix

deposition, a classic marker of tendinopathy. We postulate that altered tendon cellular metabolism following tendon injury may contribute to a chronic pathology and altered tendon healing.

Study Limitations

Experimental limitations arose during the duration of the project primarily due to the size of the tendon tissue under study. Whilst the mouse model offers many advantages over the use of larger animals (cost, use of KO mice, ease of histological evaluation for disease scoring and tissue specific protein localization), the following drawbacks were evident:

Firstly, the difficulty of obtaining adequate quantities of high quality RNA from a single murine Achilles tendon necessitates the use of tissue pools from multiple mice at any given experimental point. Due to the multifactorial nature of the pathogenesis of tendinopathy, from the disease progression after the initial injury and its severity with time, inter-animal variability occurs (Figures 7-8). Therefore, while the tendon pools used for qt-PCR represent an overall average, multiple injury state are most likely present in each sample which contributes to the variability seen across time-points.

Secondly, surgical separation of murine Achilles tendons from surrounding tissues during dissection represents a technical challenge. Whereas tissues such as the peritenon and muscle fibres at the musculotendinous joint can be readily identified and removed during dissections in larger animal species, their complete removal in the mouse foot, within a reasonable time frame to prevent post-mortem induced changes in RNA or protein abundance, is difficult. Thus, different cell types may be present in our qt-PCR samples, especially because histology/immunohistochemistry suggests activation of all surrounding tissue following injury including the peritenon, synovial fat pad, and muscle.

Lastly, the length of the mouse Achilles tendon (approx. 5-6mm) does to bode well to mechanical evaluation. In this way the ability to load tendons during explant culture is not ideal since immobilizing in a loading unit might inflict additional damage to a substantial part of the tendon. In a similar way, biomechanical testing of these tissues presents a technical challenge due to the length available for gripping (3.75mm gauge length) which results in a non-ideal aspect ratio. Additionally, slipping and failure within the clamps is quite common which leads to high error during these tests (Figure 14 and 17).

Future Directions

Future work will focus on utilizing the metabolic pathways discovered here to develop enhanced diagnostic and therapeutic tools to determine the chronicity of tendinopathy for individual patients. There currently exists an inability to diagnosis stages of chronicity in patients, which could alter treatment modalities utilized for quicker and enhanced healing. Specifically, PET scanning, a diagnostic tool available in most clinics which monitors glucose utilization, could be used with this murine model or larger animals to correlate levels of injury or clinical symptoms to variations in glucose concentration in tendon. Additionally, metabolomics could be conducted on biopsied tendon or blood samples taken near the site of injury or systemically to quantify levels of cellular output in various tendinopathy models. The benefit of these modalities is the opportunity to study the metabolic outcomes of a single tendon in conjunction with histology for chondroid deposition and mechanics for functional properties to determine specific correlations in metabolic capacity and established tendon pathological characteristics.

Appendix

Appendix A: Author Affiliations and Contributions for the Journal of Orthopedic Research Submission

Authors:

Katie J Trella^{1,4}, Jun Li², Eleni Stylianou⁶, Vincent M Wang^{5,4}, Jonathan M Frank¹, Jorge Galante¹, John D Sandy³, Anna Plaas^{2,3}, Robert Wysocki¹

Affiliations:

1. Department of Orthopedic Surgery, Rush University Medical Center, 1611 W. Harrison Street, Suite 201, Chicago, IL 60612
2. Department of Rheumatology/Internal Medicine, Rush University Medical Center, 1611 W. Harrison Street, Suite 510, Chicago, IL 60612
3. Department of Biochemistry, Rush University Medical Center, 1735 W. Harrison Street, 5th Floor, Chicago, IL 60612
4. Department of Bioengineering, University of Illinois at Chicago, 851 S. Morgan Street, 2nd Floor, Chicago, IL 60607
5. Department of Biomedical Engineering and Mechanics, Virginia Tech, Blacksburg, VA, 24061
6. Formerly Department of Pathobiology, Lerner Research Institute, Cleveland Clinic Foundation, 9500 Euclid Avenue, Cleveland, OH, 44195

Author Contribution statements: All authors have read and approved the final submitted manuscript

Trella, Katie J – Animal work, qt-PCR, methylome data analysis, manuscript preparation

Li, Jun – Animal work, histology

Sandy, John D – Experimental design, manuscript preparation

Stylianou, Eleni – Epigenetics consultant

Wang, Vincent M – Murine tendinopathy consultant

Frank, Jonathan M – Experimental design, clinical consultant

Galante, Jorge – Experimental design, clinical consultant

Plaas Anna – Experimental design, manuscript preparation

Wysocki, Robert – Experimental design, clinical consultant

Appendix B: Journal of Orthopaedic Research Permission Statement

“If you wish to reuse your own article (or an amended version of it) in a new publication of which you are the author, editor or co-editor, prior permission is not required (with the usual acknowledgements)”

Website: [http://onlinelibrary.wiley.com/journal/10.1002/\(ISSN\)1554-527X/homepage/Permissions.html](http://onlinelibrary.wiley.com/journal/10.1002/(ISSN)1554-527X/homepage/Permissions.html)

The screenshot displays the homepage of the Journal of Orthopaedic Research. At the top, the journal title and the Orthopaedic Research Society (ORS) logo are visible. The main content area includes a search bar, a list of journal statistics (edited by Linda J. Sandell, impact factor of 2.988, and ISI ranking of 9/72), and a permissions section. The permissions section contains a note about linking, instructions for reproducing content via RightsLink, and a list of steps to obtain permission. A sidebar on the right features a search bar, the ORS logo, and a vertical flow diagram with three circular nodes labeled 'Downloads', 'Citations', and 'Altmetrics'.

Journal of Orthopaedic Research
© Orthopaedic Research Society

Edited By: Linda J. Sandell
Impact Factor: 2.988
ISI Journal Citation Reports® Ranking: 2014: 9/72 (Orthopedics)
Online ISSN: 1554-527X

SEARCH
In this journal
Advanced > Saved Searches >

Published in cooperation with the Orthopaedic Research Society

ORS
Orthopaedic Research Society

Downloads

Citations

Altmetrics

Permissions

***PLEASE NOTE:** If the links highlighted here do not take you to those web sites, please copy and paste address in your browser.

Permission to reproduce Wiley journal Content:

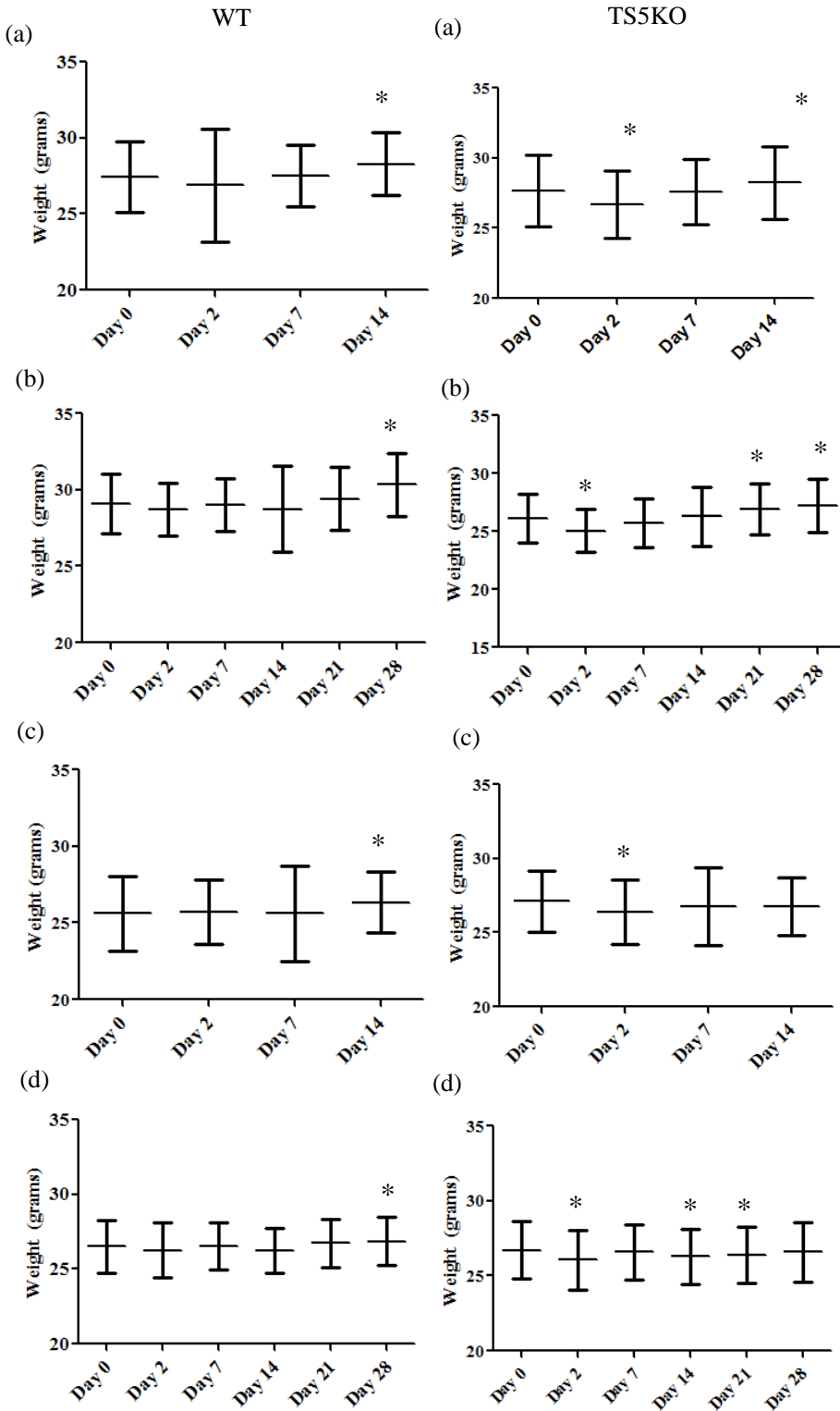
Requests to reproduce material from John Wiley & Sons publications are being handled through the RightsLink® automated permissions service.

Simply follow the steps below to obtain permission via the Rightslink® system:

- Locate the article you wish to reproduce on Wiley Online Library (<http://onlinelibrary.wiley.com>)
- Click on the 'Request Permissions' link, under the 'ARTICLE TOOLS' menu on the abstract page (also available from Table of Contents or Search Results)
- Follow the online instructions and select your requirements from the drop down options and click on 'quick price' to get a quote
- Create a RightsLink® account to complete your transaction (and pay, where applicable)
- Read and accept our Terms & Conditions and download your license
- For any technical queries please contact customer-care@copyright.com
- For further information and to view a Rightslink® demo please visit www.wiley.com and select Rights & Permissions.

AUTHORS - If you wish to reuse your own article (or an amended version of it) in a new publication of which you are the author, editor or co-editor, prior permission is not required (with the usual acknowledgements). However, a formal grant of license can be downloaded free of charge from RightsLink by selecting "Author of this Wiley article" as your requestor type.

Appendix C: Mouse weights measured each week during the experimental time-course: a) 14dCA, b) 28dCA, c) 14dTM, d) 28dTM. (* $p < 0.05$ relative to UI; One-way repeated measures ANOVA)



Appendix D: Chromatin modification enzyme array expression levels of TS5KO 14d pools for outlier analysis

Group	Gene	Pool 1	Pool 2	Pool 3	Average (STD)	Average (STD) with Pool 3 removed
DM	<i>Dnmt3a</i>	8.91	17.40	0.36	8.89 (8.52)	13.15 (6.01)
	<i>Dnmt1</i>	9.85	10.11	2.57	7.51 (4.28)	9.98 (0.18)
	<i>Dnmt3b</i>	0.82	1.87	ND	1.34 (0.74)	1.34 (0.74)
DHD	<i>Kdm1a</i>	24.90	32.39	0.50	19.26 (16.67)	28.64 (5.30)
	<i>Kdm5b</i>	18.93	32.05	5.43	18.81 (13.31)	25.49 (9.27)
	<i>Kdm4a</i>	9.19	21.93	1.25	10.79 (10.43)	15.56 (9.01)
	<i>Kdm6b</i>	9.42	20.92	0.48	10.27 (10.24)	15.17 (8.13)
	<i>Kdm5c</i>	7.76	19.67	0.03	9.15 (9.89)	13.72 (8.42)
	<i>Kdm4c</i>	10.59	15.47	1.15	9.07 (7.28)	13.03 (3.45)
HA	<i>Kat5</i>	14.17	20.71	2.72	12.54 (9.10)	17.44 (4.63)
	<i>Kat8</i>	7.26	10.04	0.31	5.87 (5.01)	8.65 (1.97)
	<i>Kat2b</i>	60.04	52.80	17.66	43.50 (22.67)	56.42 (5.12)
	<i>Kat6a</i>	24.23	34.81	1.14	20.06 (17.22)	29.52 (7.48)
	<i>Kat7</i>	16.69	31.75	1.15	16.53 (15.30)	24.22 (10.65)
	<i>Hat1</i>	17.77	14.87	11.47	14.70 (3.15)	16.32 (2.05)
	<i>Kat2a</i>	9.03	16.78	0.24	8.68 (8.28)	12.90 (5.48)
	<i>Ncoa1</i>	8.71	15.45	0.80	8.32 (7.34)	12.08 (4.76)
	<i>Ncoa3</i>	11.37	12.66	1.33	8.45 (6.20)	12.01 (0.91)
	<i>Kat6b</i>	9.45	13.84	0.52	7.94 (6.79)	11.64 (3.11)
	<i>Esco1</i>	9.14	13.66	1.87	8.22 (5.95)	11.40 (3.20)
	<i>Cdyl</i>	6.90	12.61	0.90	6.80 (5.86)	9.75 (4.04)
	<i>Atf2</i>	8.09	8.76	0.92	5.93 (4.35)	8.43 (0.47)
	<i>Csrp2bp</i>	5.32	9.42	0.22	4.99 (4.61)	7.37 (2.90)
	<i>Ncoa6</i>	5.18	5.07	0.02	3.42 (2.95)	5.13 (0.08)
<i>Ciita</i>	1.33	2.16	0.76	1.42 (0.70)	1.75 (0.58)	
<i>Esco2</i>	0.43	1.66	0.19	0.76 (0.79)	1.05 (0.87)	
HD	<i>Hdac2</i>	33.57	62.54	21.37	39.16 (21.15)	48.06 (20.49)
	<i>Hdac7</i>	42.53	46.52	3.86	30.97 (23.56)	44.52 (2.82)
	<i>Hdac1</i>	25.42	48.97	2.56	25.65 (23.21)	37.20 (16.65)
	<i>Hdac3</i>	16.33	28.78	1.29	15.47 (13.76)	22.55 (8.80)
	<i>Hdac5</i>	17.71	25.57	1.00	14.76 (12.55)	21.64 (5.56)
	<i>Hdac4</i>	7.29	13.75	0.43	7.15 (6.66)	10.52 (4.57)
	<i>Hdac8</i>	6.53	12.25	0.70	6.49 (5.77)	9.39 (4.04)
	<i>Hdac9</i>	7.03	6.68	0.22	4.65 (3.83)	6.86 (0.25)
	<i>Hdac6</i>	4.24	6.29	0.78	3.77 (2.78)	5.27 (1.45)
	<i>Hdac10</i>	3.89	6.29	0.33	3.50 (3.00)	5.09 (1.70)
	<i>Hdac11</i>	1.97	2.92	0.28	1.71 (1.34)	2.45 (0.67)

HM	<i>Ehmt2</i>	25.70	41.52	1.05	22.76 (20.39)	33.61 (11.18)
	<i>Prmt1</i>	20.58	41.56	2.36	21.503 (19.61)	31.07 (14.83)
	<i>Kmt2c</i>	22.73	31.93	1.70	18.79 (15.49)	27.33 (6.51)
	<i>Carm1</i>	19.25	32.54	0.26	17.35 (16.22)	25.89 (9.39)
	<i>Smyd1</i>	21.30	19.50	0.48	13.76 (11.53)	20.40 (1.27)
	<i>Prmt5</i>	12.05	12.84	0.17	8.36 (7.10)	12.45 (0.56)
	<i>Prmt3</i>	7.22	14.53	0.42	7.39 (7.06)	10.88 (5.17)
	<i>Ehmt1</i>	7.95	12.25	0.18	6.79 (6.12)	10.10 (3.04)
	<i>Prmt7</i>	9.25	9.07	2.31	6.88 (3.96)	9.16 (0.12)
	<i>Prmt2</i>	5.78	12.00	0.19	5.99 (5.90)	8.89 (4.40)
	<i>Dot1l</i>	5.98	11.49	0.06	5.84 (5.71)	8.73 (3.89)
	<i>Suv39h1</i>	2.84	6.49	0.04	3.12 (3.24)	4.66 (2.59)
	<i>Setdb2</i>	2.75	5.63	0.48	2.95 (2.58)	4.19 (2.04)
	<i>Prmt6</i>	2.22	4.33	0.02	2.19 (2.16)	3.27 (1.49)
<i>Smyd3</i>	2.82	3.31	0.29	2.14 (1.62)	3.06 (0.34)	
HP	<i>Rps6ka3</i>	37.22	67.76	5.78	36.92 (30.99)	52.49 (21.60)
	<i>Pak1</i>	5.99	13.35	1.62	6.99 (5.93)	9.67 (5.20)
	<i>Nek6</i>	4.32	7.58	1.50	4.47 (3.04)	5.95 (2.30)
	<i>Dzip3</i>	3.16	4.98	0.68	2.94 (2.16)	4.07 (1.29)
	<i>Rps6ka5</i>	3.44	4.43	0.21	2.70 (2.21)	3.94 (0.70)
	<i>Aurkb</i>	0.43	2.19	ND	1.31 (1.24)	1.31 (1.24)
	<i>Aurka</i>	0.68	1.10	0.02	0.60 (0.55)	0.89 (0.30)
HU	<i>Ube2b</i>	101.64	151.26	45.67	99.52 (52.83)	126.451 (35.08)
	<i>Usp16</i>	23.64	41.90	3.54	23.03 (19.19)	32.77 (12.92)
	<i>Rnf20</i>	21.65	36.61	2.16	20.14 (17.27)	29.13 (10.58)
	<i>Ube2a</i>	23.30	32.83	5.01	20.38 (14.14)	28.06 (6.74)
	<i>Usp22</i>	14.79	31.90	1.11	15.94 (15.43)	23.35 (12.10)
	<i>Mysm1</i>	10.50	22.17	2.82	11.83 (9.75)	16.34 (8.25)
	<i>Usp21</i>	13.08	15.57	1.34	10.00 (7.60)	14.32 (1.76)
	<i>Rnf2</i>	7.70	15.61	1.21	8.17 (7.21)	11.65 (5.59)
SET	<i>Kmt2e</i>	56.95	94.90	5.75	52.53 (44.74)	75.93 (26.84)
	<i>Setd7</i>	32.17	61.53	1.44	31.72 (30.05)	46.85 (20.76)
	<i>Setd2</i>	28.78	38.39	4.36	23.84 (17.55)	33.59 (6.80)
	<i>Setd8</i>	21.61	28.05	0.81	16.82 (14.23)	24.83 (4.55)
	<i>Setd1b</i>	15.11	30.49	1.38	15.66 (14.56)	22.80 (10.87)
	<i>Nsd1</i>	14.49	30.03	0.71	15.07 (14.67)	22.26 (10.99)
	<i>Setd3</i>	17.27	25.82	0.46	14.51 (12.90)	21.54 (6.05)
	<i>Whsc1</i>	12.97	28.21	0.97	14.05 (13.65)	20.59 (10.78)
	<i>Suv420h1</i>	14.10	25.62	1.38	13.70 (12.13)	19.86 (8.15)
	<i>Ash1l</i>	15.58	18.00	0.56	11.38 (9.45)	16.79 (1.71)
	<i>Setd5</i>	7.10	18.70	0.48	8.76 (9.22)	12.90 (8.21)
	<i>Setdb1</i>	7.50	15.19	0.56	7.75 (7.32)	11.35 (5.44)

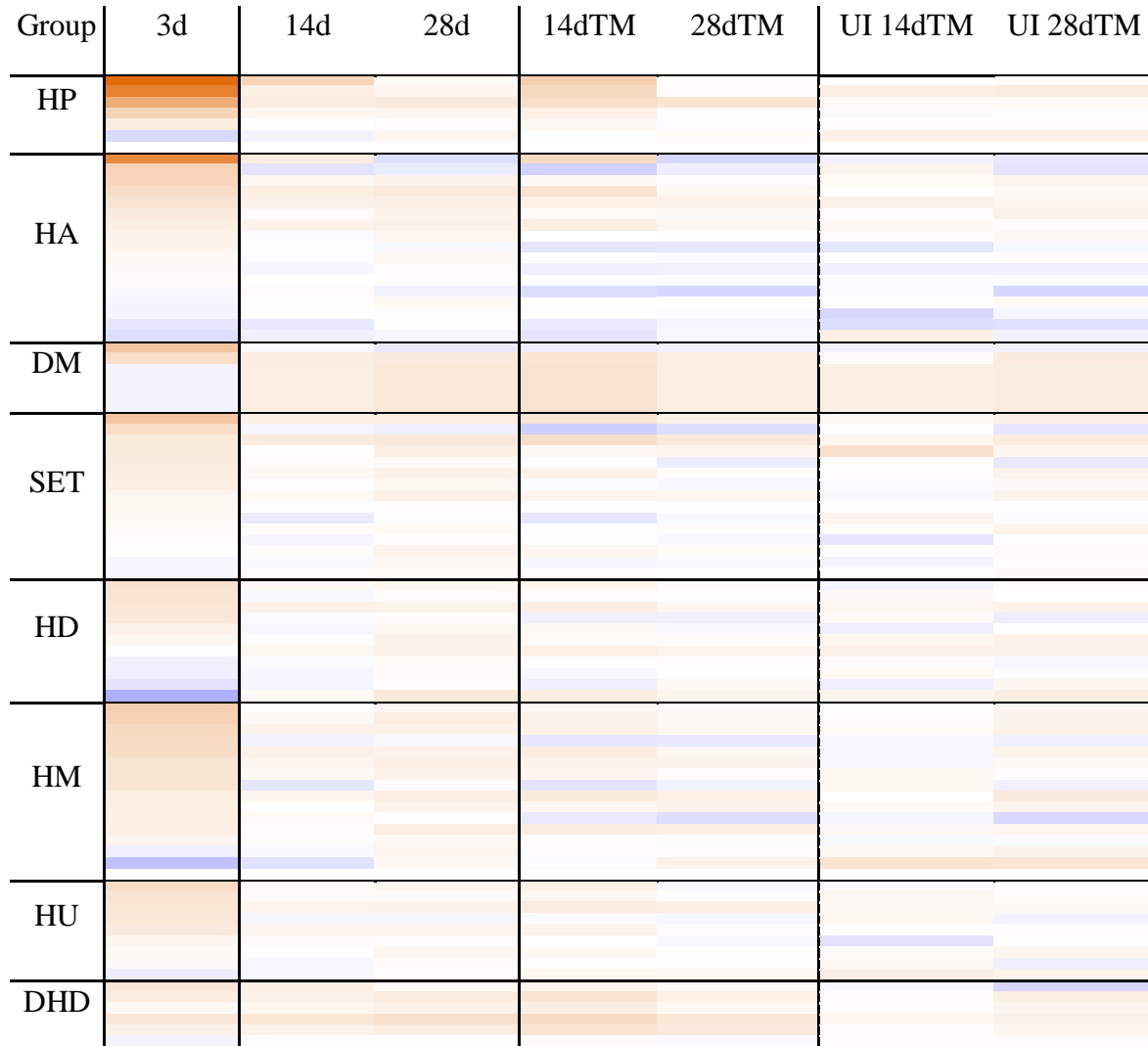
<i>Setd1a</i>	7.27	13.32	0.43	7.01 (6.45)	10.30 (4.28)
<i>Setd6</i>	9.64	10.05	1.38	7.02 (4.89)	9.85 (0.29)
<i>Setd4</i>	1.11	1.80	0.21	1.04 (0.79)	1.45 (0.49)

Abundance values ($2^{-\Delta Ct} * 1000$) presented for 3 pools of 12-20 tendons with average (standard deviation) before and after outlier removal listed in right hand columns. *Aurkc* and *Prmt8* removed as transcripts were not detected in assay

Appendix E: Thermo-Lifetech Taqman qt-PCR primer information

Gene	qt-PCR Primer
<i>B2m</i>	Mm00437762_m1
<i>Baiap211</i>	Mm00508802_m1
<i>Cend1</i>	Mm00517505_m1
<i>Cnot7</i>	Mm00516123_m1
<i>Foxf1</i>	Mm00484797_m1
<i>Foxr1</i>	Mm02600883_m1
<i>Gnas</i>	Mm01242435_m1
<i>Grm4</i>	Mm01306128_m1
<i>Hoxc4</i>	Mm00442838_m1
<i>Igfbp6</i>	Mm00599696_m1
<i>Leprel2</i>	Mm00600144_m1
<i>Mirlet7c-2</i>	Mm04238179_m1
<i>Mmp25</i>	Mm01309189_m1
<i>Peg12</i>	Mm00844053_m1
<i>Rbmxl2</i>	Mm02392382_m1
<i>Sfi1</i>	Mm03039570_m1
<i>Shisa7</i>	Mm01337245_m1
<i>Usp9x</i>	Mm00464734_m1
<i>Zrsr1</i>	Mm00495837_m1

Appendix F: Heat map representation of the chromatin modification enzyme array for all WT groups.



Max up-regulated (orange) 64-fold, max down-regulated (blue) 64-fold. Groups: DHD (DNA/Histone Demethylases), DM (DNA Methyltransferases), HA (Histone Acetyltransferases), HD (Histone Deacetylases), HM (Histone Methyltransferases), HP (Histone Phosphorylation), HU (Histone Ubiquitination), SET (SET Domain Proteins; Histone Methyltransferase Activity)

Appendix G: Heat map representation of the chromatin modification enzyme array for all TS5KO groups.



Max up-regulated (orange) 64-fold, max down-regulated (blue) 64-fold. Groups: DHD (DNA/Histone Demethylases), DM (DNA Methyltransferases), HA (Histone Acetyltransferases), HD (Histone Deacetylases), HM (Histone Methyltransferases), HP (Histone Phosphorylation), HU (Histone Ubiquitination), SET (SET Domain Proteins; Histone Methyltransferase Activity)

Appendix H: Expression levels of chromatin modification enzymes in UI mouse tendons

Group	Gene	WT				TS5KO			
		Pool 1	Pool 2	Pool 3	Average (STD)	Pool 1	Pool 2	Pool 3	Average (STD)
DM	<i>Dnmt1</i>	18.19	13.38	8.14	13.24 (5.02)	9.40	6.27	12.39	9.35 (3.06)
	<i>Dnmt3a</i>	5.30	8.49	6.36	6.71 (1.62)	2.64	7.81	6.56	5.67 (2.70)
	<i>Dnmt3b</i>	0.68	0.94	0.67	0.76 (0.15)	0.36	0.79	0.49	0.55 (0.22)
DHD	<i>Kdm5b</i>	22.12	27.48	21.69	23.77 (3.22)	8.56	17.86	8.03	11.48 (5.53)*
	<i>Kdm1a</i>	19.77	22.88	12.04	18.23 (5.58)	7.00	11.61	9.30	9.30 (2.31)
	<i>Kdm4c</i>	9.63	10.67	7.34	9.21 (1.70)	4.04	10.68	6.84	7.19 (3.33)
	<i>Kdm4a</i>	8.49	10.75	7.51	8.92 (1.66)	3.32	11.75	9.71	8.26 (4.40)
	<i>Kdm6b</i>	6.06	14.55	3.66	8.09 (5.73)	1.75	8.50	3.99	4.75 (3.44)
	<i>Kdm5c</i>	3.49	8.09	4.82	5.47 (2.37)	1.75	8.90	4.17	4.94 (3.64)
HA	<i>Kat2b</i>	60.53	68.39	79.46	69.46 (9.51)	72.02	62.86	77.00	70.63 (7.17)
	<i>Kat6a</i>	28.26	29.68	28.29	28.74 (0.81)	13.60	26.48	19.00	19.69 (6.47)
	<i>Hat1</i>	28.03	27.70	24.88	26.87 (1.73)	24.65	21.55	25.44	23.88 (2.06)
	<i>Kat7</i>	22.91	24.24	20.27	22.47 (2.02)	9.03	21.36	13.50	14.63 (6.24)
	<i>Kat5</i>	22.11	21.05	21.94	21.70 (0.57)	10.64	19.14	15.49	15.09 (4.26)
	<i>Ncoa3</i>	18.63	30.70	15.45	21.59 (8.05)	5.80	12.40	9.64	9.28 (3.31)*
	<i>Ncoa1</i>	14.05	14.07	11.91	13.34 (1.24)	4.74	13.18	8.71	8.88 (4.23)
	<i>Esco1</i>	11.40	13.18	12.17	12.25 (0.89)	5.76	10.54	6.75	7.68 (2.53)
	<i>Kat6b</i>	11.76	10.79	9.72	10.76 (1.02)	5.72	6.08	6.76	6.19 (0.53)*
	<i>Kat2a</i>	12.32	8.38	9.26	9.99 (2.07)	4.05	10.01	5.49	6.51 (3.11)
	<i>Atf2</i>	8.07	11.55	7.31	8.98 (2.26)	6.54	6.16	5.94	6.21 (0.30)
	<i>Kat8</i>	9.57	7.41	7.38	8.12 (1.26)	3.24	8.12	5.14	5.50 (2.46)
	<i>Cdyl</i>	5.15	8.34	7.05	6.84 (1.61)	2.43	6.22	5.58	4.74 (2.03)
	<i>Ncoa6</i>	8.34	5.75	6.45	6.84 (1.34)	2.55	4.63	3.07	3.42 (1.08)*
	<i>Csrp2bp</i>	5.12	5.62	4.78	5.17 (0.42)	1.96	6.22	4.69	4.29 (2.16)
<i>Ciita</i>	0.77	1.13	1.31	1.07 (0.28)	0.47	0.81	0.75	0.67 (0.18)	
<i>Esco2</i>	0.56	0.51	0.28	0.45 (0.15)	0.18	0.18	0.06	0.14 (0.07)*	
HD	<i>Hdac2</i>	44.09	53.14	48.91	48.71 (4.53)	42.57	47.55	39.42	43.18 (4.10)
	<i>Hdac7</i>	41.68	35.36	52.53	43.19 (8.69)	28.95	37.78	41.48	36.07 (6.44)
	<i>Hdac1</i>	28.54	37.51	26.03	30.69 (6.03)	9.14	27.76	20.13	19.01 (9.36)
	<i>Hdac5</i>	19.72	19.63	24.84	21.40 (2.98)	9.19	21.65	14.34	15.06 (6.26)
	<i>Hdac3</i>	13.40	20.04	15.83	16.42 (3.36)	9.54	19.00	13.31	13.95 (4.76)
	<i>Hdac4</i>	8.89	11.30	7.39	9.20 (1.97)	2.96	11.48	5.10	6.51 (4.43)
	<i>Hdac8</i>	5.86	8.76	6.96	7.20 (1.46)	2.92	6.95	5.13	5.00 (2.02)
	<i>Hdac9</i>	6.68	6.42	4.06	5.72 (1.44)	4.67	5.61	3.75	4.67 (0.93)
	<i>Hdac10</i>	6.25	6.21	3.31	5.26 (1.68)	11.99	3.88	2.78	6.22 (5.03)
	<i>Hdac6</i>	4.49	4.08	4.78	4.45 (0.35)	2.76	4.70	3.47	3.64 (0.98)
	<i>Hdac11</i>	1.49	2.60	1.71	1.93 (0.59)	0.99	2.20	1.75	1.64 (0.61)
HM	<i>Prmt1</i>	29.43	29.45	25.20	28.03 (2.45)	14.68	28.58	21.62	21.63 (6.95)
	<i>Kmt2c</i>	25.59	34.22	23.41	27.74 (5.72)	10.02	27.23	16.09	17.78 (8.73)

	<i>Ehmt2</i>	17.01	18.51	23.12	19.54 (3.19)	7.59	22.04	12.76	14.13 (7.32)
	<i>Smyd1</i>	16.97	16.57	22.98	18.84 (3.59)	19.55	39.95	21.33	26.94 (11.30)
	<i>Carm1</i>	17.13	17.03	17.85	17.34 (0.45)	8.50	18.18	11.52	12.73 (4.95)
	<i>Prmt5</i>	17.71	14.12	15.45	15.76 (1.82)	7.75	13.99	13.72	11.82 (3.53)
	<i>Prmt7</i>	13.18	10.30	12.56	12.01 (1.52)	12.98	12.68	16.25	13.97 (1.98)
	<i>Ehmt1</i>	11.37	7.69	8.35	9.14 (1.96)	4.50	8.85	4.58	5.98 (2.49)
	<i>Prmt2</i>	10.85	7.72	6.31	8.29 (2.33)	1.99	6.42	4.02	4.14 (2.22)
	<i>Prmt3</i>	7.99	7.73	6.70	7.47 (0.68)	3.42	8.40	5.83	5.88 (2.49)
	<i>Dot11</i>	5.01	7.65	3.13	5.26 (2.27)	1.58	6.86	2.84	3.76 (2.76)
	<i>Suv39h1</i>	3.48	3.82	2.69	3.33 (0.58)	1.09	3.17	2.25	2.17 (1.04)
	<i>Setdb2</i>	2.21	3.08	2.71	2.67 (0.44)	1.57	2.78	2.17	2.18 (0.61)
	<i>Smyd3</i>	2.68	2.72	1.91	2.44 (0.45)	0.96	1.99	1.90	1.62 (0.57)
	<i>Prmt6</i>	1.56	2.69	2.51	2.25 (0.61)	0.72	2.15	1.71	1.53 (0.73)
HP	<i>Rps6ka3</i>	41.52	59.19	42.52	47.74 (9.92)	27.68	50.29	25.58	34.52 (13.70)
	<i>Nek6</i>	3.62	4.00	4.02	3.88 (0.22)	2.58	4.28	3.72	3.53 (0.86)
	<i>Pak1</i>	3.47	3.62	3.57	3.55 (0.07)	3.31	4.67	3.16	3.71 (0.84)
	<i>Rps6ka5</i>	3.75	5.13	4.26	4.38 (0.70)	1.76	4.04	2.27	2.69 (1.20)
	<i>Aurka</i>	0.47	0.39	0.49	0.45 (0.05)	0.46	0.83	0.35	0.55 (0.25)
	<i>Aurkb</i>	0.67	0.23	0.26	0.39 (0.24)	0.14	0.43	0.08	0.21 (0.18)
HU	<i>Ube2b</i>	102.52	147.00	136.67	128.73 (23.28)	151.23	175.03	148.63	158.30 (14.55)
	<i>Ube2a</i>	26.89	29.57	30.17	28.88 (1.75)	25.87	25.44	31.74	27.68 (3.52)
	<i>Usp16</i>	23.75	32.11	27.83	27.89 (4.18)	17.68	30.82	22.42	23.64 (6.65)
	<i>Rnf20</i>	15.76	22.75	17.52	18.68 (3.63)	10.96	19.99	10.53	13.83 (5.34)
	<i>Usp22</i>	18.23	17.49	15.34	17.02 (1.50)	6.64	14.41	11.96	11.00 (3.97)
	<i>Mysm1</i>	13.41	19.54	14.73	15.89 (3.23)	7.63	17.14	10.10	11.63 (4.93)
	<i>Usp21</i>	15.69	14.44	17.04	15.72 (1.30)	7.75	11.73	15.22	11.57 (3.74)
	<i>Rnf2</i>	9.61	10.13	10.09	9.94 (0.29)	4.33	8.15	6.42	6.30 (1.91)
	<i>Dzip3</i>	3.84	3.47	2.58	3.30 (0.65)	1.67	2.65	1.66	1.99 (0.57)
SET	<i>Kmt2e</i>	90.90	95.25	84.66	90.27 (5.33)	28.09	74.78	45.46	49.45 (23.60)
	<i>Setd7</i>	39.63	40.29	49.11	43.01 (5.29)	21.05	46.82	42.15	36.67 (13.73)
	<i>Setd2</i>	28.18	30.36	33.87	30.80 (2.87)	13.15	26.74	18.52	19.47 (6.84)
	<i>Setd8</i>	24.28	18.34	25.76	22.79 (3.93)	15.65	21.99	20.89	19.51 (3.39)
	<i>Ash11</i>	22.28	20.75	17.82	20.28 (2.26)	7.93	15.97	9.89	11.26 (4.20)*
	<i>Setd3</i>	15.79	21.96	22.14	19.96 (3.62)	10.32	17.96	12.79	13.69 (3.90)
	<i>Nsd1</i>	16.29	21.24	13.24	16.92 (4.04)	6.48	16.53	10.93	11.32 (5.04)
	<i>Setd1b</i>	16.88	17.43	15.47	16.59 (1.01)	5.79	16.98	12.35	11.71 (5.62)
	<i>Suv420h1</i>	14.60	20.74	14.40	16.58 (3.60)	7.76	17.72	13.62	13.03 (5.01)
	<i>Setd6</i>	13.28	12.48	15.09	13.62 (1.34)	9.01	11.69	15.62	12.11 (3.32)
	<i>Setd1a</i>	10.62	10.68	9.34	10.22 (0.75)	3.24	8.42	5.25	5.64 (2.61)
	<i>Whsc1</i>	8.25	11.58	9.30	9.71 (1.70)	3.88	12.19	7.67	7.92 (4.16)
	<i>Setdb1</i>	8.08	8.32	9.23	8.54 (0.61)	4.04	7.70	5.88	5.87 (1.83)
	<i>Setd5</i>	6.05	9.30	5.26	6.87 (2.14)	2.00	7.57	5.69	5.08 (2.84)
	<i>Setd4</i>	0.91	1.01	1.34	1.08 (0.22)	0.53	1.05	1.09	0.89 (0.31)

Abundance values ($2^{-\Delta Ct} * 1000$) presented for 3 pools of 12-20 tendons with average (standard deviation) listed in right hand column. * $p < 0.05$ relative to WT UI. *Aurkc* and *Prmt8* removed as transcripts were not detected in assay

Appendix I: CpG site information for genes with DM CpG promoter sites in WT mice

Chrom	Chrom Start Site	Chrom End Site	Gene	3d	14d	28d	14dTM	28dTM
2	174297455	174297456	<i>Gnas</i>			*		
2	174297475	174297476				*		
5	1.44E+08	1.44E+08	<i>Baiap2l1</i>	*				
6	124857399	124857400	<i>Leprel2</i>			*		
6	124857418	124857419				*		
6	124857420	124857421				*		
6	124857423	124857424				*		
7	141429296	141429297	<i>Cendl1</i>	*				
7	141429290	141429291		*				
7	141429255	141429256		*				
7	107210018	107210019	<i>Rbmxl2</i>	*				
7	62464084	62464085	<i>Peg12</i>					*
7	4844837	4844838	<i>Shisa7</i>					*
8	121085119	121085120	<i>Foxfl</i>			*		
8	40511554	40511555	<i>Cnot7</i>					*
8	40511575	40511576						*
9	44440726	44440727	<i>Foxr1</i>	*		*		
11	22972184	22972185	<i>Zrsr1</i>			*		
11	3193042	3193043	<i>Sfil</i>				*	
15	85706041	85706042	<i>Mirlet7c-2</i>	*				
15	85706037	85706038		*				
15	103034611	103034612	<i>Hoxc4</i>			*		
15	103034614	103034615				*		
15	103034647	103034648				*		
15	102144621	102144622	<i>Igfbp6</i>				*	
17	27502932	27502933	<i>Grm4</i>	*				
17	23644684	23644685	<i>Mmp25</i>				*	
19	47512391	47512392	<i>Gm19557</i>	*				
19	47512352	47512353		*				
X	13072040	13072041	<i>Usp9x</i>					*

* DM relative to UI levels; Chrom=Chromosome

Appendix J: Expression levels of genes identified by methylome analysis in WT mice

Gene	UI			3d		
	1	2	3	1	2	3
<i>Baiap2l1</i>	9.74	2.20	8.25	18.03	18.81	12.62
<i>Cend1</i>	0.33	0.14	0.17	0.58	0.91	0.64
<i>Cnot7</i>	17.86	7.91	28.15	111.58	59.98	42.15
<i>Foxf1</i>	1.18	0.47	1.96	1.51	2.35	1.20
<i>Foxr1</i>	ND	ND	ND	ND	ND	ND
<i>Gnas</i>	1178.78	427.18	1157.35	1173.19	1397.87	396.88
<i>Grm4</i>	0.20	0.11	0.34	0.24	0.41	0.20
<i>Hoxc4</i>	1675.82	572.14	1317.95	565.06	516.74	297.67
<i>Igfbp6</i>	72.90	22.29	60.50	85.12	93.05	84.80
<i>Leprel2</i>	27.49	6.11	20.74	8.53	10.15	7.05
<i>Mirlet7c-2</i>	0.23	0.66	0.28	0.79	0.97	0.79
<i>Mmp25</i>	0.39	0.17	0.33	1.18	0.63	0.56
<i>Peg12</i>	35.85	4.16	6.15	4.52	3.96	2.17
<i>Rbmxl2</i>	7.89	3.43	8.98	10.89	14.99	11.03
<i>Sfi1</i>	ND	ND	ND	ND	ND	ND
<i>Shisa7</i>	12.82	3.60	22.99	27.09	35.66	71.63
<i>Usp9x</i>	33.50	7.74	25.46	11.00	15.26	7.76
<i>Zrsr1</i>	9.74	2.20	8.25	18.03	18.81	12.62
Gene	28d			14d		
	1	2	3	1	2	3
<i>Baiap2l1</i>	3.32	4.92	8.70	8.24	6.76	11.73
<i>Cend1</i>	0.12	0.10	0.17	0.19	0.41	0.50
<i>Cnot7</i>	19.03	15.13	14.84	23.18	11.14	38.83
<i>Foxf1</i>	1.09	0.79	0.80	0.27	0.77	4.53
<i>Foxr1</i>	ND	ND	ND	ND	ND	ND
<i>Gnas</i>	598.41	336.57	521.24	966.92	640.39	1483.70
<i>Grm4</i>	0.18	0.11	0.22	0.18	0.20	0.38
<i>Hoxc4</i>	756.67	695.87	848.21	2052.62	1767.41	1194.85
<i>Igfbp6</i>	62.37	29.06	43.83	73.83	85.65	173.50
<i>Leprel2</i>	12.36	10.31	19.37	15.60	15.43	10.36
<i>Mirlet7c-2</i>	0.16	0.18	0.32	1.18	0.75	1.83
<i>Mmp25</i>	0.36	0.17	0.28	0.93	0.65	0.09
<i>Peg12</i>	14.68	8.04	8.07	7.99	10.39	ND
<i>Rbmxl2</i>	9.35	4.93	5.39	5.57	5.33	17.71
<i>Sfi1</i>	ND	ND	ND	ND	ND	ND
<i>Shisa7</i>	11.19	6.75	0.58	19.54	14.77	40.79
<i>Usp9x</i>	23.26	17.94	14.43	24.52	18.65	20.35
<i>Zrsr1</i>	3.32	4.92	8.70	8.24	6.76	11.73
Gene	14dTM			28dTM		
	1	2	3	1	2	3
<i>Baiap2l1</i>	3.33	9.67	20.56	8.18	12.91	6.62

<i>Cend1</i>	0.11	0.50	1.00	0.14	0.47	0.26
<i>Cnot7</i>	13.61	24.38	44.71	19.35	7.14	2.55
<i>Foxf1</i>	0.74	3.64	4.99	1.28	2.34	1.30
<i>Foxr1</i>	ND	ND	ND	ND	ND	ND
<i>Gnas</i>	319.12	962.53	2135.05	808.70	1171.56	504.90
<i>Grm4</i>	0.13	0.28	0.59	0.28	0.31	0.12
<i>Hoxc4</i>	351.11	1060.64	2956.66	885.99	1446.59	1289.90
<i>Igfbp6</i>	76.13	158.24	301.74	67.48	85.20	41.58
<i>Leprel2</i>	6.13	13.16	24.74	21.52	36.72	19.41
<i>Mirlet7c-2</i>	0.26	1.54	2.19	0.25	0.43	0.31
<i>Mmp25</i>	0.03	4.69	12.62	4.96	0.08	0.06
<i>Peg12</i>	4.12	4.03	20.90	10.62	10.99	16.15
<i>Rbmxl2</i>	7.06	17.28	25.21	10.51	14.77	7.46
<i>Sfi1</i>	ND	ND	ND	ND	ND	ND
<i>Shisa7</i>	10.71	23.85	80.41	10.23	18.68	10.73
<i>Usp9x</i>	10.14	25.26	25.51	19.76	21.84	11.51
<i>Zrsr1</i>	3.33	9.67	20.56	8.18	12.91	6.62

Abundance values ($2^{-\Delta Ct} * 1000$) presented for 3 pools (listed as #1-3) of 12-20 tendons per experimental group

Appendix K: Expression levels of novel tendinopathy in UI TS5KO mouse tendons

Gene	Pool 1	Pool 2	Pool 3	Average (STD)
<i>Foxf1</i>	0.62	-	1.71	1.17 (0.77)
<i>Igfbp6</i>	869.53	-	1755.73	1312.63 (626.64)
<i>Leprel2</i>	30.50	-	57.69	44.09 (19.22)
<i>Mmp25</i>	0.04	-	0.11	0.07 (0.05)
<i>Peg12</i>	1.88	-	2.03	1.95 (0.10)*

Abundance values ($2^{-\Delta Ct} * 1000$) presented for 2 pools of 12-20 tendons with average (standard deviation) listed in right hand column. Genes could not be assayed in the 2nd pool as there was not sufficient RNA left for analysis. * $p < 0.05$ relative to WT UI (Appendix J)

Appendix L: Hypoxia signaling array expression levels of TS5KO 14d pools for outlier analysis

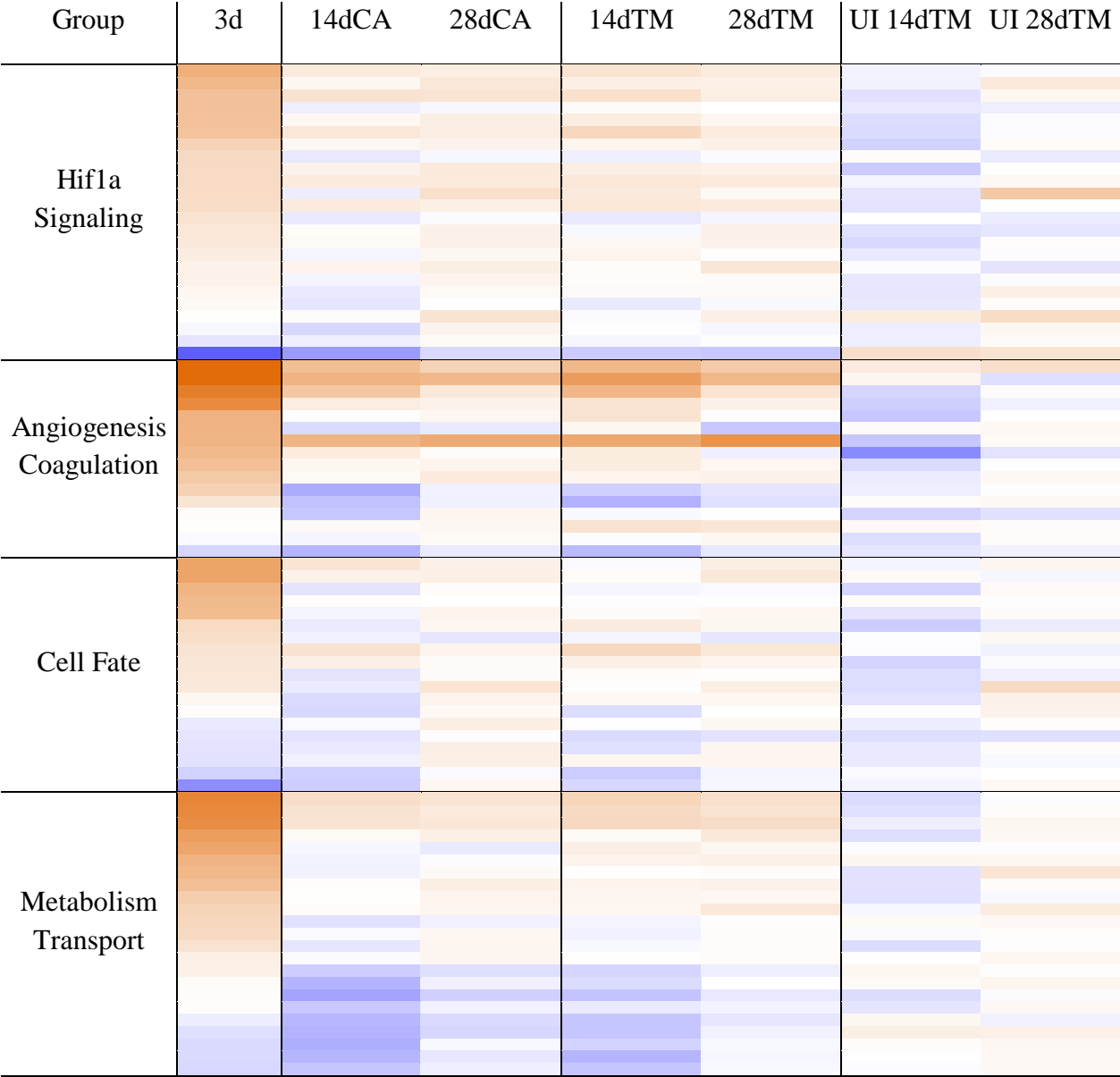
Group	Gene	Pool 1	Pool 2	Pool 3	Average (STD)	Average (STD) with Pool 3 removed
Hif1a Signaling	<i>Lgals3</i>	306.76	361.71	58.74	242.40 (161.41)	334.24 (38.85)
	<i>P4hb</i>	180.85	364.00	45.15	196.67 (160.01)	272.43 (129.50)
	<i>Ctsa</i>	52.38	71.87	2.16	42.14 (35.97)	62.12 (13.78)
	<i>P4ha1</i>	57.85	64.99	5.76	42.87 (32.33)	61.42 (5.05)
	<i>Hif1a</i>	38.79	80.15	9.56	42.83 (35.47)	59.47 (29.24)
	<i>Nfkb1</i>	42.96	34.59	2.39	26.65 (21.42)	38.78 (5.92)
	<i>Rbpj</i>	34.55	38.00	2.39	24.98 (19.64)	36.28 (2.44)
	<i>Egln1</i>	20.64	22.62	1.78	15.01 (11.50)	21.63 (1.40)
	<i>Bhlhe40</i>	22.56	20.62	1.49	14.89 (11.65)	21.59 (1.37)
	<i>Eif4ebp1</i>	18.96	21.18	8.44	16.19 (6.81)	20.07 (1.57)
	<i>Arnt</i>	16.57	17.96	0.70	11.74 (9.59)	17.27 (0.99)
	<i>Fos</i>	23.59	8.65	0.31	10.85 (11.79)	16.12 (10.56)
	<i>Egln2</i>	11.34	13.19	0.17	8.23 (7.04)	12.26 (1.30)
	<i>Per1</i>	12.94	11.33	1.36	8.54 (6.28)	12.14 (1.14)
	<i>Dnajc5</i>	10.01	12.18	0.61	7.60 (6.15)	11.09 (1.53)
	<i>Usf2</i>	10.65	11.52	0.08	7.42 (6.37)	11.08 (0.61)
	<i>Trp53</i>	6.61	8.76	0.79	5.39 (4.12)	7.68 (1.52)
	<i>Ncoa1</i>	8.91	7.50	0.84	5.75 (4.31)	8.20 (1.00)
	<i>Cops5</i>	7.56	8.72	2.91	6.40 (3.07)	8.14 (0.81)
	<i>Apex1</i>	5.24	5.74	0.77	3.92 (2.73)	5.49 (0.36)
<i>Hif1an</i>	5.07	5.48	0.36	3.64 (2.85)	5.28 (0.29)	
<i>Ankrd37</i>	4.35	5.51	1.79	3.88 (1.91)	4.93 (0.82)	
<i>Map3k1</i>	2.09	2.43	0.52	1.68 (1.02)	2.26 (0.24)	
<i>Hif3a</i>	0.26	0.12	ND	0.19 (0.10)	0.19 (0.10)	
Angiogenesis Coagulation	<i>Lox</i>	226.41	312.36	45.20	194.66 (136.38)	269.39 (60.78)
	<i>Anxa2</i>	238.06	292.46	51.65	194.06 (126.29)	265.26 (38.46)
	<i>Bnip3</i>	83.31	47.72	14.80	48.61 (34.26)	65.52 (25.16)
	<i>Angptl4</i>	59.82	65.67	3.40	42.96 (34.39)	62.74 (4.13)
	<i>Bnip3l</i>	43.31	44.78	9.19	32.42 (20.14)	44.05 (1.04)
	<i>Vegfa</i>	24.38	18.52	3.58	15.49 (10.73)	21.45 (4.14)
	<i>Serpine1</i>	27.34	15.29	1.14	14.59 (13.11)	21.31 (8.51)
	<i>Jmjd6</i>	9.45	10.19	0.56	6.73 (5.36)	9.82 (0.52)
	<i>F3</i>	6.80	9.15	1.44	5.80 (3.95)	7.97 (1.67)
	<i>Plau</i>	5.77	8.42	1.11	5.10 (3.70)	7.10 (1.88)

	<i>Mmp9</i>	1.17	12.01	0.24	4.47 (6.54)	6.59 (7.67)
	<i>Hmox1</i>	4.00	6.50	0.22	3.58 (3.16)	5.25 (1.77)
	<i>Edn1</i>	1.92	1.71	0.08	1.24 (1.00)	1.81 (0.15)
	<i>Pgf</i>	1.27	1.86	0.08	1.07 (0.91)	1.56 (0.42)
	<i>Adora2b</i>	0.38	0.20	ND	0.29 (0.12)	0.29 (0.12)
Cell Fate	<i>Txnip</i>	235.09	160.91	28.65	141.55 (104.57)	198.00 (52.46)
	<i>Igfbp3</i>	82.32	139.54	24.32	82.06 (57.61)	110.93 (40.46)
	<i>Mif</i>	73.28	114.04	19.39	68.90 (47.48)	93.66 (28.82)
	<i>Btg1</i>	44.73	64.30	2.77	37.26 (31.44)	54.51 (13.84)
	<i>Odc1</i>	35.72	51.66	3.94	30.44 (24.29)	43.69 (11.27)
	<i>Ddit4</i>	36.95	30.19	1.77	22.97 (18.67)	33.57 (4.78)
	<i>Egr1</i>	38.05	22.99	1.19	20.74 (18.53)	30.52 (10.65)
	<i>Ndr1</i>	33.82	24.68	2.38	20.30 (16.17)	29.25 (6.46)
	<i>Nampt</i>	31.14	25.73	10.30	22.39 (10.81)	28.43 (3.82)
	<i>Ier3</i>	14.84	17.07	0.91	10.94 (8.76)	15.95 (1.58)
	<i>Mxi1</i>	14.90	13.66	1.70	10.09 (7.29)	14.28 (0.88)
	<i>Ccng2</i>	10.43	12.11	1.35	7.96 (5.79)	11.27 (1.19)
	<i>Pim1</i>	6.19	9.86	1.15	5.73 (4.37)	8.03 (2.60)
	<i>Met</i>	7.99	7.76	0.26	5.34 (4.40)	7.88 (0.17)
	<i>Ruvbl2</i>	6.80	8.24	0.31	5.12 (4.23)	7.52 (1.02)
	<i>Nos3</i>	4.40	3.73	0.02	2.71 (2.36)	4.06 (0.47)
	<i>Atr</i>	3.19	4.16	0.31	2.55 (2.00)	3.67 (0.68)
		<i>Adm</i>	0.92	1.33	0.03	0.76 (0.67)
	<i>Blm</i>	1.09	1.15	0.11	0.78 (0.58)	1.12 (0.04)
Metabolism Transport	<i>Aldoa</i>	752.15	708.04	30.73	496.97 (404.38)	730.10 (31.19)
	<i>Ldha</i>	208.35	210.65	18.42	145.81 (110.33)	209.50 (1.62)
	<i>Eno1</i>	83.16	132.21	2.52	72.63 (65.48)	107.69 (34.68)
	<i>Tpi1</i>	96.72	114.66	14.62	75.33 (53.34)	105.69 (12.68)
	<i>Pkm</i>	76.31	131.26	0.42	69.330 (65.70)	103.78 (38.86)
	<i>Pgk1</i>	85.47	118.77	13.54	72.59 (53.78)	102.12 (23.55)
	<i>Vdac1</i>	96.36	97.68	22.06	72.03 (43.28)	97.02 (0.93)
	<i>Gpi1</i>	68.61	75.97	3.03	49.20 (40.16)	72.29 (5.20)
	<i>Pgam1</i>	37.84	57.46	1.19	32.16 (28.56)	47.65 (13.87)
	<i>Slc16a3</i>	7.64	56.78	0.01	21.48 (30.81)	32.21 (34.74)
	<i>Gys1</i>	23.54	22.00	0.52	15.35 (12.87)	22.77 (1.09)
	<i>Pfkl</i>	17.77	22.09	1.91	13.93 (10.63)	19.93 (3.06)
	<i>Pfkl</i>	10.87	13.08	1.06	8.34 (6.40)	11.98 (1.56)
	<i>Hk2</i>	11.56	8.13	0.49	6.72 (5.66)	9.84 (2.43)
	<i>Gbe1</i>	10.12	7.35	2.58	6.68 (3.81)	8.74 (1.96)
	<i>Pdk1</i>	7.74	9.07	0.15	5.65 (4.81)	8.40 (0.94)

<i>Tfrc</i>	8.34	7.01	1.01	5.45 (3.91)	7.68 (0.94)
<i>Ero1l</i>	6.28	8.41	1.56	5.41 (3.50)	7.34 (1.51)
<i>Slc2a1</i>	5.96	7.26	0.16	4.46 (3.78)	6.61 (0.92)
<i>Pfkfb4</i>	3.10	2.92	0.15	2.06 (1.66)	3.01 (0.13)
<i>Slc2a3</i>	1.37	1.15	0.03	0.85 (0.72)	1.26 (0.15)
<i>Pfkfb3</i>	1.17	0.82	0.14	0.71 (0.52)	0.99 (0.25)
<i>Car9</i>	0.45	0.82	0.04	0.44 (0.39)	0.64 (0.26)
<i>F10</i>	0.61	0.46	0.17	0.41 (0.22)	0.54 (0.11)

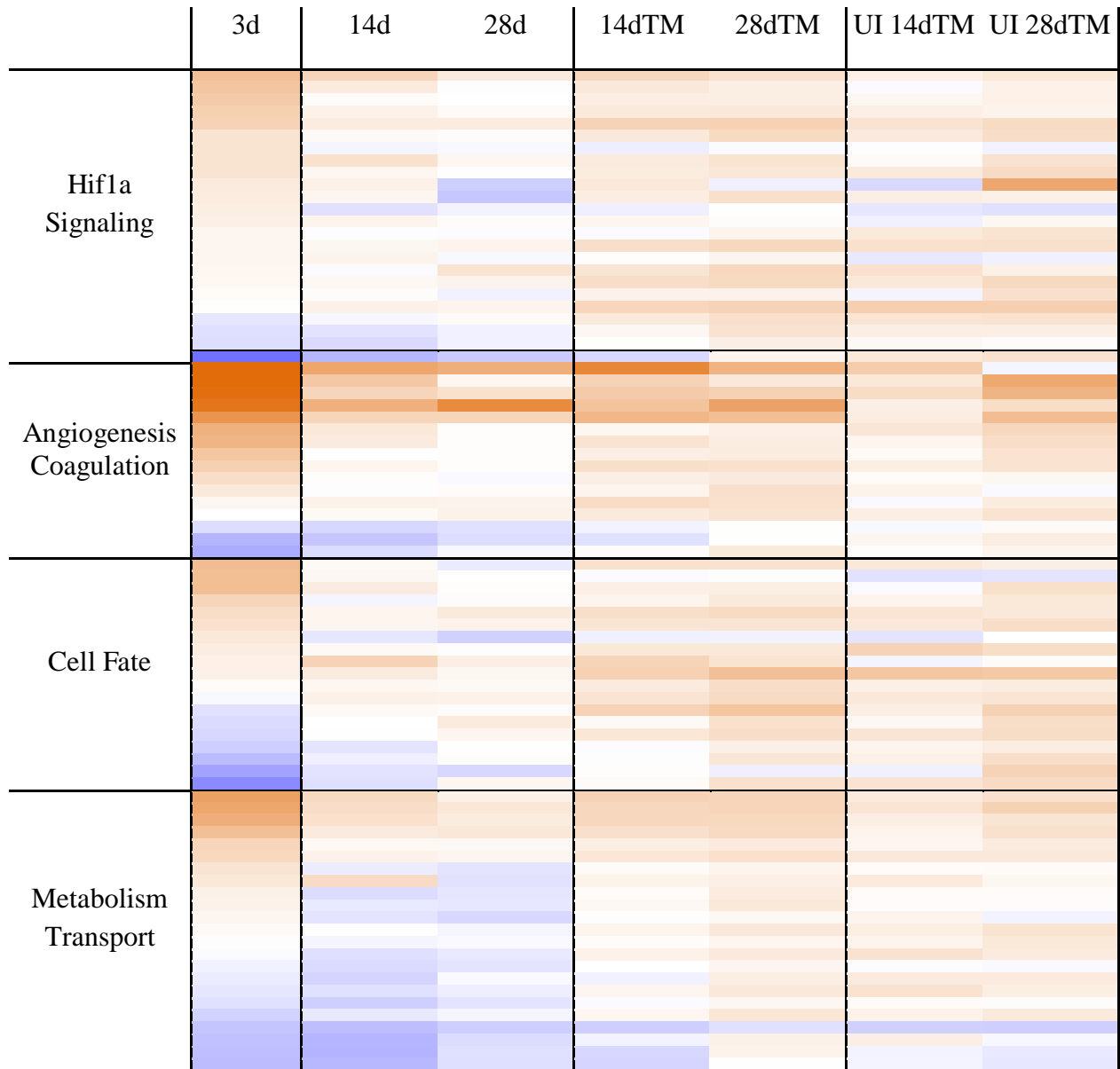
Abundance values ($2^{-\Delta Ct} * 1000$) presented for 3 pools of 12-20 tendons with average (standard deviation) before and after outlier removal listed in right hand columns. *Hnf4a* and *Epo* removed as transcripts were not detected in assay

Appendix M: Heat map representation of the hypoxia signaling array for all WT groups.



Max up-regulated (orange) 23-fold, max down-regulated (blue) 23-fold

Appendix N: Heat map representation of the hypoxia signaling array for all TS5KO groups.



Max up-regulated (orange) 23-fold, max down-regulated (blue) 23-fold

Appendix O: Expression levels of hypoxia signaling genes in UI mouse tendons

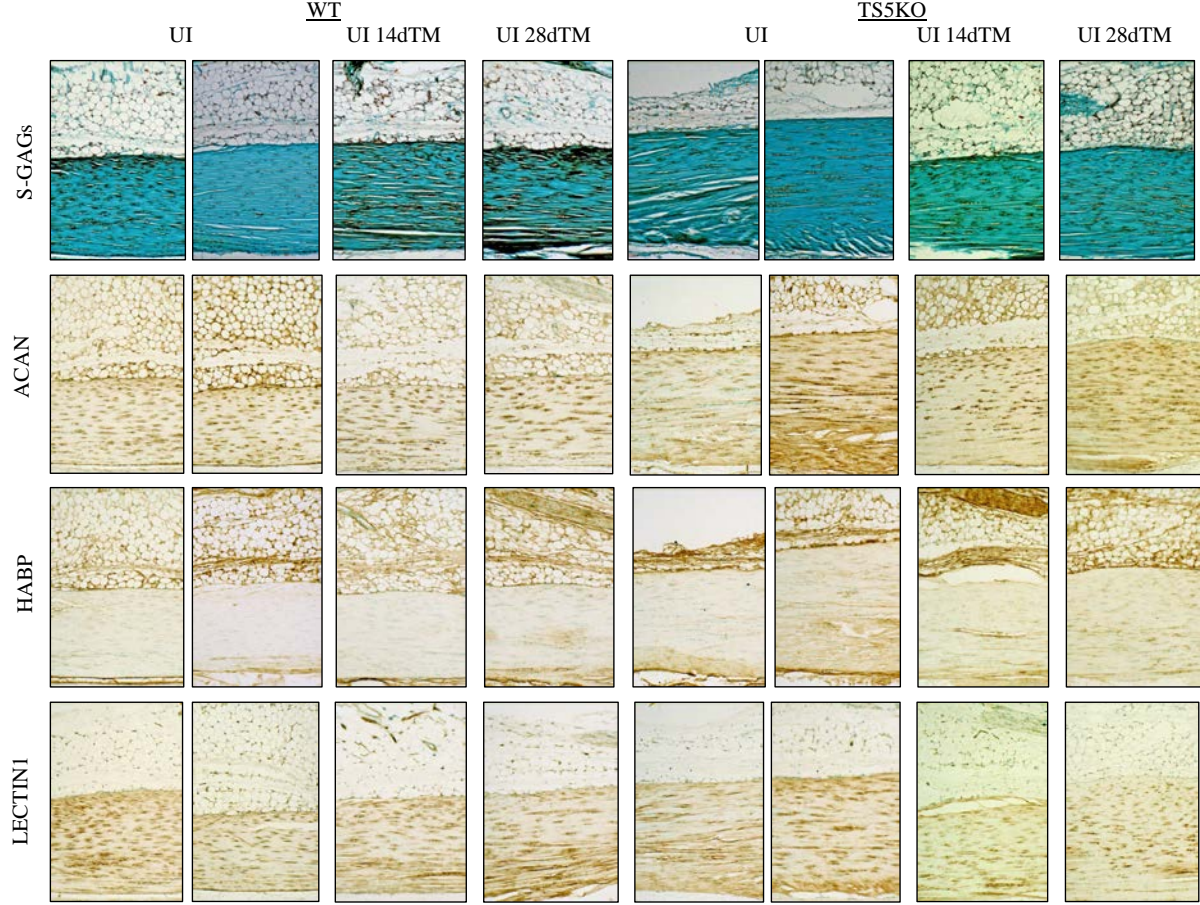
Group	Gene	Pool 1	Pool 2	Pool 3	Average (STD)	Pool 1	Pool 2	Pool 3	Average (STD)
Hif1a Signaling	<i>Lgals3</i>	328.74	188.34	397.41	304.83 (106.57)	221.64	272.99	310.79	268.47 (44.74)
	<i>P4hb</i>	266.41	138.90	183.84	196.38 (64.67)	155.90	153.64	198.95	169.50 (25.53)
	<i>Ctsa</i>	104.52	55.83	50.26	70.20 (29.85)	40.89	37.08	46.16	41.378 (4.56)
	<i>P4ha1</i>	114.34	49.53	36.94	66.94 (41.53)	60.82	58.27	56.76	58.62 (2.05)
	<i>Rbpj</i>	94.78	45.03	39.95	59.92 (30.30)	28.52	30.13	36.46	31.70 (4.20)
	<i>Egln1</i>	55.70	33.31	36.20	41.74 (12.18)	40.91	26.85	35.79	34.52 (7.12)
	<i>Hif1a</i>	54.85	26.55	33.86	38.42 (14.69)	22.34	24.39	23.36	23.36 (1.03)
	<i>Bhlhe40</i>	46.25	30.53	16.92	31.23 (14.68)	16.21	17.65	20.65	18.17 (2.27)
	<i>Eif4ebp1</i>	21.27	23.95	39.60	28.28 (9.90)	18.42	23.86	26.57	22.95 (4.15)
	<i>Nfkb1</i>	33.36	23.50	23.37	26.74 (5.73)	18.60	20.42	23.91	20.97 (2.70)
	<i>Arnt</i>	39.67	21.61	19.64	26.97 (11.04)	12.19	13.96	18.35	14.83 (3.17)
	<i>Fos</i>	51.67	14.62	4.64	23.65 (24.78)	19.60	3.34	17.91	13.62 (8.94)
	<i>Egln2</i>	22.94	15.15	13.92	17.33 (4.89)	14.05	9.21	15.24	12.84 (3.19)
	<i>Dnajc5</i>	27.28	15.69	8.59	17.19 (9.43)	8.82	8.82	12.33	9.99 (2.03)
	<i>Per1</i>	14.62	15.25	19.39	16.42 (2.59)	6.47	9.87	11.72	9.36 (2.66)*
	<i>Ncoa1</i>	19.47	12.38	13.54	15.13 (3.80)	8.82	8.97	9.48	9.09 (0.35)*
	<i>Usf2</i>	17.40	11.75	8.13	12.43 (4.67)	10.44	7.27	9.99	9.23 (1.71)
	<i>Cops5</i>	13.44	8.61	14.71	12.25 (3.22)	13.73	10.62	11.45	11.93 (1.61)
	<i>Hif1an</i>	13.55	7.19	5.81	8.85 (4.13)	10.63	5.64	7.04	7.77 (2.58)
	<i>Trp53</i>	10.77	7.31	5.45	7.85 (2.70)	5.47	5.67	6.46	5.87 (0.52)
	<i>Apex1</i>	7.98	4.99	7.48	6.82 (1.60)	5.04	4.47	5.95	5.15 (0.74)
	<i>Map3kl</i>	5.83	4.54	4.85	5.07 (0.68)	2.33	2.20	2.63	2.39 (0.22)*
	<i>Ankrd37</i>	6.17	3.25	4.17	4.53 (1.50)	4.90	3.66	3.19	3.92 (0.88)
<i>Hif3a</i>	0.38	0.51	0.49	0.46 (0.07)	ND	0.43	0.43	0.43 (0.00)	
	<i>Anxa2</i>	473.23	302.67	284.28	353.39 (104.19)	173.33	209.31	271.08	217.91 (49.44)
	<i>Lox</i>	313.69	151.60	222.60	229.29 (81.25)	125.68	193.59	219.52	179.60 (48.46)

Angiogenesis and Coagulation	<i>Bnip3</i>	191.72	113.83	145.67	150.41 (39.16)	83.47	100.29	111.21	98.32 (13.97)*
	<i>Angptl4</i>	34.04	56.95	105.39	65.46 (36.43)	15.87	72.86	50.92	46.545 (28.75)
	<i>Bnip3l</i>	76.93	46.09	69.86	64.29 (16.15)	37.38	36.49	43.27	39.05 (3.68)
	<i>Vegfa</i>	45.40	34.02	38.70	39.37 (5.72)	43.37	27.35	35.86	35.53 (8.02)
	<i>F3</i>	22.16	15.95	25.20	21.10 (4.71)	11.64	20.00	17.41	16.35 (4.28)
	<i>Jmjd6</i>	13.23	9.15	9.65	10.68 (2.23)	8.02	8.72	12.08	9.61 (2.17)
	<i>Plau</i>	12.79	6.80	5.74	8.44 (3.80)	6.11	4.74	12.28	7.71 (4.02)
	<i>Serpine1</i>	7.21	6.88	6.62	6.91 (0.30)	3.63	7.90	9.30	6.94 (2.96)
	<i>Hmox1</i>	2.61	3.89	2.34	2.95 (0.83)	1.46	2.80	2.39	2.22 (0.68)
	<i>Edn1</i>	2.33	1.59	2.03	1.98 (0.37)	2.15	1.68	1.61	1.81 (0.29)
	<i>Pgf</i>	2.18	1.51	1.83	1.84 (0.34)	1.45	1.00	1.16	1.20 (0.23)*
	<i>Mmp9</i>	1.30	1.58	1.09	1.32 (0.24)	0.81	0.53	0.88	0.74 (0.19)
	<i>Adora2b</i>	0.78	0.35	0.38	0.50 (0.24)	0.08	0.16	ND	0.12 (0.05)*
	<i>F10</i>	0.15	0.19	0.09	0.14 (0.05)	0.12	ND	0.05	0.09 (0.05)
	Cell Fate	<i>Txnip</i>	485.32	344.39	515.59	448.43 (91.37)	252.77	363.14	261.23
<i>Btg1</i>		101.59	65.38	66.19	77.72 (20.68)	33.34	44.88	58.21	45.48 (12.45)
<i>Mif</i>		69.66	61.63	79.80	70.37 (9.11)	101.03	65.65	73.15	79.94 (18.64)
<i>Nampt</i>		64.20	46.49	80.92	63.87 (17.22)	39.21	44.94	35.63	39.93 (4.70)
<i>Igfbp3</i>		59.39	36.52	71.47	55.79 (17.75)	52.15	33.63	45.67	43.82 (9.40)
<i>Ndr1</i>		79.14	45.02	39.69	54.62 (21.40)	42.88	27.90	36.39	35.72 (7.51)
<i>Egr1</i>		94.22	36.74	19.71	50.22 (39.04)	44.97	26.66	62.21	44.62 (17.78)
<i>Odc1</i>		54.53	41.77	49.59	48.63 (6.43)	68.27	52.80	56.08	59.05 (8.15)
<i>Ddit4</i>		39.02	34.69	60.45	44.72 (13.79)	14.54	39.87	19.10	24.50 (13.50)
<i>Mxi1</i>		36.69	18.56	21.27	25.51 (9.78)	14.21	13.47	15.89	14.52 (1.24)
<i>Ier3</i>		25.07	13.20	14.41	17.56 (6.53)	9.61	11.34	11.79	10.91 (1.15)
<i>Ccng2</i>		15.26	9.76	12.81	12.61 (2.76)	7.57	9.00	8.69	8.42 (0.75)*
<i>Ruvbl2</i>		13.02	10.72	9.23	10.99 (1.90)	9.86	6.33	9.71	8.63 (1.99)
<i>Pim1</i>		13.71	6.42	7.35	9.16 (3.96)	6.75	5.71	8.54	7.00 (1.43)

	<i>Met</i>	11.22	7.40	5.52	8.05 (2.90)	5.54	7.58	8.31	7.14 (1.44)
	<i>Atr</i>	12.58	3.80	6.55	7.64 (4.49)	1.88	3.46	3.96	3.10 (1.08)
	<i>Nos3</i>	5.59	4.84	3.31	4.58 (1.16)	4.75	2.40	3.47	3.54 (1.18)
	<i>Adm</i>	2.84	1.14	1.86	1.95 (0.86)	0.85	1.16	1.41	1.14 (0.28)
	<i>Blm</i>	1.85	1.25	1.47	1.52 (0.30)	1.35	0.65	1.14	1.04 (0.36)
Metabolism and Transport	<i>Aldoa</i>	1856.65	1652.10	1596.93	1701.89 (136.83)	2132.88	1637.96	1682.38	1817.74 (273.82)
	<i>Ldha</i>	362.84	304.75	384.14	350.58 (41.09)	421.47	275.67	286.20	327.78 (81.31)
	<i>Vdac1</i>	196.05	121.14	256.65	191.28 (67.88)	325.54	159.90	196.76	227.40 (86.97)
	<i>Tpi1</i>	207.42	140.98	220.75	189.72 (42.73)	235.22	123.48	154.36	171.02 (57.70)
	<i>Pgk1</i>	129.75	106.05	106.15	113.98 (13.65)	178.67	100.91	115.86	131.81 (41.27)
	<i>Gpi1</i>	149.20	74.55	76.99	100.25 (42.41)	120.37	87.25	83.18	96.93 (20.40)
	<i>Eno1</i>	112.17	75.70	62.49	83.46 (25.73)	52.66	38.65	73.33	54.88 (17.45)
	<i>Pkm</i>	113.49	67.27	41.28	74.01 (36.57)	42.22	37.20	63.96	47.79 (14.22)
	<i>Gys1</i>	75.86	47.26	37.28	53.47 (20.03)	75.42	48.20	53.73	59.11 (14.39)
	<i>Pgam1</i>	46.84	31.72	27.77	35.44 (10.07)	25.95	19.95	30.22	25.37 (5.16)
	<i>Pfkb</i>	38.67	27.78	30.22	32.22 (5.71)	19.71	19.71	29.06	22.83 (5.40)
	<i>Hk2</i>	22.80	17.54	17.49	19.28 (3.05)	23.81	10.46	18.07	17.45 (6.70)
	<i>Tfrc</i>	24.53	13.78	18.10	18.80 (5.41)	21.16	9.70	13.44	14.77 (5.85)
	<i>Gbe1</i>	20.07	15.42	18.42	17.97 (2.36)	26.53	17.55	18.73	20.94 (4.88)
	<i>Pfkl</i>	15.11	14.81	11.68	13.86 (1.90)	9.77	7.33	10.96	9.35 (1.85)
	<i>Pdk1</i>	16.14	8.99	8.14	11.09 (4.40)	15.07	7.73	11.73	11.51 (3.68)
	<i>Slc16a3</i>	11.81	10.55	8.06	10.14 (1.91)	14.80	5.81	11.49	10.70 (4.55)
	<i>Ero1l</i>	11.16	7.27	8.83	9.09 (1.96)	6.18	5.32	7.59	6.36 (1.15)
	<i>Slc2a1</i>	10.16	6.92	7.15	8.08 (1.81)	4.52	3.04	5.90	4.49 (1.43)
	<i>Pfkfb4</i>	7.29	6.94	5.02	6.42 (1.22)	6.51	2.85	4.76	4.71 (1.83)
<i>Pfkfb3</i>	1.97	2.68	1.92	2.19 (0.42)	2.58	1.01	1.14	1.58 (0.87)	
<i>Slc2a3</i>	2.63	1.57	1.43	1.88 (0.66)	1.61	1.04	1.14	1.26 (0.30)	
<i>Car9</i>	1.74	0.59	0.58	0.97 (0.67)	1.39	0.37	1.21	0.99 (0.54)	

Abundance values ($2^{-\Delta Ct} \times 1000$) presented for 3 pools of 12-20 tendons with average (standard deviation) listed in right hand column. * $p < 0.05$ relative to WT UI. *Epo* and *Hnf4a* removed as transcripts were not detected in assay

Appendix P: Histological staining in UI WT and TS5KO Achilles tendons with TM



Appendix Q: Optimization of explant culture conditions for murine Achilles tendons



Analysis of the Biomechanics of Tendinopathy in a New Murine Achilles Explant System Which Maintains Cell Viability, Gene Expression, and Material Properties

Katie J. Trella^{1,2}, Jun Li¹, Rebecca Bell^{1,2}, Daniel Gorski¹, Katalin Mikecz¹, John Sandy¹, Anna Plaas¹, Vincent Wang^{1,2}

¹Rush University Medical Center, Chicago, IL, USA
²University of Illinois, Chicago, IL, USA

Introduction

- Human **tendinopathies** are characterized by tissue swelling, loss of tensile properties [1], and mucoid deposits in association with a disorganized collagen matrix [2]
 - All of these features occur in a **novel murine Achilles tendinopathy model** induced by intratendinous injection of TGFβ1 [3]
 - Treadmill exercise** (4 weeks) and **ADAMTS proteinase** are both required to reverse murine tendinopathy [3,4]
- Study Objective:**

 - To establish a murine Achilles tendon explant system in which cell viability, gene expression, and material properties are maintained ex-vivo
 - To identify candidate biomechanical and biological pathways involved in murine Achilles tendinopathy using this explant system

Methods

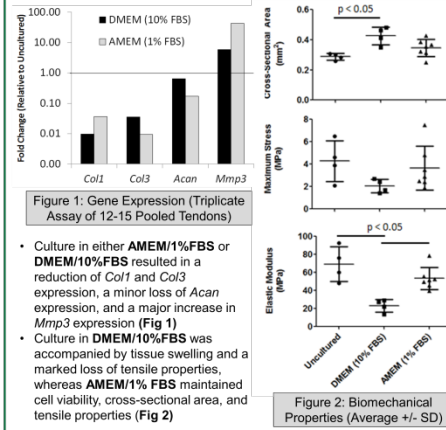
- Tissue Harvest**
- Achilles tendons released at origin and insertion from 12-week old C57BL/6 wild-type mice dissected into either PBS, PBS:DMEM(1:1), or CO₂ Independent MEM (collection media)
- Explant culture**
- Performed under variable conditions (**Table 1**)
- | Conditions | Levels |
|---------------------------|---------------------------------|
| Culture Medium (%FBS) | DMEM (1%* or 10%), AMEM (1%) |
| Glucose Concentration* | 5.5mM, 11mM, 24.7mM |
| Glucosamine Concentration | 0mM, 5mM |
| Time in Culture | 1,2,4 or 7 days |
| Mechanical Loading | Free Floating, Static Extension |
- *Data not presented

- Mechanical Testing following Explant:**
- Cross-sectional area measured with digital calipers and laser micrometer, grip to grip length set to 3.75mm
 - Tensile testing using electromechanical testing system
 - Preload (0.05N for 2 min) and load to failure (0.05 mm/sec)
 - Statistics: 1-way ANOVA with Tukey's post-hoc test ($p < 0.05$)
- qPCR following Explant:**
- 12-15 identically-treated tendons were combined from each experimental group for preparation of about 0.5µg mRNA
 - ΔCt (Ct for gene of interest minus Ct for *Gapdh*) was the mean of a triplicate assay on each RNA preparation
 - Fold change calculated as $2^{\Delta\Delta Ct}$ relative to uncultured
 - Performed for *Col1a*, *Col3a1*, *Acan*, and *Mmp3* [5]
- Histology following Explant:**
- Paraffin sections (6µm) stained with SafraninO

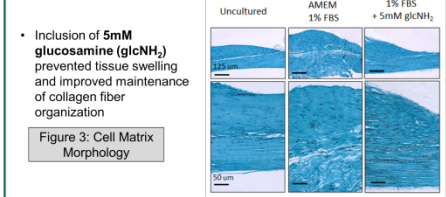
Results

- A. Effect of Tissue Collection Media on Gene Expression and Mechanical Properties:**
- CO₂-independent MEM prevented induction of *Mmp3* expression, a marker of tendon tissue damage [6], whereas PBS or 1:1 PBS:DMEM resulted in a 6.3, and 2.0-fold upregulation of *Mmp3* expression, respectively
 - The composition of the collection media had no marked effect ($p > 0.05$) on tensile properties, relative to freshly excised tissue

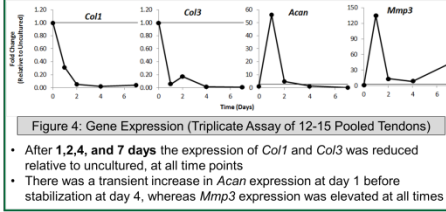
B. Effect of Explant Media Composition on Gene Expression and Mechanical Properties following 7 days in Explant Culture:



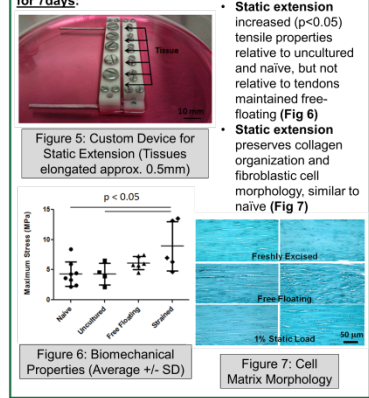
C. Effect of Glucosamine Supplementation on Tissue Morphology in AMEM/1%FBS for 4 days



D. Effect of Time in Culture on Gene Expression in AMEM/1%FBS/5mM glcNH₂



E. Effect of Static Extension on Mechanical Properties and Tissue Morphology in AMEM/1%FBS/5mM glcNH₂ for 7 days:



Conclusion

Figure 8: Current Working Model of Murine Achilles Tendon Explant System

- We have optimized culture conditions which include the use of CO₂ independent MEM for collection and AMEM/1% FCS supplemented with 5mM glcNH₂ for explant media. These conditions preserve cell viability, cross-sectional area, and biomechanical properties of murine Achilles tendons for up to 7 days.
- This explant system enables mechanistic studies of mechanobiologic factors known or expected to impact tendon maintenance and repair in vivo

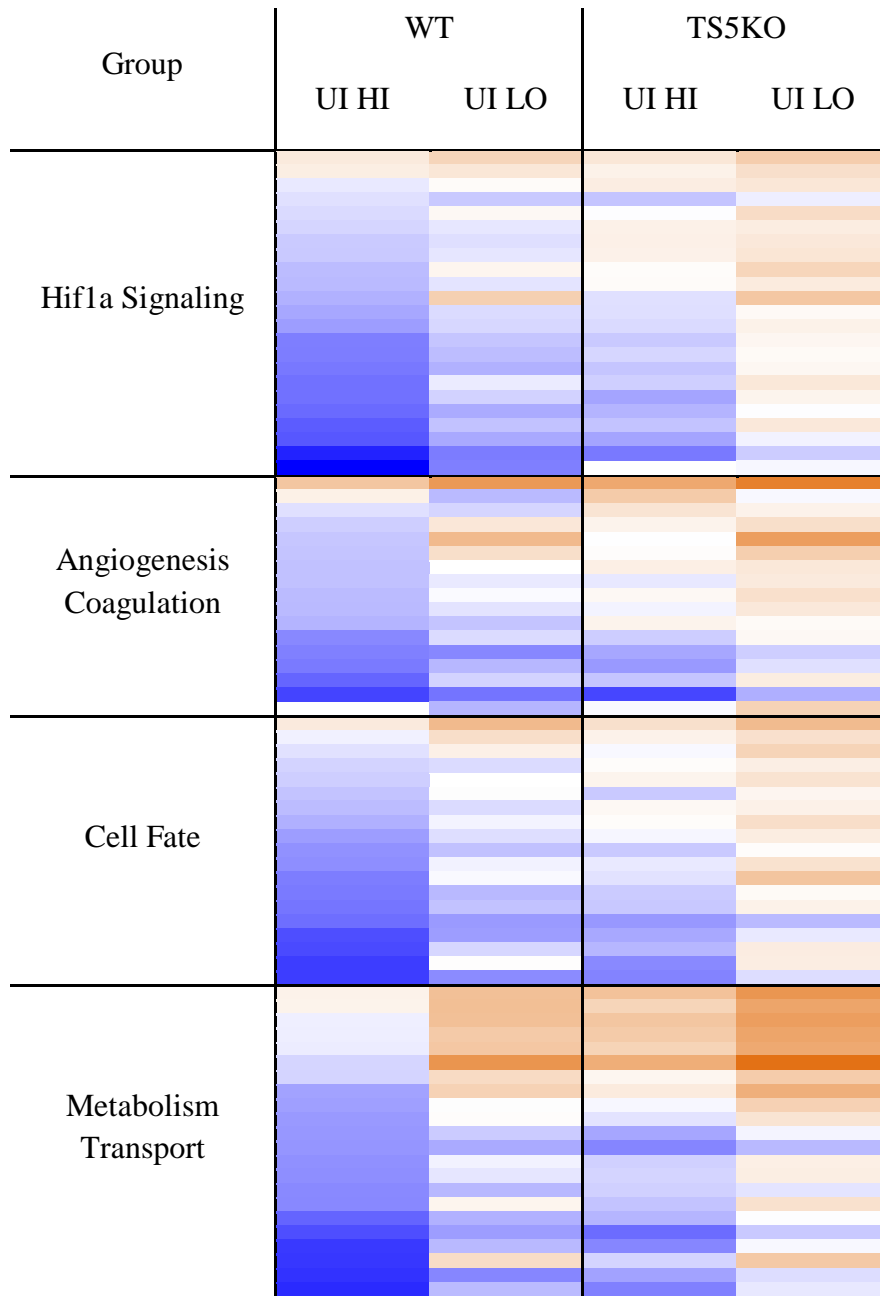
References

- [1] Arya, et al. J Appl Physiol. 2010;108(3):670-675
- [2] Kannus, et al. J Bone Joint Surg Am. 1991;73(10):1507-1525
- [3] Bell, et al. J Biomech. 2013;46(3):498-505
- [4] Bell, et al. J Orthop Res. In Review. 2013.
- [5] Velasco, et al. J Biol Chem. 2012;286(29): 26016-26027
- [6] Leigh, et al. J Orthop Res. 2008;26(10):1306-1312

Acknowledgements

Funding was provided by the Charles J. and Margaret Roberts Trust (RUMC), Katz Rubschlager Endowment (RUMC) and the Rush Arthritis Institute.

Appendix R: Heat map representation of the hypoxia signaling array for all explant UI groups



Max up-regulated (orange) 64-fold, max down-regulated (blue) 64-fold

Protocols

Complete Protocol for qRT-PCR

Plaas-Sandy Lab 2011

By: Daniel J Gorski (Updated by Katie J Trella 4.16.2013)

Preparation for mRNA isolation from Tissue

Remove RNA later from tubes containing tissues from RNA later

Snap freeze tissue in liquid nitrogen.

Pulverize tissue with a chilled mortar and pestle.

Place pulverized tissue in 1mL Trizol at room temperature.

Vortex Trizol and tissue for 1min, let sit at room temp for 10min (Repeat 3x)

Proceed to Trizol purification (or store at -20°C overnight)

Preparation for mRNA isolation from cells grown in monolayer

Remove Media

Add 1mL Trizol, directly to flask/dish (rock back and forth)

Incubate samples for 1-2 mins at 37°C

Disturb bottom of flask/dish with cell scraper

Rock for ~20 min

Disturb bottom of flask/dish with cell scraper

Pipette Trizol suspension into RNase/DNase Free 1.5mL centrifuge tube

Proceed to Trizol purification (Store at -20°C overnight)

mRNA purification using Trizol

Cat No. 15596-018 (Invitrogen)

Add 0.2mls chloroform, vortex 3min

Incubate 2-3mins at 15-30°C

Centrifuge samples @14,000g for 15mins at 4°C

Samples are then separated into lower red phenol-chloroform phase, an interphase, and a colorless upper aqueous phase. RNA remains in aqueous phase.

Transfer aqueous phase to separate tube (~0.7mL), save the other phases if DNA or protein isolation is needed.

Precipitate RNA by adding 0.6 mLs isopropyl alcohol, make sure tubes are even then invert multiple times

Incubate 5 mins at 15-30C (or -20C overnight)

Centrifuge @14,000g for 15mins at 4C, RNA pellet will be gel-like on side and bottom.

Remove (pour off) supernatant, wash pellet once with 75% ethanol at least 1 mL, Mix the sample by vortexing

Centrifuge @14,000rpm for 10mins at 4°C

Pour off EtOH

Dry the RNA pellet with the cap open 30-45min (Turn on 55°C water bath)

Do not let the sample dry completely; it will decrease its solubility. Partially dissolved RNA samples have an A260/280 ratio <1.6.

Dissolve the RNA in RNAase free (DEPC) 100ul water for 5min in 55°C water bath

Fast spin down

Store at -80°C

***Technically this mRNA prep can be used for qRT-PCR, but we like to further purify it with a spin column kit from Qiagen. Using only the RNA cleanup protocol from the RNeasy Mini Kit (below is an adapted protocol referencing reagents and solutions provided in the kit, there are certain steps and precautions omitted here that must be read.)**

mRNA cleanup using RNeasy Mini Kit by Qiagen
Cat No. 74104

1. Adjust the sample to a volume of 100 µl with RNase-free water (should already be 100µL). Add 350 µl Buffer RLT, and mix well.

2. Add 250 µl ethanol (96–100%) to the diluted RNA, and mix well by pipetting. Do not centrifuge. Proceed immediately to step 3.

3. Transfer the sample (700 µl) to an RNeasy Mini spin column placed in a 2 ml collection tube (supplied). Close the lid gently, and centrifuge for 15 s at $\approx 8000 \times g$ (10,000 rpm). Discard the flow-through. ***Reuse the collection tube in step 4.**

Note: After centrifugation, carefully remove the RNeasy spin column from the collection tube so that the column does not contact the flow-through. Be sure to empty the collection tube completely.

4. Add 500 µl Buffer RPE to the RNeasy spin column. Close the lid gently, and centrifuge for 15 s at $\approx 8000 \times g$ ($\approx 10,000$ rpm) to wash the spin column membrane. Discard the flow-through. Reuse the collection tube in step 5.

Note: When using a new kit from Qiagen make sure to add ethanol to Buffer RPE before use (check box on top of RPE container when completed)

5. Add 500 µl Buffer RPE to the RNeasy spin column. Close the lid gently, and centrifuge for 2 min at $\approx 8000 \times g$ ($\approx 10,000$ rpm) to wash the spin column membrane. Discard the flow-through. ***Reuse collection tube for step 6.**

6. Centrifuge spin column at max speed for 30sec, to completely remove any remaining Buffer RPE on the column. Discard flow through. At this point you may discard the collection tube as well, **but have a labeled 1.5mL collection tube waiting to place the spin column in.**

Note: The long centrifugation dries the spin column membrane, ensuring that no ethanol is carried over during RNA elution. Residual ethanol may interfere with downstream reactions. **After centrifugation, carefully remove the RNeasy spin column from the collection tube so that the column does not contact the flow-through. Otherwise, carryover of ethanol will occur.**

7. Place the RNeasy spin column in a new 1.5 ml collection tube (supplied). Add 30 µl RNase-free water directly to the spin column membrane. Let sit for 10 min. Centrifuge for 1 min at $\approx 11,000 \times g$ ($\approx 10,000$ rpm) to elute the RNA.

8. Store at -80°C

[mRNA] quantification

Measure the A260/280 of the mRNA sample, looking for a ratio >1.8
Measure the concentration of the mRNA, and calculate how much volume is needed to pipette 0.5 or 1µg of RNA (for use in cDNA synthesis step).

cDNA synthesis using SuperScript™ First-Strand Synthesis System for RT-PCR (Invitrogen)

Cat. No: 11904-018

The following 20µl reaction volume can be used for 10pg - 5µg of total RNA or 10pg - 500ng of mRNA

Add the following components to a nuclease-free microcentrifuge tube:

1 µl of oligo(dT)₂₀ (50µM); *or* 200-500 ng of oligo(dT)₁₂₋₁₈; *or* 50-250 ng of random primers; *or* 2 pmol of gene-specific primer

1 µl 10 mM dNTP mix (10 mM each dATP, dGTP, dCTP, and dTTP at neutral pH)

10pg - 5µg total RNA *or* 10pg - 500ng mRNA

Sterile, distilled water to 13µl

Heat mixture to 65°C for 5 minutes and incubate on ice for at least 1 minute

Collect the contents of the tube by brief centrifugation and add:

4 µl 5X First-Strand Buffer

1 µl 0.1 M DTT

1 µl RNaseOUT™ Recombinant RNase Inhibitor (Cat. No. 10777-019, 40 units/µl) Note: When using less than 50ng of starting RNA, the addition of RNaseOUT™ is essential

1 µl of SuperScript™ III RT (200 units/µl) Note: If generating cDNA longer than 5 kb at temperatures above 50°C using a gene-specific primer or oligo(dT)₂₀, the amount of SuperScript™ III RT may be raised to 400 U (2 µl) to increase yield

Mix by pipetting gently up and down. If using random primers, incubate tube at 25°C for 5 minutes

Incubate at 50°C for 30-60 minutes. Increase the reaction temperature to 55°C for gene-specific primer.

Reaction temperature may also be increased to 55°C for difficult templates or templates with high secondary structure.

Inactivate the reaction by heating at 70°C for 15 minutes

The cDNA can now be used as a template for amplification in PCR. However, amplification of some PCR targets (that > 1 kb) may require the removal of RNA complementary to the cDNA. To remove RNA complementary to the cDNA, add 1µl (2 units) of *E. coli* RNase H and incubate at 37°C for 20 minutes.

qRT-PCR using ABI Taqman Primers

Make 1:10, 1:100, 1:1000 dilutions in DEPC water of cDNA preps.

Note: 1:10 Dilution is made from 20 ul cDNA from rxn and 180ul Water, which yields a total of 200 ul. When conducting analysis in triplicates ~6 genes can be used on 1 cDNA prep (with some extra), otherwise more preps should be made



2. Following the protocol provided by “ABI Taqman Gene Expression Assays” for the 20uL/well reaction add to each well (60 well plates):

ABI Gene Expression Mix 10 ul/rxn
ABI 20X primers 1 ul/rxn
cDNA (diluted) 9ul/rxn

Important Note: For gene targets other than control (GAPDH), only use **1:10 cDNA dilution in triplicate reactions (27 ul of cDNA from each sample required per gene)**. For control, use 1:10, 1:100, 1:1000 dilutions in triplicate, then create standard curve to confirm PCR efficiency and pipetting accuracy. Most qRT-PCR instrument software will be able to create a standard curve for you.

3. Make sure samples are well mixed by using a multichannel pipette.
4. Spin down plate briefly.
5. Run reactions on PCR machine with these conditions: 50°C for 2 min, 95°C for 10 min, 95°C for 15 sec, 60°C for 1 min. Repeat 39x (Step 3-4 of reaction).

Important Note: When comparing data on two or more separate plates, you must manually set the baseline threshold to the same value after the run is complete. For example, an experiment needs five 96 well plates to be complete. I will let the qRT-PCR software calculate the baseline threshold for the first plate i.e. **341.57 (or 0.34157)**, and then I will manually set the next 4 plates to have a baseline threshold of 341.57. You must do this for the Ct values to be comparable.

Brief data analysis:

Calculate average Ct for GOIs from the triplicate values, removing outliers (SD >0.3)

Calculate average Ct from Control gene triplicate using only 1:10 dilution values.

Calculate Delta Ct

$\Delta Ct = Ct (GOI) - Ct (Control)$

Calculate Delta Delta Ct (for comparison of timepoints, genotypes, etc...)

$\Delta\Delta Ct = \Delta Ct (KO) - \Delta Ct (WT)$

Calculate Fold Change (2 to the power of negative delta delta Ct)

Fold Change = $2^{-\Delta\Delta Ct}$

Purification of DNA (> 500 bp) for Methylation Analysis
Adapted by Anna Plaas and Katie Trella
1/19/2015

ZR FFPE DNA Mini Prep (50 preps)
Zymo (Cat # - D3065) – FORMALIN FIXED TISSUE

Zymo Contact: Ryan Sasada
Phone: (949)-679-1190 (x260)
E-mail: rsasada@zymoresearch.com

Buffer Preparations:

- Add 260 uL of **Proteinase K Storage Buffer** to each **Proteinase K tube** (store at -20°C)
 - Final concentration is ~20 mg/mL
- Resuspend lyophilized **RNase A** in 300 uL of **ddH₂O (UltraPure DNase/RNase FREE Water)**

Proteinase K Digestion:

- To each tissue sample (< 25 mg) in a sterile DNase/RNase Free microcentrifuge tube add:
 - 45uL **ddH₂O (UltraPure DNase/RNase FREE Water)**
 - 45uL **2X Digestion Buffer**
 - 10uL **Proteinase K**
- Incubate at 55°C overnight (or 1-4 hours for rapid digestion)

** If your tissue sample is too large for the digestion volume, scale up the digestion to 200 uL while keeping the amount of proteinase K the same (Double the reagent volumes of **RNase A** and **Genomic Lysis Buffer** in the next steps)

DNA Isolation:

1. Add 5uL of **RNase A**, mix, and then incubate for 5 minutes at room temperature
2. Add 350uL **Genomic Lysis Buffer**, vortex
3. Centrifuge at 10,000xg for 1 minute to remove insoluble debris
4. Transfer the supernatant to the **Zymo-Spin™ IIC Column** in a **Collection Tube**
5. Centrifuge at 10,000xg for 1 minute (discard collection tube)
6. Add 200uL of **DNA Pre-Wash Buffer** to the spin column in a new **Collection Tube**
7. Centrifuge at 10,000xg for 1 minute (discard flow-through)
8. Add 400uL of g-DNA Wash Buffer to the spin column
9. Centrifuge at 10,000xg for 1 minute (discard collection tube)
10. Transfer the **Zymo-Spin™ IIC Column** to a clean DNase/RNase free microcentrifuge tube
11. Add 100uL **DNA Elution Buffer** to the spin column
12. Incubate for 5 minutes at room temperature
13. Centrifuge at top speed (~21,000xg) for 30 seconds to elute the DNA
14. Store at -20°C

ZR FFPE DNA Mini Prep (50 preps)
Zymo (Cat # - D4068) – FRESH TISSUE

Buffer Preparations:

- Add 1060 uL of **Proteinase K Storage Buffer** to each **Proteinase K tube** (store at -20°C)

Proteinase K Digestion:

- To each tissue sample (< 25 mg) in a sterile DNase/RNase Free micro-centrifuge tube add:
 - 95uL **ddH₂O (UltraPure DNase/RNase FREE Water)**
 - 95uL **Solid Tissue Buffer (Blue)**
 - 10uL **Proteinase K**
- Incubate at 55°C for 1 hour

** If your tissue sample is too large for the digestion volume, scale up the digestion to 400uL while keeping the amount of proteinase K the same (Double the reagent volume **Genomic Binding Buffer** in the next steps)

DNA Isolation:

1. Centrifuge at 12,000xg for 1 minute to remove insoluble debris
2. Transfer the supernatant to a clean micro-centrifuge tube
3. Add 400uL (2x volume) of **Genomic Binding Buffer** and mix thoroughly
4. Transfer the mixture to a **Zymo-Spin™ IIC Column** in a **Collection Tube**
5. Centrifuge at 12,000xg for 1 minute (discard collection tube)
6. Add 400uL of **DNA Pre-Wash Buffer** to the spin column in a new **Collection Tube**
7. Centrifuge at 12,000xg for 1 minute (discard flow-through)
8. Add 700uL of **g-DNA Wash Buffer** to the spin column
9. Centrifuge at 12,000xg for 1 minute (discard flow-through)
10. Add 200uL of **g-DNA Wash Buffer** to the spin column
11. Centrifuge at 12,000xg for 3 minutes (discard collection tube)
12. Transfer the **Zymo-Spin™ IIC Column** to a clean DNase/RNase free micro-centrifuge tube
13. Add 100uL **DNA Elution Buffer** to the spin column
14. Incubate for 5 minutes at room temperature
15. Centrifuge at top speed (~21,000xg) for 1 minute to elute the DNA
16. Store at -20°C

Alamar Blue Assay Protocol
Adapted by Katie Trella 9.16.13

Description for Life Tech: “AlamarBlue® is a proven cell viability indicator that uses the natural reducing power of living cells to convert resazurin to the fluorescent molecule, resorufin. The active ingredient of alamarBlue® (resazurin) is a nontoxic, cell permeable compound that is blue in color and virtually nonfluorescent. Upon entering cells, resazurin is reduced to resorufin, which produces very bright red fluorescence. Viable cells continuously convert resazurin to resorufin, thereby generating a quantitative measure of viability—and cytotoxicity”

AlamarBlue from Molecular Probes (Life Technologies – Invitrogen)

- 25 mL (DAL1025) - \$176.00
- 100 mL (DAL1100) - \$379.00

Protocol [1-2]

- Following experimental explant conditions, transfer tendons individually and 1 mL of culture medium to a multi-well plate. Add 1/10th the volume of alamarBlue reagent (100 uL)
 - Use medium with 10% alamar blue, without any tendon explant, as a reagent blank
 - NOTE: FBS and BSA cause some quenching of fluorescence. We recommend using the same serum concentration in controls to account for this quenching. Other media components, such as phenol red do not interfere with this assay
- Incubate 24 hours at 37°C in a cell culture incubator (protected from direct light)
- After incubation with alamar blue, pipette 1 mL reaction mixtures into cuvettes for measurement of fluorescence
 - Read fluorescence using an excitation wavelength of 530 nm (excitation range 540-570nm). Read fluorescence emission at 590 nm (emission range 580-610nm)

** Note if reading is above threshold for the machine (999.999) take 500 uL of a blank and 500 uL of the sample and mix together. Re-measure. Do the following calculation to calculate the original fluorescence**

New Measurement – ½ Blank = ½ Original Sample
½ Original Sample * 2 = Original Sample (**Then make it relative by subtracting blank)

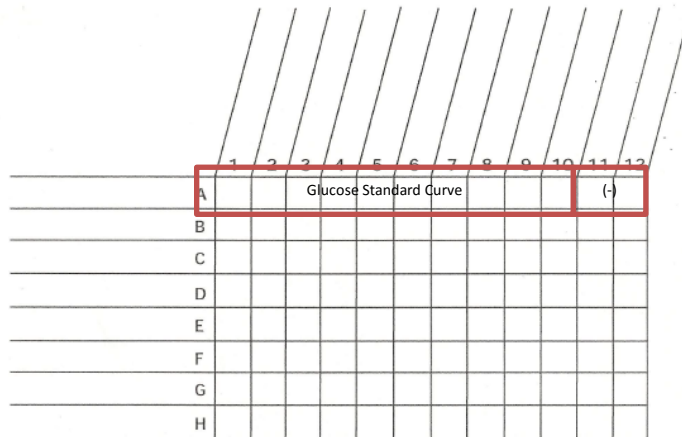
Amplex Red Glucose Assay Protocol for cell culture media
 Written by Dan Gorski 2014
 Updated by Katie Trella 11/10/2015

Life Tech Cat #: A22189
 Store all contents $\leq -20^{\circ}\text{C}$

Prepare stock solutions

1. 10mM stock solution of Amplex Red reagent
 1. Dissolve the contents of 1 vial of Amplex red reagent (154ug) in 60uL DMSO
2. 1X Reaction Buffer
 1. Add 4 mL of 5X Reaction Buffer to 16mL DI
3. 10 U/mL stock solution of horseradish peroxidase (HRP)
 1. Dissolve HRP (10 U) in 1mL of 1X Reaction Buffer
 2. Aliquot and store at -20°C
4. 400 mM (72 mg/mL) glucose stock solution
 1. 72 mg D-glucose in 1 mL of DI
5. 100 U/mL glucose oxidase solution
 1. Dissolve contents of the glucose oxidase vial in 1.0 mL of 1x Reaction Buffer
 2. Aliquot and store at -20°C
6. 20 mM H₂O₂ working solution
 1. Dilute the ~3% H₂O₂ stock solution into the appropriate volume of 1X Reaction Buffer. The actual % of stock solution will be indicated on the label
 - For example: if 3.0% (0.88 M) H₂O₂ stock – dilute 22.7 uL in 977 uL of 1X Reaction Buffer

Prepare 96-well plate layout



Prepare sample dilutions

1. 3uL of sample in 147uL 1x Reaction Buffer in separate tubes
 - Triplicates of each sample
 - Triplicates of blank media (preconditioned media controls)

Prepare glucose standards (200uM and 20uM) from 400mM stock solution

1. 200mM standard = 100uL 1x Reaction buffer + 100uL 400mM standard
 - 200uM = 999uL 1x Reaction buffer + 1uL 200mM standard
 - 20uM = 900uL 1x Reaction buffer + 100uL 200uM standard

Make enough standard solutions to finish all experiments

Experimental Protocol

1. Pipette Glucose Standard Curve into first row of plate (10 wells + 2 wells negative control)
 - Add 1x Reaction Buffer First, then add Standard (either 200uM or 20uM)

Final Concentration (uM)	uL Glucose Standard	[Glucose Standard uM]	uL 1x rxn Buffer
50	25	200	25
25	12.5	200	37.5
12.5	6.25	200	43.75
5	2.5	200	47.5
3.75	18.75	20	31.25
2.5	12.5	20	37.5
1.25	6.25	20	43.75
0.75	3.75	20	46.25
0.5	2.5	20	47.5
0.25	1.25	20	48.75
0	0	n.a.	50

2. Pipette media blanks (preconditioned media controls)
 - 45uL 1x Reaction Buffer
 - 5uL pre-diluted sample
3. Pipette samples
 - 45uL 1x Reaction Buffer
 - 5uL pre-diluted sample
4. Prepare working solution of 100uM Amplex Red Reagent, 0.2 U/mL HRP, and 2 U/mL glucose oxidase
 - 50uL of 10mM Amplex Red Reagent stock solution
 - 100uL of 10 U/mL HRP stock solution
 - 100uL of 100 U/mL glucose oxidase solution
 - 4.75 mL of 1x Reaction Buffer
5. Pipette 50uL of Amplex Red Working Solution into wells containing standard curve, controls, and samples
6. Cover with tinfoil
7. Incubate at Room Temperature for 30min (or longer if necessary)
 - If measurements are too low after 30 minutes, re-cover and wait 15 minutes, then re-measure

Taking Measurements (using Biotek – Gen5 in Maki’s Lab)

1. Turn on machine
2. Open Gen 5.1.10
3. Go to Experiment → Browse → Load (Amplex Red Glucose Assay)

4. Highlight All → Read → Emission 590nm (Excitation 530-560nm)

Calculations

Sample concentration (uM) is a 1:1000 dilution of what sample is (mM) since it is in 1mL

1. Calculate relative glucose concentration using negative control

$$[\text{glucose}]_{\text{Relative}} = [\text{glucose}]_{\text{EACH SAMPLES}} - [\text{glucose}]_{\text{Average from Negative Controls}}$$

2. Calculate glucose consumed in system

$$[\text{glucose}]_{\text{Consumed}} = [\text{glucose}]_{\text{Average from MEDIA BLANKS}} - [\text{glucose}]_{\text{SAMPLES (RELATIVE)}}$$

Explant Tensile Testing Protocol

Computer 1: Obtaining Images during Testing

1. Open DMAS Sync
2. Open DMAS Calibration:
File → Calibrate Capture Models → DMAS New Calibration Frame 45 X 45
Display → Options → Video Size 50 %
Line up crosshairs with physical crosshairs → Control Click to Zoom
Origin → Counterclockwise → Middle
File → Save (overwrites existing file)
3. DMAS Capture
File → New Data Set → 45 X 45 → Preview → Open Shutters
4. When ready to test
 - a. Stop Preview
 - b. Change to Input 00 and Start/Stop
 - i. Capture won't start until program receives trigger from MTS computer

Computer 2: Tensile Testing

1. Open Testworks (no passwords)
2. Configure → Device → Δ Load Cell → Calibrate
3. Zero Load
4. Load specimen into the device
 - a. Prior to clamping specimen measure length with calipers (1x), width with calipers (5x across length), and thickness with laser micrometer (5x across length)
5. Fill with Saline
6. Rest for 10 minutes in lax position
7. Unlock button on Machine → Scroll down slightly then scroll up till 0.01 N
8. Zero Extension
9. Preload to 0.05 → Set time to Zero → Wait 2 minutes
 - a. Continue to adjust extension till 2 minutes is up
 - b. Write down extension
10. Zero Extension
11. Start Pull to Failure Program
12. Once failure occurs, stop
13. Save File
14. Backup all files

References

1. Abate, M., et al., *Pathogenesis of tendinopathies: inflammation or degeneration?* Arthritis Res Ther, 2009. **11**(3): p. 235.
2. Scott, A. and M.C. Ashe, *Common tendinopathies in the upper and lower extremities.* Curr Sports Med Rep, 2006. **5**(5): p. 233-41.
3. September, A.V., M. Posthumus, and M. Collins, *Application of Genomics in the Prevention, Treatment and Management of Achilles Tendinopathy and Anterior Cruciate Ligament Ruptures.* Recent Patents on DNA and Gene Sequences, 2012. **6**: p. 212-223.
4. Magnan, B., et al., *The pathogenesis of Achilles tendinopathy: a systematic review.* Foot Ankle Surg, 2014. **20**(3): p. 154-9.
5. Collins, M. and M. Posthumus, *Type V collagen genotype and exercise-related phenotype relationships: a novel hypothesis.* Exerc Sport Sci Rev, 2011. **39**(4): p. 191-8.
6. Parkinson, J., et al., *Involvement of Proteoglycans in Tendinopathy.* Journal of Musculoskeletal and Neuronal Interactions, 2011. **11**(2): p. 86-93.
7. Funakoshi, T., et al., *Lubricin distribution in the goat infraspinatus tendon: a basis for interfascicular lubrication.* J Bone Joint Surg Am, 2008. **90**(4): p. 803-14.
8. Ritty, T.M., K. Ditsios, and B.C. Starcher, *Distribution of the elastic fiber and associated proteins in flexor tendon reflects function.* Anat Rec, 2002. **268**(4): p. 430-40.
9. Cheng, V.W.T. and H.R.C. Screen, *The micro-structural strain response of tendon.* Journal of Materials Science, 2007. **42**(21): p. 8957-8965.
10. Hayashi, M., et al., *The effect of lubricin on the gliding resistance of mouse intrasynovial tendon.* PLoS One, 2013. **8**(12): p. e83836.

11. Screen, H.R., et al., *Tendon functional extracellular matrix*. J Orthop Res, 2015. **33**(6): p. 793-9.
12. Rees, S.G., C.M. Dent, and B. Caterson, *Metabolism of proteoglycans in tendon*. Scand J Med Sci Sports, 2009. **19**(4): p. 470-8.
13. Scott, J.E., C.R. Orford, and E.W. Hughes, *Proteoglycan-collagen arrangements in developing rat tail tendon. An electron microscopical and biochemical investigation*. Biochem J, 1981. **195**(3): p. 573-81.
14. Yoon, J.H. and J. Halper, *Tendon proteoglycans: biochemistry and function*. J Musculoskelet Neuronal Interact, 2005. **5**(1): p. 22-34.
15. Ezura, Y., et al., *Differential expression of lumican and fibromodulin regulate collagen fibrillogenesis in developing mouse tendons*. J Cell Biol, 2000. **151**(4): p. 779-88.
16. Benjamin, M. and J.R. Ralphs, *Fibrocartilage in tendons and ligaments--an adaptation to compressive load*. J Anat, 1998. **193** (Pt 4): p. 481-94.
17. Waggett, A.D., et al., *Characterization of collagens and proteoglycans at the insertion of the human Achilles tendon*. Matrix Biol, 1998. **16**(8): p. 457-70.
18. Birch, H.L., et al., *Matrix metabolism rate differs in functionally distinct tendons*. Matrix Biol, 2008. **27**(3): p. 182-9.
19. Innes, J.F. and P. Clegg, *Comparative rheumatology: what can be learnt from naturally occurring musculoskeletal disorders in domestic animals?* Rheumatology (Oxford), 2010. **49**(6): p. 1030-9.
20. Screen, H.R., et al., *The influence of swelling and matrix degradation on the microstructural integrity of tendon*. Acta Biomaterialia, 2006. **2**(5): p. 505-13.

21. Screen, H.R.C., et al., *An investigation into the effects of the hierarchical structure of tendon fascicles on micromechanical properties*. Proceedings of the Institution of Mechanical Engineers, Part H: Journal of Engineering in Medicine, 2004. **218**(2): p. 109-119.
22. Screen, H.R., S. Toorani, and J.C. Shelton, *Microstructural stress relaxation mechanics in functionally different tendons*. Med Eng Phys, 2013. **35**(1): p. 96-102.
23. Thorpe, C.T., et al., *Distribution of proteins within different compartments of tendon varies according to tendon type*. J Anat, 2016.
24. Rigozzi, S., et al., *Tendon glycosaminoglycan proteoglycan sidechains promote collagen fibril sliding-AFM observations at the nanoscale*. J Biomech, 2013. **46**(4): p. 813-8.
25. Dymant, N.A., et al., *The paratenon contributes to scleraxis-expressing cells during patellar tendon healing*. PLoS One, 2013. **8**(3): p. e59944.
26. Mienaltowski, M.J., S.M. Adams, and D.E. Birk, *Tendon proper- and peritenon-derived progenitor cells have unique tenogenic properties*. Stem Cell Res Ther, 2014. **5**(4): p. 86.
27. Cadby, J.A., et al., *Differences between the cell populations from the peritenon and the tendon core with regard to their potential implication in tendon repair*. PLoS One, 2014. **9**(3): p. e92474.
28. Han, W.M., et al., *Macro- to microscale strain transfer in fibrous tissues is heterogeneous and tissue-specific*. Biophys J, 2013. **105**(3): p. 807-17.
29. Kannus, P. and L. Jozsa, *Histopathological changes preceding spontaneous rupture of a tendon. A controlled study of 891 patients*. J Bone Joint Surg Am, 1991. **73**: p. 1507-1525.

30. Corps, A.N., et al., *Increased expression of aggrecan and biglycan mRNA in Achilles tendinopathy*. Rheumatology (Oxford), 2006. **45**(3): p. 291-4.
31. de Mos, M., et al., *In vitro model to study chondrogenic differentiation in tendinopathy*. Am J Sports Med, 2009. **37**(6): p. 1214-22.
32. Khan, M., et al., *Patellar tendinosis (jumper's knee): Findings at histopathologic examination, US, and MR imaging*. Musculoskelet Rad, 1996. **200**: p. 821-827.
33. Attia, M., et al., *Greater glycosaminoglycan content in human patellar tendon biopsies is associated with more pain and a lower VISA score*. Br J Sports Med, 2014. **48**(6): p. 469-75.
34. Jarvinen, M., et al., *Histopathological findings in chronic tendon disorders*. Scand J Med Sci Sports, 1997. **7**(2): p. 86-95.
35. Pingel, J., et al., *3-D ultrastructure and collagen composition of healthy and overloaded human tendon: evidence of tenocyte and matrix buckling*. J Anat, 2014. **224**(5): p. 548-55.
36. Spiesz, E.M., et al., *Tendon extracellular matrix damage, degradation and inflammation in response to in vitro overload exercise*. J Orthop Res, 2015. **33**(6): p. 889-97.
37. Plaas, A., et al., *Aggrecanolytic in human osteoarthritis: confocal localization and biochemical characterization of ADAMTS5-hyaluronan complexes in articular cartilages*. Osteoarthritis Cartilage, 2007. **15**(7): p. 719-34.
38. Velasco, J., et al., *Adamts5 deletion blocks murine dermal repair through CD44-mediated aggrecan accumulation and modulation of transforming growth factor beta1 (TGFbeta1) signaling*. J Biol Chem, 2011. **286**(29): p. 26016-27.

39. Bell, R., et al., *Controlled treadmill exercise eliminates chondroid deposits and restores tensile properties in a new murine tendinopathy model*. Journal of Biomechanics, 2013. **46**(3): p. 498-505.
40. Dirks, R.C. and S.J. Warden, *Models for the study of tendinopathy*. Journal of Musculoskeletal and Neuronal Interactions, 2011. **11**(2): p. 141-149.
41. Lui, P.P., et al., *What are the validated animal models for tendinopathy?* Scand J Med Sci Sports, 2011. **21**(1): p. 3-17.
42. Mienaltowski, M.J. and D.E. Birk, *Mouse models in tendon and ligament research*. Adv Exp Med Biol, 2014. **802**: p. 201-30.
43. Wang, V.M., et al., *Murine tendon function is adversely affected by aggrecan accumulation due to the knockout of ADAMTS5*. J Orthop Res, 2012. **30**(4): p. 620-6.
44. Bell, R., et al., *ADAMTS5 is required for biomechanically-stimulated healing of murine tendinopathy*. Journal of Orthopaedic Research, 2013. **31**(10): p. 1540-8.
45. Plaas, A., et al., *Biochemical identification and immunolocalization of aggrecan, ADAMTS5 and inter-alpha-trypsin-inhibitor in equine degenerative suspensory ligament desmitis*. J Orthop Res, 2011. **29**(6): p. 900-6.
46. Li, J., et al., *Knockout of ADAMTS5 does not eliminate cartilage aggrecanase activity but abrogates joint fibrosis and promotes cartilage aggrecan deposition in murine osteoarthritis models*. J Orthop Res, 2011. **29**(4): p. 516-22.
47. Gorski, D.J., et al., *Deletion of ADAMTS5 does not affect aggrecan or versican degradation but promotes glucose uptake and proteoglycan synthesis in murine adipose derived stromal cells*. Matrix Biol, 2015.

48. Andres, B.M. and G.A. Murrell, *Treatment of tendinopathy: what works, what does not, and what is on the horizon*. Clin Orthop Relat Res, 2008. **466**(7): p. 1539-54.
49. Greis, A.C., S.M. Derrington, and M. McAuliffe, *Evaluation and nonsurgical management of rotator cuff calcific tendinopathy*. Orthop Clin North Am, 2015. **46**(2): p. 293-302.
50. Fahlstrom, M., et al., *Chronic Achilles tendon pain treated with eccentric calf-muscle training*. Knee Surg Sports Traumatol Arthrosc, 2003. **11**(5): p. 327-33.
51. Verrall, G., S. Schofield, and T. Brustad, *Chronic Achilles Tendinopathy Treated With Eccentric Stretching Program*. Foot & Ankle International, 2011. **32**(09): p. 843-849.
52. Silbernagel, K.G., A. Brorsson, and M. Lundberg, *The majority of patients with Achilles tendinopathy recover fully when treated with exercise alone: a 5-year follow-up*. Am J Sports Med, 2011. **39**(3): p. 607-13.
53. Maxson, S., et al., *Concise review: role of mesenchymal stem cells in wound repair*. Stem Cells Transl Med, 2012. **1**(2): p. 142-9.
54. Lee, C.H., et al., *Harnessing endogenous stem/progenitor cells for tendon regeneration*. J Clin Invest, 2015. **125**(7): p. 2690-701.
55. Susztak, K., *Understanding the epigenetic syntax for the genetic alphabet in the kidney*. J Am Soc Nephrol, 2014. **25**(1): p. 10-7.
56. Wada, S., et al., *H3K9MTase G9a is essential for the differentiation and growth of tenocytes in vitro*. Histochem Cell Biol, 2015. **144**(1): p. 13-20.
57. Liu, H., et al., *Crucial transcription factors in tendon development and differentiation: their potential for tendon regeneration*. Cell Tissue Res, 2014. **356**(2): p. 287-98.

58. Kim, G.K., *The Risk of Fluoroquinolone-induced Tendinopathy and Tendon Rupture: What Does The Clinician Need To Know?* J Clin Aesthet Dermatol, 2010. **3**(4): p. 49-54.
59. Millar, N.L., et al., *Hypoxia: a critical regulator of early human tendinopathy.* Ann Rheum Dis, 2012. **71**(2): p. 302-10.
60. Badal, S., Y.F. Her, and L.J. Maher, 3rd, *Nonantibiotic Effects of Fluoroquinolones in Mammalian Cells.* J Biol Chem, 2015. **290**(36): p. 22287-97.
61. Schubeler, D., *Function and information content of DNA methylation.* Nature, 2015. **517**(7534): p. 321-6.
62. Wasserstein, R.L. and N.A. Lazar, *The ASA's statement on p-values: context, process, and purpose.* The American Statistician, DOI: 10.1080/00031305.2016.1154108, 2016.
63. Eyre, D.R., et al., *A novel 3-hydroxyproline (3Hyp)-rich motif marks the triple-helical C terminus of tendon type I collagen.* J Biol Chem, 2011. **286**(10): p. 7732-6.
64. Hudson, D.M., et al., *Peptidyl 3-hydroxyproline binding properties of type I collagen suggest a function in fibril supramolecular assembly.* Biochemistry, 2012. **51**(12): p. 2417-24.
65. Malin, D., et al., *Forkhead box F1 is essential for migration of mesenchymal cells and directly induces integrin-beta3 expression.* Mol Cell Biol, 2007. **27**(7): p. 2486-98.
66. Saunders, C.J., M. Jalali Sefid Dashti, and J. Gamielien, *Semantic interrogation of a multi knowledge domain ontological model of tendinopathy identifies four strong candidate risk genes.* Sci Rep, 2016. **6**: p. 19820.
67. Smith, S.M., C.E. Thomas, and D.E. Birk, *Pericellular proteins of the developing mouse tendon: a proteomic analysis.* Connect Tissue Res, 2012. **53**(1): p. 2-13.

68. Raykha, C., et al., *IGF-II and IGFBP-6 regulate cellular contractility and proliferation in Dupuytren's disease*. *Biochim Biophys Acta*, 2013. **1832**(10): p. 1511-9.
69. Zhang, C., et al., *IGF binding protein-6 expression in vascular endothelial cells is induced by hypoxia and plays a negative role in tumor angiogenesis*. *Int J Cancer*, 2012. **130**(9): p. 2003-12.
70. Bechard, M., et al., *Frat is a phosphatidylinositol 3-kinase/Akt-regulated determinant of glycogen synthase kinase 3beta subcellular localization in pluripotent cells*. *Mol Cell Biol*, 2012. **32**(2): p. 288-96.
71. Ko, C.Y., et al., *Glycogen synthase kinase-3beta-mediated CCAAT/enhancer-binding protein delta phosphorylation in astrocytes promotes migration and activation of microglia/macrophages*. *Neurobiol Aging*, 2014. **35**(1): p. 24-34.
72. Dean, B.J., et al., *Are inflammatory cells increased in painful human tendinopathy? A systematic review*. *Br J Sports Med*, 2016. **50**(4): p. 216-20.
73. Chamberlain, C.S., et al., *The influence of macrophage depletion on ligament healing*. *Connect Tissue Res*, 2011. **52**(3): p. 203-11.
74. Dantas Machado, A.C., et al., *Evolving insights on how cytosine methylation affects protein-DNA binding*. *Brief Funct Genomics*, 2015. **14**(1): p. 61-73.
75. Baubec, T. and D. Schubeler, *Genomic patterns and context specific interpretation of DNA methylation*. *Curr Opin Genet Dev*, 2014. **25**: p. 85-92.
76. Jones, P.A. and P.W. Laird, *Cancer epigenetics comes of age*. *Nat Genet*, 1999. **21**(2): p. 163-7.
77. Fenwick, S.A., B.L. Hazleman, and G.P. Riley, *The vasculature and its role in the damaged and healing tendon*. *Arthritis Research*, 2002. **4**(4): p. 252-260.

78. Lee, W.Y., P.P. Lui, and Y.F. Rui, *Hypoxia-mediated efficient expansion of human tendon-derived stem cells in vitro*. Tissue Eng Part A, 2012. **18**(5-6): p. 484-98.
79. Zhang, J. and J.H. Wang, *Human tendon stem cells better maintain their stemness in hypoxic culture conditions*. PLoS One, 2013. **8**(4): p. e61424.
80. Vailas, A.C., et al., *Physical activity and hypophysectomy on the aerobic capacity of ligaments and tendons*. J Appl Physiol Respir Environ Exerc Physiol, 1978. **44**(4): p. 542-6.
81. Hunt, T.K., B. Zederfeldt, and T.K. Goldstick, *Oxygen and healing*. Am J Surg, 1969. **118**(4): p. 521-5.
82. Gordillo, G.M. and C.K. Sen, *Revisiting the essential role of oxygen in wound healing*. Am J Surg, 2003. **186**(3): p. 259-63.
83. Prockop, D.J., et al., *The biosynthesis of collagen and its disorders (first of two parts)*. N Engl J Med, 1979. **301**(1): p. 13-23.
84. Prockop, D.J., et al., *The biosynthesis of collagen and its disorders (second of two parts)*. N Engl J Med, 1979. **301**(2): p. 77-85.
85. Nauta, T.D., V.W. van Hinsbergh, and P. Koolwijk, *Hypoxic signaling during tissue repair and regenerative medicine*. Int J Mol Sci, 2014. **15**(11): p. 19791-815.
86. Benson, R.T., et al., *Tendinopathy and tears of the rotator cuff are associated with hypoxia and apoptosis*. J Bone Joint Surg Br, 2010. **92**(3): p. 448-53.
87. Rathbun, J.B. and I. MacNab, *The microvascular pattern of the human rotator cuff*. Journal of bone and Joint Surgery, 1970. **52B**(3): p. 540-553.
88. Davidson, Y.S., et al., *The effect of aging on skeletal muscle capillarization in a murine model*. J Gerontol A Biol Sci Med Sci, 1999. **54**(10): p. B448-51.

89. Malhotra, R. and F.C. Brosius, 3rd, *Glucose uptake and glycolysis reduce hypoxia-induced apoptosis in cultured neonatal rat cardiac myocytes*. J Biol Chem, 1999. **274**(18): p. 12567-75.
90. Masoud, G.N. and W. Li, *HIF-1alpha pathway: role, regulation and intervention for cancer therapy*. Acta Pharm Sin B, 2015. **5**(5): p. 378-89.
91. Jones, G.C., et al., *Expression profiling of metalloproteinases and tissue inhibitors of metalloproteinases in normal and degenerate human achilles tendon*. Arthritis Rheum, 2006. **54**(3): p. 832-42.
92. Karousou, E., et al., *Collagens, proteoglycans, MMP-2, MMP-9 and TIMPs in human achilles tendon rupture*. Clin Orthop Relat Res, 2008. **466**(7): p. 1577-82.
93. Parkinson, J., et al., *Change in proteoglycan metabolism is a characteristic of human patellar tendinopathy*. Arthritis Rheum, 2010. **62**(10): p. 3028-35.
94. Voloshin, I., et al., *Proinflammatory cytokines and metalloproteases are expressed in the subacromial bursa in patients with rotator cuff disease*. Arthroscopy, 2005. **21**(9): p. 1076 e1-1076 e9.
95. Yu, T.Y., et al., *Aging is associated with increased activities of matrix metalloproteinase-2 and -9 in tenocytes*. BMC Musculoskelet Disord, 2013. **14**: p. 2.
96. Guerra Fda, R., et al., *LLLT improves tendon healing through increase of MMP activity and collagen synthesis*. Lasers Med Sci, 2013. **28**(5): p. 1281-8.
97. Gillard, J.A., et al., *Matrix metalloproteinase activity and immunohistochemical profile of matrix metalloproteinase-2 and -9 and tissue inhibitor of metalloproteinase-1 during human dermal wound healing*. Wound Repair Regen, 2004. **12**(3): p. 295-304.

98. Loiselle, A.E., et al., *Bone marrow-derived matrix metalloproteinase-9 is associated with fibrous adhesion formation after murine flexor tendon injury*. PLoS One, 2012. **7**(7): p. e40602.
99. Loiselle, A.E., et al., *Remodeling of murine intrasynovial tendon adhesions following injury: MMP and neotendon gene expression*. J Orthop Res, 2009. **27**(6): p. 833-40.
100. Orner, C.A., et al., *Low-Dose and Short-Duration Matrix Metalloproteinase 9 Inhibition Does Not Affect Adhesion Formation during Murine Flexor Tendon Healing*. Plast Reconstr Surg, 2016. **137**(3): p. 545e-53e.
101. Tsai, W.C., et al., *High glucose concentration up-regulates the expression of matrix metalloproteinase-9 and -13 in tendon cells*. BMC Musculoskelet Disord, 2013. **14**: p. 255.
102. Khan, K.M., et al., *Histopathology of common tendinopathies*. Sports Medicine, 1999. **27**(6): p. 393-408.
103. Khan, W.S., et al., *Bone marrow-derived mesenchymal stem cells express the pericyte marker 3G5 in culture and show enhanced chondrogenesis in hypoxic conditions*. J Orthop Res, 2010. **28**(6): p. 834-40.
104. Khan, W.S., A.B. Adesida, and T.E. Hardingham, *Hypoxic conditions increase hypoxia-inducible transcription factor 2alpha and enhance chondrogenesis in stem cells from the infrapatellar fat pad of osteoarthritis patients*. Arthritis Res Ther, 2007. **9**(3): p. R55.
105. Pfander, D., et al., *HIF-1alpha controls extracellular matrix synthesis by epiphyseal chondrocytes*. J Cell Sci, 2003. **116**(Pt 9): p. 1819-26.

106. Robins, J.C., et al., *Hypoxia induces chondrocyte-specific gene expression in mesenchymal cells in association with transcriptional activation of Sox9*. Bone, 2005. **37**(3): p. 313-22.
107. Kowalski, T.J., et al., *Hypoxic culture conditions induce increased metabolic rate and collagen gene expression in ACL-derived cells*. J Orthop Res, 2016. **34**(6): p. 985-94.
108. Ramchurn, N., et al., *Upper limb musculoskeletal abnormalities and poor metabolic control in diabetes*. Eur J Intern Med, 2009. **20**(7): p. 718-21.
109. de Oliveira, R.R., et al., *Alterations of tendons in patients with diabetes mellitus: a systematic review*. Diabet Med, 2011. **28**(8): p. 886-95.
110. Gaida, J.E., J.L. Cook, and S.L. Bass, *Adiposity and tendinopathy*. Disabil Rehabil, 2008. **30**(20-22): p. 1555-62.
111. Ozgurtas, T., et al., *Is high concentration of serum lipids a risk factor for Achilles tendon rupture?* Clin Chim Acta, 2003. **331**(1-2): p. 25-8.
112. Pineda, C., et al., *Joint and tendon subclinical involvement suggestive of gouty arthritis in asymptomatic hyperuricemia: an ultrasound controlled study*. Arthritis Res Ther, 2011. **13**(1): p. R4.
113. Perry, M.B., et al., *Musculoskeletal findings and disability in alkaptonuria*. J Rheumatol, 2006. **33**(11): p. 2280-5.
114. Abate, M., et al., *Occurrence of tendon pathologies in metabolic disorders*. Rheumatology (Oxford), 2013. **52**(4): p. 599-608.
115. Reddy, G.K., *Cross-linking in collagen by nonenzymatic glycation increases the matrix stiffness in rabbit achilles tendon*. Exp Diabetes Res, 2004. **5**(2): p. 143-53.

116. David, M.A., et al., *Tendon repair is compromised in a high fat diet-induced mouse model of obesity and type 2 diabetes*. PLoS One, 2014. **9**(3): p. e91234.
117. Bedi, A., et al., *Diabetes mellitus impairs tendon-bone healing after rotator cuff repair*. J Shoulder Elbow Surg, 2010. **19**(7): p. 978-88.
118. Screen, H.R., et al., *Cyclic tensile strain upregulates collagen synthesis in isolated tendon fascicles*. Biochem Biophys Res Commun, 2005. **336**(2): p. 424-9.
119. Abreu, E.L., D. Leigh, and K.A. Derwin, *Effect of altered mechanical load conditions on the structure and function of cultured tendon fascicles*. J Orthop Res, 2008. **26**(3): p. 364-73.
120. Gardner, K., et al., *Re-establishment of cytoskeletal tensional homeostasis in lax tendons occurs through an actin-mediated cellular contraction of the extracellular matrix*. J Orthop Res, 2012. **30**(11): p. 1695-701.
121. Cousineau-Pelletier, P. and E. Langelier, *Relative contributions of mechanical degradation, enzymatic degradation, and repair of the extracellular matrix on the response of tendons when subjected to under- and over- mechanical stimulations in vitro*. J Orthop Res, 2010. **28**(2): p. 204-10.
122. Lavagnino, M., K. Gardner, and S.P. Arnoczky, *Age-related changes in the cellular, mechanical, and contractile properties of rat tail tendons*. Connect Tissue Res, 2013. **54**(1): p. 70-5.
123. Leigh, D.R., E.L. Abreu, and K.A. Derwin, *Changes in gene expression of individual matrix metalloproteinases differ in response to mechanical unloading of tendon fascicles in explant culture*. J Orthop Res, 2008. **26**(10): p. 1306-12.

124. Maeda, E., et al., *Time dependence of cyclic tensile strain on collagen production in tendon fascicles*. Biochem Biophys Res Commun, 2007. **362**(2): p. 399-404.
125. Marsolais, D., et al., *Inflammatory cells do not decrease the ultimate tensile strength of intact tendons in vivo and in vitro: protective role of mechanical loading*. J Appl Physiol (1985), 2007. **102**(1): p. 11-7.
126. Hsieh, A.H., R.L. Sah, and K.L.P. Sung, *Biomechanical regulation of type I collagen gene expression in ACLs in organ culture*. Journal of Orthopaedic Research, 2002. **20**: p. 325-331.
127. Scott, A., et al., *High strain mechanical loading rapidly induces tendon apoptosis: an ex vivo rat tibialis anterior model*. Br J Sports Med, 2005. **39**(5): p. e25.
128. Ikeda, J., et al., *Effects of synovial interposition on healing in a canine tendon explant culture model*. J Hand Surg Am, 2010. **35**(7): p. 1153-9.
129. Lee, J., M.H. Green, and D. Amiel, *Synergistic Effect of Growth Factors on Cell Outgrowth from Explants of Rabbit Anterior Cruciate and Medial Collateral Ligaments*. Journal of Orthopaedic Research, 1995. **13**: p. 435-441.
130. Majima, T., et al., *Compressive compared with Tensile Loading of Medial Collateral Ligament Scar In Vitro Uniquely Influences mRNA Levels for Aggrecan, Collagen Type II, and Collagenase*. Journal of Orthopaedic Research, 2000. **18**: p. 524-531.
131. Manske, P.R., et al., *Intrinsic flexor-tendon repair. A morphological study in vitro*. J Bone Joint Surg Am, 1984. **66**(3): p. 385-96.
132. Yoshikawa, Y. and S.-O. Abrahamsson, *Dose-related cellular effects of platelet-derived growth factor-BB differ in various types of rabbit tendons in vitro*. Acta Orthop Scand, 2001. **72**(3): p. 287-292.

133. Yamamoto, E., et al., *Effects of Static Stress on the Mechanical Properties of Cultured Collagen Fascicles From the Rabbit Patellar Tendon*. Journal of Biomechanical Engineering, 2002. **124**: p. 85-93.
134. Legerlotz, K., et al., *Cyclic loading of tendon fascicles using a novel fatigue loading system increases interleukin-6 expression by tenocytes*. Scand J Med Sci Sports, 2013. **23**(1): p. 31-7.
135. Rees, S.G., et al., *Inhibition of aggrecan turnover in short-term explant cultures of bovine tendon*. Matrix Biol, 2007. **26**(4): p. 280-90.
136. Samiric, T., M.Z. Ilic, and C.J. Handley, *Characterisation of proteoglycans and their catabolic products in tendon and explant cultures of tendon*. Matrix Biol, 2004. **23**(2): p. 127-40.
137. Dakin, S.G., et al., *Proteomic analysis of tendon extracellular matrix reveals disease stage-specific fragmentation and differential cleavage of COMP (cartilage oligomeric matrix protein)*. J Biol Chem, 2014. **289**(8): p. 4919-27.
138. Haupt, J.L., B.P. Donnelly, and A.J. Nixon, *Effects of platelet-derived growth factor-BB on the metabolic function or morphologic features of equine tendon in explant culture*. Am J Vet Res, 2006. **69**(9): p. 1595-1599.
139. Dudhia, J., et al., *Aging enhances a mechanically-induced reduction in tendon strength by an active process involving matrix metalloproteinase activity*. Aging Cell, 2007. **6**: p. 547-556.
140. Devkota, A.C., et al., *Distributing a fixed amount of cyclic loading to tendon explants over longer periods induces greater cellular and mechanical responses*. J Orthop Res, 2007. **25**(8): p. 1078-86.

141. Wong, M.W., et al., *The effect of glucocorticoids on tendon cell viability in human tendon explants*. Acta Orthop, 2009. **80**(3): p. 363-7.
142. Tsubone, T., et al., *Effect of TGF-beta inducible early gene deficiency on flexor tendon healing*. J Orthop Res, 2006. **24**(3): p. 569-75.
143. Trella, K.J., et al. *Analysis of the biomechanics of tendinopathy in a new murine Achilles explant system which maintains cell viability, gene expression, and material properties*. in *Trans Orthop Res Soc*. 2013. San Antonio, TX.
144. Zhou, M., et al., *A stable nonfluorescent derivative of resorufin for the fluorometric determination of trace hydrogen peroxide: applications in detecting the activity of phagocyte NADPH oxidase and other oxidases*. Analytical Biochemistry, 1997. **253**: p. 162-168.
145. Eliasson, P., et al., *Ruptured human Achilles tendon has elevated metabolic activity up to 1 year after repair*. Eur J Nucl Med Mol Imaging, 2016.
146. Greve, K., et al., *Metabolic activity in early tendon repair can be enhanced by intermittent pneumatic compression*. Scand J Med Sci Sports, 2012. **22**(4): p. e55-63.
147. Hannukainen, J., et al., *In vivo measurements of glucose uptake in human Achilles tendon during different exercise intensities*. Int J Sports Med, 2005. **26**(9): p. 727-31.
148. Burner, T., et al., *Hyperglycemia reduces proteoglycan levels in tendons*. Connect Tissue Res, 2012. **53**(6): p. 535-41.
149. Tsai, T.L., P.A. Manner, and W.J. Li, *Regulation of mesenchymal stem cell chondrogenesis by glucose through protein kinase C/transforming growth factor signaling*. Osteoarthritis Cartilage, 2013. **21**(2): p. 368-76.

150. Clarkin, C.E., et al., *Regulation of UDP-glucose dehydrogenase is sufficient to modulate hyaluronan production and release, control sulfated GAG synthesis, and promote chondrogenesis*. J Cell Physiol, 2011. **226**(3): p. 749-61.

Katie J. Trella
Curriculum Vitae

EDUCATION:

University of Illinois at Chicago

Chicago, IL

PhD Bioengineering

May 2016

Co-Advisors: Vincent M. Wang, PhD/Anna Plaas, PhD

Assistant Professor of Orthopedic Surgery/Professor of Rheumatology
Rush University Medical Center

Rose-Hulman Institute of Technology

Terre Haute, IN

BS Biomedical Engineering

May 2011

Biomaterials Concentration

Minor in Biochemistry/Molecular Biology

Advisor: Glen A. Livesay, PhD

Professor of Bioengineering

RESEARCH EXPERIENCE:

Rush University Medical Center, Department of Orthopedic Surgery

Chicago, IL

Research Assistant

Oct 2011 – Present

Projects: **Mechanical Stimulation on Hypoxic Conditions for Tendon Healing**

(Thesis)

Effect of Hypoxia on Tendon Explants (Thesis)

Thesis work funded by NIH-RO1 (PI: Vincent Wang, PhD)

Knockout of Hyaluronan Synthase on Murine Tendon Function (Lead

Researcher)

Epigenetic Regulation in Murine Tendinopathy (Lead Researcher)

Funded by American Society for the Hand (PI: Robert Wysocki, MD)

Epigenetic Regulation in Human Tendinopathy (Collaborator)

Grant submitted (PI: Robert Wysocki, MD)

Equine Degenerative Suspensory Ligament Desmitis (Collaborator)

Clinical Lead: Jorge Galante, MD

Quadriceps and Achilles Tendon Allografts in PCL Reconstruction

(Collaborator)

Clinical Lead: Brian Forsythe, MD

Rose-Hulman Institute of Technology

Terre Haute, IN

Research Assistant

Apr 2009 – May 2011

Projects: **Markerless Tracking of Regional Surface Strains** (Thesis)

TEACHING EXPERIENCE

University of Illinois at Chicago, Department of Bioengineering

Chicago, IL

Classes:

BioE 101 Introduction to Bioengineering (Miiri Kotche, PhD)

BioE 250 Clinical Problems in Bioengineering (Miiri Kotche, PhD)

PEER REVIEWED PUBLICATIONS:

1. ET Sayegh, JD Sandy, MS Virk, AA Romeo, RW Wysocki, JO Galante, **KJ Trella**, A Plaas, and VM Wang. Recent Scientific Advances Towards the Development of Tendon Healing Strategies. *Current Tissue Engineering* (2015); 4(2):128-143.
2. **KJ Trella**. Markerless Tracking of Regional Surface Strains in Collagenous Biological Materials, *BS Biomedical Engineering Thesis*. Rose-Hulman Institute of Technology, Terre Haute, IN, May 18, 2011
3. **KJ Trella** and GA Livesay. Development and Implementation of a Custom Program for Post Hoc Strain Tracking in Biological Specimens using Cross Correlation. *Biomedical Sciences Instrumentation* (2011) 47:106-111

CONFERENCE PRESENTATIONS:

1. **KJ Trella**, J Li, J Galante, VM Wang, JD Sandy, E Stylianou, A Plaas, R Wysocki. Examination of Genome Wide Methylation Changes in a Murine Model of Tendinopathy using MiniSeq Technology. *Orthopaedic Research Society*, Orlando, FL, 2016. **Podium 0353**.
2. **KJ Trella**, J Li, JD Sandy, A Plaas, VM Wang. The Stress Response of Murine Achilles Tendons to Explant Culture can be Blocked by TGF- β 1 or Low Oxygen Tension. *Orthopaedic Research Society*, Orlando, FL, 2016. **Poster 0643**.
3. **KJ Trella**, J Li, J Frank, J Galante, R Wysocki, JD Sandy, A Plaas, VM Wang. Treadmill Running Mitigates the Post-Injury Hypoxic Response in a Murine Model of Tendinopathy. *Biomedical Engineering Society Annual Meeting*. Tampa, FL, 2015. **Podium**
4. **KJ Trella**, J Li, J Frank, J Galante, R Wysocki, JD Sandy, A Plaas, VM Wang. Treadmill Running Promotes Epigenetic Changes in a Murine Model of Tendon Repair. *The American Society for Pharmacology and Experimental Therapeutics: Great Lakes Chapter Annual Meeting*. Chicago, IL, 2015. **Poster**
5. **KJ Trella**. J Li, C DeLa Motte, JD Sandy, VM Wang, A Plaas. Tendons from Has1^{-/-} and Has3^{-/-} exhibit discrete abnormalities in mechanical properties and gene expression. *10th International Conference on Hyaluronan Sciences*. Florence, Italy, 2015. **Poster 132**
6. **KJ Trella**, J Li, J Frank, J Galante, JD Sandy, A Plaas, R Wysocki, VM Wang. Does Hypoxia Contribute to Tendinopathy? Evidence from an In-Vivo Murine Model. *International Symposium on Tendons and Ligaments*, Las Vegas, NV, 2015. **Podium**.

7. **KJ Trella**, J Li, EF Shewman, JD Sandy, A Plaas, VM Wang. Development of a Novel Murine Achilles Tendon Explant System. *International Symposium on Tendons and Ligaments*, Las Vegas, NV, 2015. **Poster**
8. **KJ Trella**, J Li, J Frank, K Mikecz, J Galante, J Sandy, A Plaas, VM Wang, R Wysocki. Epigenetic Changes in a Murine Model of Tendinopathy. *Orthopaedic Research Society*, Las Vegas, NV, 2015. **Poster 1355**.
9. **KJ Trella**, J Li, C DeLa Motte, J Sandy, A Plaas, VM Wang. Ablation of Hyaluronan Synthase 1 Or 3 Primarily Affects The Phenotype Of The Achilles Rather Than The Flexor Digitorum Longus Tendon In Skeletally Mature Mice. *Orthopaedic Research Society*, Las Vegas, NV, 2015. **Poster 1359**.
10. **KJ Trella**, EF Shewman, F Tenuto, F McCormick, MB Ellman, NN Verma, BR Bach, B Forsythe. Biomechanical Evaluation of Posterior Cruciate Ligament Reconstruction with Quadriceps vs. Achilles Tendon-Bone Block Allograft. *Orthopaedic Research Society*, New Orleans, LA, 2014. **Poster 1717**
11. **KJ Trella**, J Li, R Bell, D Gorski, K Mikecz, J Sandy, A Plaas, V Wang. Analysis of the Biomechanics of Tendinopathy in a New Murine Achilles Explant System which Maintains Cell Viability, Gene Expression, and Material Properties. *Orthopaedic Research Society*, San Antonio, TX, 2013. **Poster 1326**
12. **KJ Trella** and GA Livesay. Development and Implementation of a Custom Program for Post Hoc Strain Tracking in Biological Specimens using Cross Correlation, *Rocky Mountain Bioengineering Symposium*, Denver, CO, 2011. **Podium**.
13. **KJ Trella**, KE Hickman, GA Livesay. Design and Fabrication of a Horizontal Micro-Tensile Tester with Analysis Software for Testing of Collagenous Specimens, *Interdisciplinary Research Collaborative (IRC) Undergraduate Student Research Symposium*, Rose-Hulman Institute of Technology, Terre Haute, IN, 2010. **Poster**

INVITED TALKS

1. **KJ Trella**, R Bell, J Li, R Wysocki, J Sandy, A Plaas, V Wang. The Role of Mechanical Stimulation and ADAMTS5 in Tendinopathy. *Engineering in Medicine and Biology*, Chicago, IL 2014.
2. **KJ Trella**. Development of a New Murine Achilles Tendon Explant System for use in Therapeutic and Mechanobiologic Studies of Tendinopathy. *Musculoskeletal Monthly Seminar Series*, Department of Anatomy and Cell Biology, Rush University Medical Center, Chicago, IL, December 2012.

PROFESSIONAL SERVICE:

Manuscript Review

British Journal of Sports Medicine, Journal of Orthopaedic Research, Medical Engineering and Physics

Society Membership

Orthopaedic Research Society (Associate Member) 2014 – Present

Biomedical Engineering Society (Student Member) 2015 – Present
American Association for the Advancement of Science (Student Member)
2015 – Present

SKILLS:

Software Experience

Digital Motion Analysis Software, GPower, GraphPad, Maple, MATLAB, Microsoft Office, Mimics, Minitab, ImageJ, Solid Edge, LabView, Statistical Analysis Software, TestWorks

Experimental Experience

Animal Protocols

Murine Breeding, Murine Genotyping

Biochemical Analysis

Alamar Blue Viability Assay, Hoechst DNA Assay, RNA Isolation, RT-PCR, Gel electrophoresis, Western Blot

Biomechanical Analysis

Material Testing Systems

Cell Culture Protocols

Mammalian Cell Culture, Murine Explant Culture

Imaging Techniques

Digital Imaging Tracking, Image Processing, Two-Photon Excitation Microscopy

HONORS:

Graduate Student Poster Award: 3rd Place 2015

Treadmill Running Promotes Epigenetic Changes in a Murine Model of Tendon Repair. KJ Trella, J Li, J Frank, J Galante, R Wysocki, JD Sandy, A Plaas, VM Wang.. *The American Society for Pharmacology and Experimental Therapeutics: Great Lakes Chapter Annual Meeting*. Chicago, IL, 2015. Poster

Best Poster Award 2015

Development of a Novel Murine Achilles Tendon Explant System. KJ Trella, J Li, EF Shewman, JD Sandy, A Plaas, VM Wang. *International Symposium on Tendons and Ligaments*, Las Vegas, NV, 2015. Poster

UIC Graduate Student Council Travel Award 2012

Analysis of the Biomechanics of Tendinopathy in a New Murine Achilles Explant System which Maintains Cell Viability, Gene Expression, and Material Properties. KJ Trella, J Li, R Bell, D Gorski, K Mikecz, J Sandy, A Plaas, V Wang. *Orthopedic Research Society*, San Antonio, TX, 2013. Poster 1326

RMBS Program Chairman Award	2011
Development and Implementation of a Custom Program for Post Hoc Strain Tracking in Biological Specimens using Cross Correlation. KJ Trella and GA Livesay. <i>Rocky Mountain Bioengineering Symposium</i> , Denver, CO, 2011. Talk	
Delta Delta Delta Gamma Pi Chapter Academic Award	2011
Delta Delta Delta Gamma Pi Chapter Leadership Award	2011
Rose-Hulman Dean's List Qualifier (9 out of 12 semesters)	2007-2011
Rose-Hulman Merit Scholarship	2007-2011